

# Navier-Stokes/Darcy Coupling: Modeling, Analysis, and Numerical Approximation

Marco DISCACCIATI <sup>1</sup>, and Alfio QUARTERONI <sup>1,2</sup>,

<sup>1</sup>IACS - Chair of Modeling and Scientific Computing  
Ecole Polytechnique Fédérale de Lausanne  
CH-1015 Lausanne — Switzerland  
alfio.quarteroni@epfl.ch

<sup>2</sup>MOX, Politecnico di Milano  
P.zza Leonardo da Vinci 32  
I-20133 Milano — Italy  
marco.discacciati@epfl.ch

Received: November 21, 2008  
Accepted: April 16, 2009

## ABSTRACT

This paper is an overview of known and new results about the coupling of Navier-Stokes and Darcy equations to model the filtration of incompressible fluids through porous media. We discuss coupling conditions and we analyze the global coupled model in order to prove its well-posedness and to characterize effective algorithms to compute the solution of its numerical approximation.

*Key words:* Navier-Stokes equations, Darcy's law, Interface conditions, Domain decomposition, Finite elements, Environmental flows, Blood flow.

*2000 Mathematics Subject Classification:* 76D05, 76S05, 65M60, 65M55, 86A05, 76Z05.

## 1. Introduction

The filtration of fluids through porous media is an interesting research subject with many relevant applications. To quote some examples, these phenomena occur in physiology when studying the filtration of blood through arterial vessel walls, in industrial processes involving, e.g., air or oil filters, in the environment concerning the percolation of waters of hydrological basins through rocks and sand.

The modeling of such physical processes requires to consider different systems of partial differential equations in each subregion of the domain of interest. Typically,

---

The supports of the FNS Project 200020-117587 "Interface operators and solutions algorithms for fluid-structure interaction problems with applications" and of the European Project ERC-2008-AdG\_/20080228 "MATHCARD" are kindly acknowledged.

the motion of incompressible free fluids are described by the Navier-Stokes equations while Darcy equations are adopted to model the filtration process. These equations must be linked through suitably chosen conditions that describe the fluid flow across the surface of the porous media through which the filtration occurs. In this respect, we are facing a global heterogeneous partial differential model as those considered, e.g., in [110, Chapter 8].

This system may be possibly completed by considering the transport of passive scalars in the main field and in the porous medium representing different substances, e.g., solutes, chemical pollutants, etc.

For example, in hydrological environmental applications, we can model the transport of contaminants in coastal areas, rivers, basins, or lakes. In this case, the coupling of the Navier-Stokes equations for free-surface flows, with the ground-water flow in the porous media, together with a numerical model of transport-diffusion of a chemical pollutant in the two regions, would help in assessing the short and medium-term effects of polluting agents.

On the other hand, in bio-engineering applications, blood oxygenators and hemodialysis devices are based on the transport of chemicals from the main blood stream in the arteries through a porous membrane. Similar problems occur within human arteries when chemical substances (such as lipo-proteins, drugs or oxygen) are carried through the vessel wall from the main blood stream. Here, the problem is made more difficult by the complex mechanical behavior of the material constituting the several layers of a vessel wall. In both cases we are facing a coupling between fluid flow in heterogeneous media and transport-diffusion (and possibly reaction) phenomena.

Those coupled problems have received an increasing attention during the last years both from the mathematical and the numerical point of view.

Starting from the original experimental works of Beavers and Joseph on the coupling conditions between a fluid and a porous medium, mathematical investigations have been carried out in [66, 83, 84, 85, 89, 95].

Under these conditions, the analysis of the coupled Stokes/Darcy problem has been studied in [40, 49, 53, 55, 56, 68, 69, 70, 71, 72, 88, 112, 113] in the steady case, and in [43, 124] in the time-dependent case. Moreover, extensions to the Navier-Stokes equations [13, 53, 75] and to the Shallow Water Equations [55, 97, 98] have been considered.

Applications in the biomedical context have been investigated as well. Let us mention, e.g., [18, 82, 107, 124].

A vast literature on the approximation methods, as well as on numerical algorithms for the solutions of the associated systems is available (see Section 7).

In this paper, we give an overview on the coupled free/porous-media flow problem. Precisely, the paper is structured as follows.

In Section 2 we present the differential model introducing the Navier-Stokes equations for the fluid and Darcy equations for the porous media. The coupling conditions (the so-called Beavers-Joseph-Saffman conditions) are discussed in Section 3, besides

explaining their physical meaning we comment also on their mathematical justification via homogenization theory.

In Section 4 we deal with the analysis of the linear Stokes/Darcy model. We show that the problem features a saddle-point structure and its well-posedness can be proved using classical results on saddle-point problems.

Section 5 introduces the multi-domain formulation of the Stokes/Darcy problem. The idea is that, based on the naturally decoupled structure of the fluid-porous media problem, it would be interesting to reduce the size of the global problem by keeping separated the fluid and the porous media parts and exchanging information between surface and groundwater flows only through boundary conditions at the interface. Therefore, we introduce and analyze the Steklov-Poincaré interface equation associated to the Stokes/Darcy problem, in order to reformulate it solely in terms of interface unknowns. This re-interpretation will be crucial to set up iterative procedures between the subdomains as we will see in Section 8.

In Section 6 we extend the approach to the non-linear Navier-Stokes/Darcy problem. In this case, we will use the multi-domain formulation of the problem also to prove the existence and uniqueness of the solution under suitable hypotheses on the data.

Then, after giving an overview on the most common discretization strategies based on the finite element method (Section 7), in Section 8 we study possible iterative methods to solve the linear Stokes/Darcy problem and we discuss their effectiveness in Section 9 by showing several numerical results. We will see how the characteristic physical parameters, such as the fluid viscosity and the porosity of the porous medium, have a major influence on the convergence behavior of these methods. This will lead us to investigate more robust algorithms such as the Robin-Robin methods that we present in Section 10.

Section 11 is devoted to the non-linear Navier-Stokes/Darcy problem. In particular, we investigate theoretically and experimentally fixed-point and Newton methods to compute its solution.

Finally, Section 12 briefly introduces some recent results in hemodynamic applications in the context of filtration of blood through the arterial walls described as poroelastic structures.

## 2. Setting of the problem

In this section we introduce the setting of a coupled free/porous-media flow problem keeping in mind two diverse applications. On one hand we consider the coupling between surface and groundwater flows, on the other hand we consider the filtration of blood through the arterial wall. In both cases we make some model simplifications. In the first one, we assume that the free fluid has a fixed upper surface, i.e., we neglect the case of free surface. This amounts to considering a computational domain close enough to the porous media and we impose a suitable boundary condition on the top

artificial boundary to simulate the presence of a volume of water above. The extension of our analysis to the free-surface case can be found in [97, 55] and references therein.

Concerning blood flow applications, we refer to Section 12.

Our computational domain will be a region naturally split into two parts: one occupied by the fluid, the other by the porous media. More precisely, let  $\Omega \subset \mathbb{R}^d$  ( $d = 2, 3$ ) be a bounded domain, partitioned into two non intersecting subdomains  $\Omega_f$  and  $\Omega_p$  separated by an interface  $\Gamma$ , i.e.,  $\bar{\Omega} = \bar{\Omega}_f \cup \bar{\Omega}_p$ ,  $\Omega_f \cap \Omega_p = \emptyset$  and  $\bar{\Omega}_f \cap \bar{\Omega}_p = \Gamma$ . We suppose the boundaries  $\partial\Omega_f$  and  $\partial\Omega_p$  to be Lipschitz continuous. From the physical point of view,  $\Gamma$  is a surface separating the domain  $\Omega_f$  filled by a fluid, from a domain  $\Omega_p$  formed by a porous medium. As mentioned above, we assume that  $\Omega_f$  has a fixed surface. The fluid in  $\Omega_f$ , that will be referred to as *free fluid* in the following, can filtrate through the adjacent porous medium. This would consist of water in the first kind of application, blood in the second one. In Figure 1 we show a schematic representation of the computational domain.

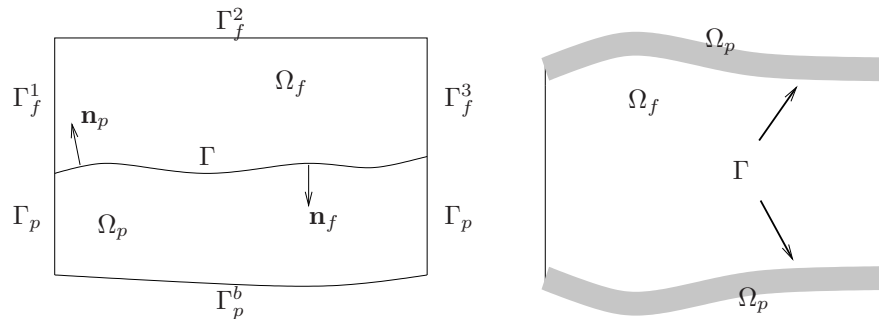


Figure 1 – Schematic representation of a 2D section of two possible computational domains: the surface-groundwater setting on the left, and the blood-flow problem on the right.

### 2.1. The surface-groundwater flow problem

In order to describe the motion of the fluid in  $\Omega_f$ , we introduce the Navier-Stokes equations:  $\forall t > 0$ ,

$$\partial_t \mathbf{u}_f - \nabla \cdot \mathbb{T}(\mathbf{u}_f, p_f) + (\mathbf{u}_f \cdot \nabla) \mathbf{u}_f = \mathbf{f} \quad \text{in } \Omega_f, \tag{2.1}$$

$$\nabla \cdot \mathbf{u}_f = 0 \quad \text{in } \Omega_f, \tag{2.2}$$

where  $\mathbb{T}(\mathbf{u}_f, p_f) = \nu(\nabla \mathbf{u}_f + \nabla^T \mathbf{u}_f) - p_f \mathbf{l}$  is the Cauchy stress tensor,  $\mathbf{l}$  being the identity tensor,  $\nu > 0$  is the kinematic viscosity of the fluid,  $\mathbf{f}$  a given volumetric force, while  $\mathbf{u}_f$  and  $p_f$  are the fluid velocity and pressure, respectively,  $\partial_t$  denotes the time derivative,  $\partial_i = \partial/\partial x_i$  is the spatial derivative with respect to the coordinate

$x_i$ , while  $\nabla$  and  $\nabla \cdot$  are, respectively, the gradient and the divergence operator with respect to the space coordinates. Moreover,

$$\nabla \cdot \mathbb{T} = \left( \sum_{j=1}^d \partial_j \mathbb{T}_{ij} \right)_{i=1, \dots, d}.$$

Finally, we recall that

$$(\mathbf{v} \cdot \nabla) \mathbf{w} = \sum_{i=1}^d v_i \partial_i \mathbf{w},$$

for all vector functions  $\mathbf{v} = (v_1, \dots, v_d)$  and  $\mathbf{w} = (w_1, \dots, w_d)$ .

The filtration of an incompressible fluid through porous media is often described using Darcy's law. The latter provides the simplest linear relation between velocity and pressure in porous media under the physically reasonable assumption that fluid flows are usually very slow and all the inertial (non-linear) terms may be neglected.

Groundwater flows could be treated microscopically by the laws of hydrodynamics if the granular skeleton of the porous medium were a simple geometrical assembly of unconnected tubes. However, the seepage path is tortuous and it branches into a multitude of tributaries. Darcy's law avoids the insurmountable difficulties of the hydrodynamic microscopic picture by introducing a macroscopic concept. In fact, it considers a fictitious flow velocity, the *Darcy velocity* or *specific discharge*  $\mathbf{q}$  through a given cross section of the porous medium, rather than the true velocity  $\mathbf{u}_p$  with respect to the porous matrix:

$$\mathbf{u}_p = \frac{\mathbf{q}}{n}, \quad (2.3)$$

with  $n$  being the *volumetric porosity*, defined as the ratio between the volume of void space and the total volume of the porous medium.

This simplifying concept was introduced by the nature of Darcy's experiment (see [50]) which only permitted the measurement of averaged hydraulic values from the percolation of water through a column of horizontally stratified beds of sand in a cylindrical pipe.

To introduce Darcy's law, we define a scalar quantity  $\varphi$  called *piezometric head* which essentially represents the fluid pressure in  $\Omega_p$ :

$$\varphi = z + \frac{p_p}{g},$$

where  $z$  is the elevation from a reference level, accounting for the potential energy per unit weight of fluid,  $p_p$  is the ratio between the fluid pressure in  $\Omega_p$  and its viscosity  $\rho_f$ , and  $g$  is the gravity acceleration.

Then, Darcy's law can be written as

$$\mathbf{q} = -K \nabla \varphi, \quad (2.4)$$

Table 1 – Typical values of hydraulic conductivity  $K$ .

$K$ (m/s):	1	$10^{-1}$	$10^{-2}$	$10^{-3}$	$10^{-4}$	$10^{-5}$	$10^{-6}$	$10^{-7}$	$10^{-8}$	$10^{-9}$	$10^{-10}$	$10^{-11}$	$10^{-12}$
Permeability	Pervious				Semipervious				Impervious				
Soils	Clean gravel	Clean sand or sand and gravel			Very fine sand, silt, loam								
					Peat	Stratified clay			Unweathered clay				
Rocks					Oil rocks		Sandstone		Good limestone, dolomite		Breccia, granite		

where  $K$  is a symmetric positive definite tensor  $K = (K_{ij})_{i,j=1,\dots,d}$ ,  $K_{ij} \in L^\infty(\Omega_p)$ ,  $K_{ij} > 0$ ,  $K_{ij} = K_{ji}$ , called *hydraulic conductivity tensor*, which depends on the properties of the fluid as well as on the characteristics of the porous medium. In fact, its components are proportional to  $n\varepsilon^2$ , where  $\varepsilon$  is the characteristic length of the pores; then,  $K \propto \varepsilon^2$ . The hydraulic conductivity  $K$  is therefore a macroscopic quantity characterizing porous media; in Table 1 we report some typical values that it may assume (see [20]).

Finally, we notice that the hydraulic conductivity tensor  $K$  can be diagonalized by introducing three mutually orthogonal axes called *principal directions of anisotropy*. In the following, we will always suppose that the principal axes are in the  $x$ ,  $y$  and  $z$  directions so that the tensor will be considered diagonal:  $K = \text{diag}(K_1, K_2, K_3)$ . Moreover, let us denote  $\mathbf{K} = K/n$ .

In conclusion, the motion of an incompressible fluid through a saturated porous medium is described by the following equations:

$$\mathbf{u}_p = -\mathbf{K}\nabla\varphi \quad \text{in } \Omega_p, \tag{2.5}$$

$$\nabla \cdot \mathbf{u}_p = 0 \quad \text{in } \Omega_p. \tag{2.6}$$

Extensions of Darcy’s law are given, e.g., by the Forchheimer’s or Brinkman’s equations when the Reynolds number in  $\Omega_p$  is not small (see [67, 73, 95, 38]), or by more complicated models like Richards’ equations apt to describe saturated-unsaturated fluid flows (see, e.g., [24] and references therein).

### 3. Interface conditions to couple surface and groundwater flows

We consider now the issue of finding effective coupling conditions across the interface  $\Gamma$  which separates the fluid flow in  $\Omega_f$  and the porous medium. This is a classical problem which has been investigated from both a physical and a rigorous mathematical point of view.

A mathematical difficulty arises from the fact that we need to couple two different systems of partial differential equations: Darcy equations (2.5)–(2.6) contain second

order derivatives for the pressure and first order for the velocity, while in the Navier-Stokes system it is the opposite.

In the following,  $\mathbf{n}_p$  and  $\mathbf{n}_f$  denote the unit outward normal vectors to the surfaces  $\partial\Omega_p$  and  $\partial\Omega_f$ , respectively, and we have  $\mathbf{n}_f = -\mathbf{n}_p$  on  $\Gamma$ . We suppose  $\mathbf{n}_f$  and  $\mathbf{n}_p$  to be regular enough. Moreover, we shall indicate  $\mathbf{n} = \mathbf{n}_f$  for simplicity of notation, and by  $\partial_n$  the partial derivative along  $\mathbf{n}$ .

Three conditions are to be prescribed on  $\Gamma$ .

- (i) The obvious condition to assign at a permeable interface is the continuity of the normal velocity, which is a consequence of the incompressibility of both fluids:

$$\mathbf{u}_f \cdot \mathbf{n} = \mathbf{u}_p \cdot \mathbf{n} \quad \text{on } \Gamma.$$

- (ii) Moreover, a suitable condition relating the pressures of the two fluids across  $\Gamma$  has to be prescribed.
- (iii) Finally, in order to have a completely determined flow of the free fluid, we have to specify a further condition on the tangential component of the fluid velocity at the interface.

Concerning the third point, a classically used condition for the free fluid is the vanishing of the tangential velocity at the interface,  $\mathbf{u}_f \cdot \boldsymbol{\tau}_j = 0$  on  $\Gamma$ , where  $\boldsymbol{\tau}_j$  ( $j = 1, \dots, d - 1$ ) are linear independent unit tangential vectors to the boundary  $\Gamma$ . However, this condition, which is correct in the case of a permeable surface, is not completely satisfactory for a permeable interface. (Let us remark that this condition has been used in [124] for blood flow simulations.) Beavers and Joseph proposed a new condition postulating that the difference between the slip velocity of the free fluid and the tangential component of the velocity through the porous medium is proportional to the shear rate of the free fluid (see [21]). They verified this law experimentally and found that the proportionality constant depends linearly on the square root of the permeability. Precisely, the coupling condition that they advocated reads:

$$\boldsymbol{\tau}_j \cdot \partial_n \mathbf{u}_f = \frac{\alpha_{BJ}}{\sqrt{K}} (\mathbf{u}_f - \mathbf{u}_p) \cdot \boldsymbol{\tau}_j \quad \text{on } \Gamma, \tag{3.1}$$

where  $\alpha_{BJ}$  is a dimensionless constant which depends only on the structure of the porous medium.

This experimentally found coupling condition was further studied by Saffman (see [115]) who pointed out that the velocity  $\mathbf{u}_p$  was much smaller than the other quantities appearing in equation (3.1) and that, in fact, it could be dropped. The new proposed interface condition reads therefore

$$\boldsymbol{\tau}_j \cdot \partial_n \mathbf{u}_f = \frac{\alpha_{BJ}}{\sqrt{K}} \mathbf{u}_f \cdot \boldsymbol{\tau}_j + O(\sqrt{K}) \quad \text{on } \Gamma. \tag{3.2}$$

This problem was later reconsidered in [66] and [89] using an asymptotic expansion argument and distinguishing two cases. First, the authors considered the case of a pressure gradient on the side of the porous medium normal to the interface (see Figure 2, left); they found that the flow is balanced on both sides of the interface and that the velocities across  $\Gamma$  are of the same order. Then, using an asymptotic expansion, they obtained the following interface laws:

$$\mathbf{u}_f \cdot \mathbf{n} = \mathbf{u}_p \cdot \mathbf{n}, \quad p_f = \text{const} \quad \text{on } \Gamma.$$

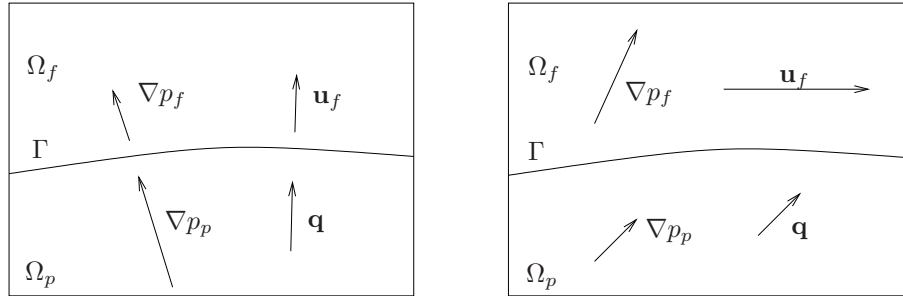


Figure 2 – Two configurations for the pressure gradient: on the left, normal to the interface  $\Gamma$ ; on the right, oblique to  $\Gamma$ .

Secondly, they studied the case of pressure gradient not normal (oblique) to the interface (see Figure 2, right). In this case, it is found in [66] and [89] that the velocity  $\mathbf{u}_f$  is much larger than the filtration velocity in the porous body and, in the first approximation, the flow around the porous medium is the same as if the body were impervious. Then, investigation in the vicinity of  $\Gamma$  lead to the existence of an intermediate layer, of characteristic thickness  $\varepsilon$  (the representative length of the porous matrix), which allows the asymptotic matching of the free fluid with the flow in the porous body. The free fluid contains a Prandtl’s type boundary layer near  $\Gamma$  for large Reynolds number  $Re_f$  (see Figure 3). We recall that  $Re_f = L_f U_f / \nu$ ,  $L_f$  being a characteristic length of the domain  $\Omega_f$  and  $U_f$  a characteristic velocity of the fluid. The conclusion drawn is that a suitable interface condition across  $\Gamma$  is the continuity of the pressure.

In practice, however, when solving the effective equations, the boundary conditions on  $\Gamma$  are not enough to guarantee the well-posedness of the fluid problem, as opposed to the interface equations of Beavers and Joseph that yield a well-posed problem in the free fluid domain.

A first attempt toward an analytical study of the interface conditions between a free fluid and a porous medium can be found in [105]; a mathematical investigation



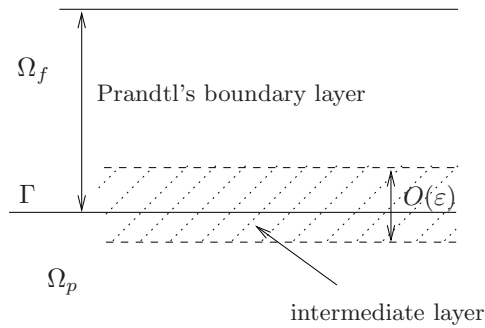


Figure 3 – The intermediate layer of thickness  $O(\varepsilon)$  and the Prandtl’s boundary layer if  $Re_f \gg 1$ .

using homogenization theory has been conducted by Jäger and Mikelić (see [83, 84, 85]). For the reader’s convenience, in Section 3.1 we briefly review their approach and the main results they achieved. This section however is not essential to understand the remaining of the paper and it might be skipped by the reader not interested in the involved mathematical details.

Notice that, strictly speaking, (3.2) is not a coupling condition in the sense that it does not relate quantities from the two subdomains  $\Omega_f$  and  $\Omega_p$ , but it is actually a boundary condition on  $\Gamma$  for the fluid problem. Moreover, neglecting the term  $O(\sqrt{K})$ , we can rewrite (3.2) as

$$\sqrt{K} \cdot \boldsymbol{\tau}_j \cdot \partial_n \mathbf{u}_f = \alpha_{BJ} \mathbf{u}_f \cdot \boldsymbol{\tau}_j. \tag{3.3}$$

Since  $K \propto \varepsilon^2$ , we can see that the term involving the normal derivative of  $\mathbf{u}_f$  is multiplied by  $\varepsilon$ . Since the velocity itself can be supposed at least of order  $O(\varepsilon)$  in the neighborhood of  $\Gamma$ , the left-hand term in (3.3) might be neglected in first approximation.

We point out that the conditions studied by Jäger and Mikelić have been adopted also in [88, 113, 40].

Finally, let us remark that the condition  $\boldsymbol{\tau}_j \cdot \partial_n \mathbf{u}_f = 0$  can be regarded as a simplified form of (3.3). In fact, although not completely justified from the physical point of view, it is perfectly acceptable from the mathematical viewpoint since it allows to write a well-posed problem for the fluid part, and, in this sense, it could be adopted as well.

As concerns the condition of the balance of pressures across the interface, a common choice (see, e.g., [53, 75, 88]) reads

$$-\mathbf{n} \cdot \mathbb{T}(\mathbf{u}_f, p_f) \cdot \mathbf{n} = g\varphi \quad \text{on } \Gamma. \tag{3.4}$$

This condition, which actually allows the pressure to be discontinuous across  $\Gamma$ , is well-suited for the analysis of the coupled fluid-groundwater flow problem. Indeed, it can be naturally incorporated in its weak formulation as it is a Neumann-type boundary condition on  $\Gamma$  for the Navier-Stokes equations (2.1)–(2.2). We will show it in details in Section 4. Let us notice that if one adopted the divergence form of the Navier-Stokes momentum equation:

$$\partial_t \mathbf{u}_f - \nabla \cdot \mathbb{T}(\mathbf{u}_f, p_f) + \nabla \cdot (\mathbf{u}_f \mathbf{u}_f^T) = \mathbf{f} \quad \text{in } \Omega_f,$$

then, (3.4) should be replaced by the following one (see [75])

$$-\mathbf{n} \cdot \mathbb{T}(\mathbf{u}_f, p_f) \cdot \mathbf{n} + \frac{1}{2}(\mathbf{u}_f \cdot \mathbf{u}_f) = g\varphi \quad \text{on } \Gamma, \tag{3.5}$$

that is, pressure  $p_f$  in (3.4) has to be replaced by the total pressure  $p_f + \frac{1}{2}|\mathbf{u}_f|^2$  in (3.5).

At the end of this section, let us write the coupled Navier-Stokes/Darcy model:

$$\begin{aligned} \partial_t \mathbf{u}_f - \nabla \cdot \mathbb{T}(\mathbf{u}_f, p_f) + (\mathbf{u}_f \cdot \nabla) \mathbf{u}_f &= \mathbf{f} & \text{in } \Omega_f, \\ \nabla \cdot \mathbf{u}_f &= 0 & \text{in } \Omega_f, \end{aligned} \tag{3.6}$$

$$\mathbf{u}_p = -\mathbf{K} \nabla \varphi \quad \text{in } \Omega_p, \tag{3.7}$$

$$\nabla \cdot \mathbf{u}_p = 0 \quad \text{in } \Omega_p, \tag{3.8}$$

$$\mathbf{u}_f \cdot \mathbf{n} = \mathbf{u}_p \cdot \mathbf{n} \quad \text{on } \Gamma, \tag{3.9}$$

$$-\mathbf{n} \cdot \mathbb{T}(\mathbf{u}_f, p_f) \cdot \mathbf{n} = g\varphi \quad \text{on } \Gamma, \tag{3.10}$$

$$\frac{\nu \alpha_{BJ}}{\sqrt{\mathbf{K}}} \mathbf{u}_f \cdot \boldsymbol{\tau}_j - \boldsymbol{\tau}_j \cdot \mathbb{T}(\mathbf{u}_f, p_f) \cdot \mathbf{n} = 0 \quad \text{on } \Gamma. \tag{3.11}$$

Moreover, let us point out that using Darcy’s law we can rewrite the system (2.5)–(2.6) as an elliptic equation for the scalar unknown  $\varphi$ :

$$-\nabla \cdot (\mathbf{K} \nabla \varphi) = 0 \quad \text{in } \Omega_p. \tag{3.12}$$

In this case, the differential formulation of the coupled Navier-Stokes/Darcy problem becomes:

$$\partial_t \mathbf{u}_f - \nabla \cdot \mathbb{T}(\mathbf{u}_f, p_f) + (\mathbf{u}_f \cdot \nabla) \mathbf{u}_f = \mathbf{f} \quad \text{in } \Omega_f, \tag{3.13}$$

$$\nabla \cdot \mathbf{u}_f = 0 \quad \text{in } \Omega_f \tag{3.14}$$

$$-\nabla \cdot (\mathbf{K} \nabla \varphi) = 0 \quad \text{in } \Omega_p, \tag{3.15}$$

with the interface conditions on  $\Gamma$ :

$$\mathbf{u}_f \cdot \mathbf{n} = -\mathbf{K} \partial_n \varphi, \tag{3.16}$$

$$-\mathbf{n} \cdot \mathbb{T}(\mathbf{u}_f, p_f) \cdot \mathbf{n} = g\varphi, \tag{3.17}$$

$$\frac{\nu \alpha_{BJ}}{\sqrt{\mathbf{K}}} \mathbf{u}_f \cdot \boldsymbol{\tau}_j - \boldsymbol{\tau}_j \cdot \mathbb{T}(\mathbf{u}_f, p_f) \cdot \mathbf{n} = 0. \tag{3.18}$$

The global problem is then non-linear. A linearization can be obtained by replacing the Navier-Stokes momentum equation (3.13) with the Stokes one:

$$\partial_t \mathbf{u}_f - \nabla \cdot \mathbb{T}(\mathbf{u}_f, p_f) = \mathbf{f} \quad \text{in } \Omega_f, \tag{3.19}$$

i.e., dropping the non-linear convective terms. This replacement is justified when the Reynolds number  $Re_f$  of the fluid is low, i.e., in case of slow motion of fluids with high viscosity. This linearized problem is also interesting since a steady Stokes problem can be generated when considering a semi-implicit time advancement of the Navier-Stokes equations where all terms but the non-linear convective one have been dealt with implicitly.

**3.1. Mathematical derivation of the law of Beavers, Joseph and Saffman via homogenization**

To derive the law of Beavers, Joseph and Saffman, Jäger and Mikelić [84] proceed as follows. Consider a porous medium containing a large number of periodically distributed channels of characteristic size  $\varepsilon$  much smaller than the characteristic length  $L_p$  of the porous domain, as represented in Figure 4.

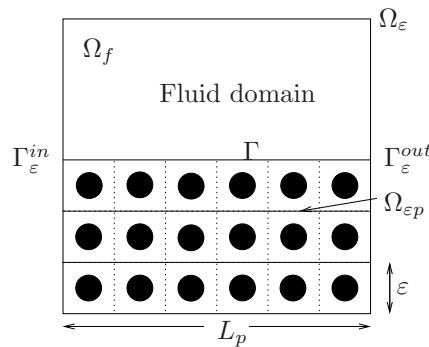


Figure 4 – Schematic representation of the domain  $\Omega_\varepsilon$ , with porous matrix of width  $\varepsilon$  and characteristic length  $L_p$ .

Then, mimicking the experimental setting of Beavers and Joseph, consider a uniform pressure gradient in the longitudinal direction of  $\Omega_\varepsilon = \Omega_f \cup \Gamma \cup \Omega_{\varepsilon p} \subset \mathbb{R}^2$ : For a fixed  $\varepsilon > 0$ , let  $\mathbf{u}^\varepsilon$  and  $p^\varepsilon$  represent the solution of the homogeneous Navier-Stokes equations:

$$\begin{aligned} -\nu \Delta \mathbf{u}^\varepsilon + (\mathbf{u}^\varepsilon \cdot \nabla) \mathbf{u}^\varepsilon + \nabla p^\varepsilon &= \mathbf{0} \quad \text{in } \Omega_\varepsilon, \\ \nabla \cdot \mathbf{u}^\varepsilon &= 0 \quad \text{in } \Omega_\varepsilon, \end{aligned}$$

with

$$p^\varepsilon = p_0 \text{ on } \Gamma_\varepsilon^{in} \quad \text{and} \quad p^\varepsilon = p_b \text{ on } \Gamma_\varepsilon^{out},$$

and homogeneous boundary conditions on the velocity (see [84]).

*Remark 3.1.* Adopting the Navier-Stokes equations not only in  $\Omega_f$  but also in  $\Omega_{\varepsilon p}$  is motivated by the fact that Darcy's law can be obtained from the (Navier-)Stokes equations through homogenization, at least in the interior of  $\Omega_{\varepsilon p}$ . A proof can be found, e.g., in [117] where it is shown that the sequences of functions (depending on  $\varepsilon$ )  $\mathbf{u}^\varepsilon$  and  $p^\varepsilon$  in  $\Omega_{\varepsilon p}$  which satisfy the Stokes equations

$$\begin{aligned} -\Delta \mathbf{u}^\varepsilon + \nabla p^\varepsilon &= \mathbf{f} && \text{in } \Omega_{\varepsilon p}, \\ \nabla \cdot \mathbf{u}^\varepsilon &= 0 && \text{in } \Omega_{\varepsilon p}, \\ \mathbf{u}^\varepsilon &= \mathbf{0} && \text{on } \partial\Omega_{\varepsilon p}, \end{aligned}$$

tend to the asymptotic velocity  $\mathbf{u}_p^0$  and pressure  $p_p^0$ :

$$\begin{aligned} \frac{\mathbf{u}^\varepsilon}{\varepsilon^2} &\rightharpoonup \mathbf{u}_p^0 && \text{weakly in } L^2(\Omega_p), \\ p^\varepsilon &\rightarrow p_p^0 && \text{strongly in } L^2(\Omega_p), \end{aligned}$$

where  $\mathbf{u}_p^0$  and  $p_p^0$  satisfy the boundary value problem

$$\begin{aligned} \mathbf{u}_p^0 &= -\mathbf{K}(\nabla p_p^0 - \mathbf{f}) && \text{in } \Omega_p, \\ \nabla \cdot \mathbf{u}_p^0 &= 0 && \text{in } \Omega_p, \\ \mathbf{u}_p^0 \cdot \mathbf{n}_p &= 0 && \text{on } \partial\Omega_p. \end{aligned}$$

From the convergence proof it can be seen that  $\mathbf{K} \propto \varepsilon^2/\nu$ .

Jäger and Mikelić proved that, consistently with the considerations by Ene and Sánchez-Palencia, the velocity field is of order  $O(1)$  in  $\Omega_f$ , of order  $O(\varepsilon^2)$  in  $\Omega_{\varepsilon p}$ , and that there is a boundary layer of thickness  $O(\varepsilon)$  for the velocity at the interface, while the pressure fields are of order  $O(1)$  in both media. In particular, the effective velocity field in  $\Omega_f$  is described by the solution  $\mathbf{u}_f^0$  of Stokes equations with the no-slip condition  $\mathbf{u}_f^0 = \mathbf{0}$  on  $\Gamma$ , giving an  $L^2$ -approximation of order  $O(\varepsilon)$  for the velocity  $\mathbf{u}^\varepsilon$ .

However, since this approximation is too rough as it cannot account for the velocity in the porous medium which is  $O(\varepsilon^2)$ , in [84] higher order terms in  $\varepsilon$  are considered for the velocity, introducing a boundary layer problem across  $\Gamma$  whose solution decays exponentially away from  $\Gamma$  and which accounts for the shear effects near the interface.

This correction yields the following interface conditions for the macroscale problem:

$$\mathbf{u}_f \cdot \boldsymbol{\tau}_j - \varepsilon C_1^{bl} \boldsymbol{\tau}_j \cdot \partial_n \mathbf{u}_f = 0 \quad \text{on } \Gamma \tag{3.20}$$

and

$$p_p = p_f - \nu C_2^{bl} \mathbf{n} \cdot \partial_n \mathbf{u}_f \quad \text{on } \Gamma, \tag{3.21}$$

where  $C_1^{bl}$  and  $C_2^{bl}$  ( $bl$  stands for boundary layer) are two suitable positive constants.

Finally, the following estimates hold (see [84]):

$$\begin{aligned} \|\nabla(\mathbf{u}^\varepsilon - \mathbf{u}_f)\|_{L^1(\Omega_f)} &\leq C\varepsilon|\log \varepsilon|, \\ \|\mathbf{u}^\varepsilon - \mathbf{u}_f\|_{H^{1/2-\gamma}(\Omega_f)} &\leq C'\varepsilon^{3/2}|\log \varepsilon|, \end{aligned}$$

where  $0 < \gamma < 1/2$  (the log term being due to the presence of corners in the domain).

Notice that (3.20) is exactly Saffman’s modification of Beavers and Joseph’s law with  $\sqrt{K}/\alpha_{BJ} = \varepsilon C_1^{bl}$ , while condition (3.21) shows that, somehow contrary to intuition, the effective pressure in the system free flow/porous medium is not necessarily continuous and, therefore this contradicts the continuity assumption of Sánchez-Palencia [66, 89].

As for the quantitative value of the constants  $C_1^{bl}$ ,  $C_2^{bl}$ , the latter have been computed for some configurations of porous media; on the base of the results reported in [85], it may be speculated that  $C_1^{bl}, C_2^{bl} \sim 1$ . In the computations that are presented in this paper we have actually set  $C_1^{bl} = \alpha_{BJ}$  and  $C_2^{bl} = 1$ .

#### 4. Weak formulation and analysis

From now on, we focus on the coupled problem (3.13)–(3.18), however we consider the steady Navier-Stokes problem by dropping the time-derivative in the momentum equation (3.13):

$$-\nabla \cdot \mathbb{T}(\mathbf{u}_f, p_f) + (\mathbf{u}_f \cdot \nabla)\mathbf{u}_f = \mathbf{f} \quad \text{in } \Omega_f. \tag{4.1}$$

A similar kind of “steady” problem can be found when using an implicit time-advancing scheme on the time-dependent problem (3.13). In that case, however, an extra reaction term  $\alpha\mathbf{u}_f$  would show up on the left-hand side of (4.1), where the positive coefficient  $\alpha$  plays the role of inverse of the time-step. This reaction term would not affect our forthcoming analysis, though.

Let us discuss now about possible boundary conditions to be prescribed on the external boundary of  $\Omega_f$  and  $\Omega_p$ .

We split the boundaries  $\partial\Omega_f$  and  $\partial\Omega_p$  of  $\Omega_f$  and  $\Omega_p$  as  $\partial\Omega_f = \Gamma \cup \Gamma_f^1 \cup \Gamma_f^2 \cup \Gamma_f^3$  and  $\partial\Omega_p = \Gamma \cup \Gamma_p \cup \Gamma_p^b$ , as shown in Figure 1, left.

For the Darcy equation we assign the piezometric head  $\varphi = \varphi_p$  on  $\Gamma_p$ ; moreover, we require that the normal component of the velocity vanishes on the bottom surface, that is,  $\mathbf{u}_p \cdot \mathbf{n}_p = 0$  on  $\Gamma_p^b$ .

For the Navier-Stokes problem, several combinations of boundary conditions could be considered, representing different kinds of flow problems; we indicate some of them.

A first possibility is to assign the velocity vector  $\mathbf{u}_f = \mathbf{0}$  on  $\Gamma_f^1 \cup \Gamma_f^3$  and a natural boundary condition  $\mathbb{T}(\mathbf{u}_f, p_f) \cdot \mathbf{n}_f = \mathbf{g}$  on  $\Gamma_f^2$  (a fictitious boundary), where  $\mathbf{g}$  is a given vector function, representing the flux across  $\Gamma_f^2$  of the fluid column standing above.

Alternatively, we can prescribe a non-null inflow  $\mathbf{u}_f = \mathbf{u}_{in}$  on the left-hand boundary  $\Gamma_f^1$ , a slip condition  $\mathbf{u}_f \cdot \mathbf{n}_f = 0$  and  $\boldsymbol{\tau}_i \cdot \mathbf{T}(\mathbf{u}_f, p_f) \cdot \mathbf{n}_f = 0$  on  $\Gamma_f^2$  and an outflow condition  $\mathbf{T}(\mathbf{u}_f, p_f) \cdot \mathbf{n}_f = 0$  on the right-hand boundary  $\Gamma_f^3$  which describes a free outflow or a free stress at the outflow boundary.

A third possibility consists of assigning again a non-null inflow  $\mathbf{u}_f = \mathbf{u}_{in}$  on the left-hand boundary  $\Gamma_f^1$  and a no-slip condition  $\mathbf{u}_f = \mathbf{0}$  on the remaining boundary  $\Gamma_f^2 \cup \Gamma_f^3$ .

Our analysis considers the last choice we have indicated, but it can be modified to accommodate the other boundary conditions as well. From now on, we denote  $\Gamma_f^1$  as  $\Gamma_f^{in}$  (standing for  $\Gamma_f^{inflow}$ ) and the remaining boundary  $\Gamma_f^2 \cup \Gamma_f^3$  simply by  $\Gamma_f$ . Thus, we supplement the coupled problem (3.13)–(3.18) with the boundary conditions:

$$\mathbf{u}_f = \mathbf{u}_{in} \quad \text{on } \Gamma_f^{in}, \tag{4.2}$$

$$\mathbf{u}_f = \mathbf{0} \quad \text{on } \Gamma_f,$$

$$\varphi = \varphi_p \quad \text{on } \Gamma_p,$$

$$\mathbb{K} \partial_n \varphi = 0 \quad \text{on } \Gamma_p^b. \tag{4.3}$$

We introduce the following functional spaces:

$$H_{\Gamma_f} = \{v \in H^1(\Omega_f) : v = 0 \text{ on } \Gamma_f\},$$

$$H_{\Gamma_f \cup \Gamma_f^{in}} = \{v \in H_{\Gamma_f} : v = 0 \text{ on } \Gamma_f^{in}\}, \quad H_f = (H_{\Gamma_f \cup \Gamma_f^{in}})^d,$$

$$H_f^0 = \{\mathbf{v} \in H_f : \mathbf{v} \cdot \mathbf{n}_f = 0 \text{ on } \Gamma\},$$

$$\widetilde{H}_f = \{\mathbf{v} \in (H^1(\Omega_f))^d : \mathbf{v} = \mathbf{0} \text{ on } \Gamma_f \cup \Gamma\},$$

$$Q = L^2(\Omega_f), \quad Q_0 = \{q \in Q : \int_{\Omega_f} q = 0\},$$

$$H_p = \{\psi \in H^1(\Omega_p) : \psi = 0 \text{ on } \Gamma_p\}, \quad H_p^0 = \{\psi \in H_p : \psi = 0 \text{ on } \Gamma\}.$$

We denote by  $|\cdot|_1$  and  $\|\cdot\|_1$  the  $H^1$ -seminorm and norm, respectively, and by  $\|\cdot\|_0$  the  $L^2$ -norm; it will always be clear from the context whether we are referring to spaces on  $\Omega_f$  or  $\Omega_p$ .

The space  $W = H_f \times H_p$  is a Hilbert space with norm

$$\|\underline{\mathbf{w}}\|_W = (\|\mathbf{w}\|_1^2 + \|\psi\|_1^2)^{1/2} \quad \forall \underline{\mathbf{w}} = (\mathbf{w}, \psi) \in W.$$

Finally, we consider on  $\Gamma$  the trace space  $\Lambda = H_{00}^{1/2}(\Gamma)$  and denote its norm by  $\|\cdot\|_\Lambda$  (see [90]).

We introduce a continuous extension operator

$$E_f : (H^{1/2}(\Gamma_f^{in}))^d \rightarrow \widetilde{H}_f. \tag{4.4}$$

Then  $\forall \mathbf{u}_{in} \in (H_{00}^{1/2}(\Gamma_f^{in}))^d$  we can construct a vector function  $E_f \mathbf{u}_{in} \in \widetilde{H}_f$  such that  $E_f \mathbf{u}_{in}|_{\Gamma_f^{in}} = \mathbf{u}_{in}$ .

*Remark 4.1.* Alternatively, we could consider a divergence free extension  $\widetilde{E}_f \mathbf{u}_{in}$  of  $\mathbf{u}_{in}$ . To this aim, let  $\mathcal{E}_f \mathbf{u}_{in} \in (H_{\Gamma_f})^d$  such that  $\mathcal{E}_f \mathbf{u}_{in} = \mathbf{u}_{in}$  on  $\Gamma_f^{in}$ . Then, we construct a function  $\mathbf{w}_{in}$  which is the solution of the following problem: find  $\mathbf{w}_{in} \in H_f$  such that for all  $q \in Q$

$$-\int_{\Omega_f} q \nabla \cdot \mathbf{w}_{in} = \int_{\Omega_f} q \nabla \cdot (\mathcal{E}_f \mathbf{u}_{in}) . \tag{4.5}$$

The solvability of (4.5) is guaranteed by the inf-sup condition: there exists a constant  $\beta^* > 0$  such that

$$\forall q \in Q \quad \exists \mathbf{v} \in H_f, \mathbf{v} \neq \mathbf{0} : \quad -\int_{\Omega_f} q \nabla \cdot \mathbf{v} \geq \beta \|\mathbf{v}\|_1 \|q\|_0 \tag{4.6}$$

(see, e.g., [110, pages 157–158]). Finally, we indicate by  $\widetilde{E}_f \mathbf{u}_{in} = \mathcal{E}_f \mathbf{u}_{in} + \mathbf{w}_{in}$  the divergence-free extension of  $\mathbf{u}_{in}$ . We remark that  $\widetilde{E}_f \mathbf{u}_{in} = \mathbf{u}_{in}$  on  $\Gamma_f^{in}$ ,  $\widetilde{E}_f \mathbf{u}_{in} = \mathbf{0}$  on  $\Gamma_f$  and that, thanks to (4.5), it holds

$$\int_{\Omega_f} q \nabla \cdot (\widetilde{E}_f \mathbf{u}_{in}) = 0, \quad \forall q \in Q .$$

We point out that the extension  $\widetilde{E}_f \mathbf{u}_{in}$  cannot satisfy the additional constraint  $\widetilde{E}_f \mathbf{u}_{in} \cdot \mathbf{n}_f = 0$  on  $\Gamma$ , except for the special case of  $\mathbf{u}_{in}$  such that  $\int_{\Gamma_f^{in}} \mathbf{u}_{in} \cdot \mathbf{n}_f = 0$ .

We introduce another continuous extension operator:

$$E_p : H^{1/2}(\Gamma_p^b) \rightarrow H^1(\Omega_p) \quad \text{such that } E_p \varphi_p = 0 \text{ on } \Gamma .$$

Then, for all  $\varphi \in H^1(\Omega_p)$  we define the function  $\varphi_0 = \varphi - E_p \varphi_p$ .

Finally, we define the following bilinear forms:

$$\begin{aligned} a_f(\mathbf{v}, \mathbf{w}) &= \int_{\Omega_f} \frac{\nu}{2} (\nabla \mathbf{v} + \nabla^T \mathbf{v}) \cdot (\nabla \mathbf{w} + \nabla^T \mathbf{w}) \quad \forall \mathbf{v}, \mathbf{w} \in (H^1(\Omega_f))^d, \\ b_f(\mathbf{v}, q) &= -\int_{\Omega_f} q \nabla \cdot \mathbf{v} \quad \forall \mathbf{v} \in (H^1(\Omega_f))^d, \quad \forall q \in Q, \\ a_p(\varphi, \psi) &= \int_{\Omega_p} \nabla \psi \cdot \mathbb{K} \nabla \varphi \quad \forall \varphi, \psi \in H^1(\Omega_p), \end{aligned}$$

and, for all  $\mathbf{v}, \mathbf{w}, \mathbf{z} \in (H^1(\Omega_f))^d$ , the trilinear form

$$c_f(\mathbf{w}; \mathbf{z}, \mathbf{v}) = \int_{\Omega_f} [(\mathbf{w} \cdot \nabla) \mathbf{z}] \cdot \mathbf{v} = \sum_{i,j=1}^d \int_{\Omega_f} w_j \frac{\partial z_i}{\partial x_j} v_i .$$

Now, if we multiply (4.1) by  $\mathbf{v} \in H_f$  and integrate by parts we obtain

$$a_f(\mathbf{u}_f, \mathbf{v}) + c_f(\mathbf{u}_f; \mathbf{u}_f, \mathbf{v}) + b_f(\mathbf{v}, p_f) - \int_{\Gamma} \mathbf{n} \cdot \mathbb{T}(\mathbf{u}_f, p_f) \mathbf{v} = \int_{\Omega_f} \mathbf{f} \mathbf{v}.$$

Notice that we can write

$$- \int_{\Gamma} \mathbf{n} \cdot \mathbb{T}(\mathbf{u}_f, p_f) \mathbf{v} = - \int_{\Gamma} [\mathbf{n} \cdot \mathbb{T}(\mathbf{u}_f, p_f) \cdot \mathbf{n}] \mathbf{v} \cdot \mathbf{n} - \int_{\Gamma} \sum_{j=1}^{d-1} [\mathbf{n} \cdot \mathbb{T}(\mathbf{u}_f, p_f) \cdot \boldsymbol{\tau}_j] \mathbf{v} \cdot \boldsymbol{\tau}_j,$$

so that we can incorporate in weak form the interface conditions (3.17) and (3.18) as follows:

$$- \int_{\Gamma} \mathbf{n} \cdot \mathbb{T}(\mathbf{u}_f, p_f) \mathbf{v} = \int_{\Gamma} g\varphi(\mathbf{v} \cdot \mathbf{n}) + \int_{\Gamma} \sum_{j=1}^{d-1} \frac{\nu\alpha_{BJ}}{\sqrt{K}} (\mathbf{u}_f \cdot \boldsymbol{\tau}_j) (\mathbf{v} \cdot \boldsymbol{\tau}_j).$$

Finally, we consider the lifting  $E_f \mathbf{u}_{in}$  of the boundary datum and we split  $\mathbf{u}_f = \mathbf{u}_f^0 + E_f \mathbf{u}_{in}$  with  $\mathbf{u}_f^0 \in H_f$ ; we recall that  $E_f \mathbf{u}_{in} = 0$  on  $\Gamma$  and we get

$$a_f(\mathbf{u}_f^0, \mathbf{v}) + c_f(\mathbf{u}_f^0 + E_f \mathbf{u}_{in}; \mathbf{u}_f^0 + E_f \mathbf{u}_{in}, \mathbf{v}) + b_f(\mathbf{v}, p_f) + \int_{\Gamma} g\varphi(\mathbf{v} \cdot \mathbf{n}) + \int_{\Gamma} \sum_{j=1}^{d-1} \frac{\nu\alpha_{BJ}}{\sqrt{K}} (\mathbf{u}_f \cdot \boldsymbol{\tau}_j) (\mathbf{v} \cdot \boldsymbol{\tau}_j) = \int_{\Omega_f} \mathbf{f} \mathbf{v} - a_f(E_f \mathbf{u}_{in}, \mathbf{v}). \quad (4.7)$$

From (3.14) we find

$$b_f(\mathbf{u}_f^0, q) = -b_f(E_f \mathbf{u}_{in}, q) \quad \forall q \in Q. \quad (4.8)$$

On the other hand, if we multiply (3.15) by  $\psi \in H_p$  and integrate by parts we get

$$a_p(\varphi, \psi) + \int_{\Gamma} K \partial_n \varphi \psi = 0.$$

Now we incorporate the interface condition (3.16) in weak form as

$$a_p(\varphi, \psi) - \int_{\Gamma} (\mathbf{u}_f \cdot \mathbf{n}) \psi = 0,$$

and, considering the splitting  $\varphi = \varphi_0 + E_p \varphi_p$  we obtain

$$a_p(\varphi_0, \psi) - \int_{\Gamma} (\mathbf{u}_f \cdot \mathbf{n}) \psi = -a_p(E_p \varphi_p, \psi). \quad (4.9)$$



We multiply (4.9) by  $g$  and sum to (4.7) and (4.8). Then, we define

$$\begin{aligned} \mathcal{A}(\underline{v}, \underline{w}) &= a_f(\mathbf{v}, \mathbf{w}) + g a_p(\varphi, \psi) + \int_{\Gamma} g \varphi(\mathbf{w} \cdot \mathbf{n}) - \int_{\Gamma} g \psi(\mathbf{v} \cdot \mathbf{n}) \\ &\quad + \int_{\Gamma} \sum_{j=1}^{d-1} \frac{\nu \alpha_{BJ}}{\sqrt{K}} (\mathbf{w} \cdot \boldsymbol{\tau}_j)(\mathbf{v} \cdot \boldsymbol{\tau}_j), \\ \mathcal{C}(\underline{v}; \underline{w}, \underline{u}) &= c_f(\mathbf{v}; \mathbf{w}, \mathbf{u}), \\ \mathcal{B}(\underline{w}, q) &= b_f(\mathbf{w}, q), \end{aligned}$$

for all  $\underline{v} = (\mathbf{v}, \varphi)$ ,  $\underline{w} = (\mathbf{w}, \psi)$ ,  $\underline{u} = (\mathbf{u}, \xi) \in W$ ,  $q \in Q$ . Finally, we define the following linear functionals:

$$\begin{aligned} \langle \mathcal{F}, \underline{w} \rangle &= \int_{\Omega_f} \mathbf{f} \cdot \mathbf{w} - a_f(E_f \mathbf{u}_{in}, \mathbf{w}) - g a_p(E_p \varphi_p, \psi), \\ \langle \mathcal{G}, q \rangle &= -b_f(E_f \mathbf{u}_{in}, q), \end{aligned} \tag{4.10}$$

for all  $\underline{w} = (\mathbf{w}, \psi) \in W$ ,  $q \in Q$ .

Adopting these notations, the weak formulation of the coupled Navier-Stokes/Darcy problem reads:

find  $\underline{u} = (\mathbf{u}_f^0, \varphi_0) \in W$ ,  $p_f \in Q$  such that

$$\mathcal{A}(\underline{u}, \underline{v}) + \mathcal{C}(\underline{u} + \underline{u}^*; \underline{u} + \underline{u}^*, \underline{v}) + \mathcal{B}(\underline{v}, p_f) = \langle \mathcal{F}, \underline{v} \rangle \quad \forall \underline{v} = (\mathbf{v}, \psi) \in W, \tag{4.11}$$

$$\mathcal{B}(\underline{u}, q) = \langle \mathcal{G}, q \rangle \quad \forall q \in Q, \tag{4.12}$$

with  $\underline{u}^* = (E_f \mathbf{u}_{in}, 0) \in \widetilde{H}_f \times H^1(\Omega_p)$ .

Remark that the interface conditions (3.16)–(3.18) have been incorporated in the above weak model as natural conditions on  $\Gamma$ . In particular, (3.17) and (3.18) are natural conditions for the Navier-Stokes problem, while (3.16) becomes a natural condition for Darcy’s problem.

#### 4.1. Analysis of the linear coupled Stokes/Darcy problem

In this section we consider the analysis of the coupled problem where we replace the Navier-Stokes equations by the Stokes equations, i.e., we neglect the non-linear convective term. The weak formulation of the Stokes/Darcy problem can be obtained straightforwardly from (4.11)–(4.12) dropping the trilinear form  $\mathcal{C}(\cdot; \cdot, \cdot)$ . Thus, we have:

find  $\underline{u} = (\mathbf{u}_f^0, \varphi_0) \in W$ ,  $p_f \in Q$  such that

$$\mathcal{A}(\underline{u}, \underline{v}) + \mathcal{B}(\underline{v}, p_f) = \langle \mathcal{F}, \underline{v} \rangle \quad \forall \underline{v} = (\mathbf{v}, \psi) \in W, \tag{4.13}$$

$$\mathcal{B}(\underline{u}, q) = \langle \mathcal{G}, q \rangle \quad \forall q \in Q. \tag{4.14}$$

In order to prove existence and uniqueness for the solution of the Stokes/Darcy coupled problem, we introduce some preliminary results on the properties of the bilinear forms  $\mathcal{A}$  and  $\mathcal{B}$  and of the functional  $\mathcal{F}$ .

**Lemma 4.2.** *The following results hold:*

- (i)  $\mathcal{A}(\cdot, \cdot)$  is continuous and coercive on  $W$  and, in particular, it is coercive on the kernel of  $\mathcal{B}$

$$W^0 = \{\underline{v} \in W : \mathcal{B}(\underline{v}, q) = 0, \forall q \in Q\};$$

- (ii)  $\mathcal{B}(\cdot, \cdot)$  is continuous on  $W \times Q$  and satisfies the following inf-sup condition: there exists a positive constant  $\beta > 0$  such that

$$\forall q \in Q \quad \exists \underline{w} \in W, \underline{w} \neq (0, 0) : \mathcal{B}(\underline{w}, q) \geq \beta \|\underline{w}\|_W \|q\|_0. \tag{4.15}$$

- (iii)  $\mathcal{F}$  is a continuous linear functional on  $W$ .

- (iv)  $\mathcal{G}$  is a continuous linear functional on  $Q$ .

*Proof.*

- (i) The following trace inequalities hold (see [90]):

$$\exists C_f > 0 \quad \text{such that} \quad \|\mathbf{v}_\Gamma\|_\Lambda \leq C_f \|\mathbf{v}\|_1 \quad \forall \mathbf{v} \in H_f; \tag{4.16}$$

$$\exists C_p > 0 \quad \text{such that} \quad \|\psi_\Gamma\|_\Lambda \leq C_p \|\psi\|_1 \quad \forall \psi \in H_p. \tag{4.17}$$

Thanks to the Cauchy–Schwarz inequality and the above trace inequalities the continuity of  $\mathcal{A}(\cdot, \cdot)$  follows:

$$\begin{aligned} |\mathcal{A}(\underline{v}, \underline{w})| &\leq 2\nu \|\mathbf{v}\|_1 \|\mathbf{w}\|_1 + g \max_j \|\mathbf{K}_j\|_\infty \|\psi\|_1 \|\varphi\|_1 \\ &\quad + g C_f C_p \|\varphi\|_1 \|\mathbf{w}\|_1 + g C_f C_p \|\psi\|_1 \|\mathbf{v}\|_1 \\ &\quad + (d-1)(\nu \alpha_{BJ} / \sqrt{\mathbf{K}}) C_f^2 \|\mathbf{v}\|_1 \|\mathbf{w}\|_1. \end{aligned}$$

We define

$$\gamma = \max\{\gamma_1, \gamma_2\}, \tag{4.18}$$

where

$$\begin{aligned} \gamma_1 &= \max\{2\nu + (d-1)C_f^2(\nu \alpha_{BJ} / \sqrt{\mathbf{K}}), g C_f C_p\}, \\ \gamma_2 &= \max\{g \max_j \|\mathbf{K}_j\|_\infty, g C_f C_p\}, \end{aligned}$$

so that

$$|\mathcal{A}(\underline{v}, \underline{w})| \leq \gamma (\|\mathbf{v}\|_1 + \|\varphi\|_1) (\|\mathbf{w}\|_1 + \|\psi\|_1) \leq 2\gamma \|\underline{v}\|_W \|\underline{w}\|_W,$$

which follows from the inequality  $(x + y) \leq \sqrt{2}(x^2 + y^2)^{1/2}$ ,  $\forall x, y \in \mathbb{R}^+$ .

The coercivity is a consequence of the Korn inequality (see, e.g., [51, page 416] or [110, page 149]):  $\forall \mathbf{v} = (v_1, \dots, v_d) \in H_f$

$$\exists \kappa_f > 0 \quad \text{such that} \quad \int_{\Omega_f} \sum_{j,l=1}^d (\partial_l v_j + \partial_j v_l)^2 \geq \kappa_f \|\mathbf{v}\|_1^2, \tag{4.19}$$

and the Poincaré inequality (see [90] and [109, page 11]):

$$\exists C_{\Omega_p} > 0 \quad \text{such that} \quad \|\psi\|_0^2 \leq C_{\Omega_p} \|\nabla \psi\|_0^2 \quad \forall \psi \in H_p.$$

In fact we have for all  $\underline{v} = (\mathbf{v}, \varphi) \in W$ ,

$$\begin{aligned} \mathcal{A}(\underline{v}, \underline{v}) &= a_f(\mathbf{v}, \mathbf{v}) + g a_p(\varphi, \varphi) + \int_{\Gamma} \sum_j^{d-1} \frac{\nu \alpha_{BJ}}{\sqrt{K}} (\mathbf{v} \cdot \boldsymbol{\tau}_j)^2 \\ &\geq a_f(\mathbf{v}, \mathbf{v}) + g a_p(\varphi, \varphi) \\ &\geq \nu \kappa_f \|\mathbf{v}\|_1^2 + g m_K \min(1, C_{\Omega_p}^{-1}) \|\varphi\|_1^2 \geq \alpha \|\underline{v}\|_W^2, \end{aligned}$$

where

$$\alpha = \min\{\nu \kappa_f, g m_K \min(1, C_{\Omega_p}^{-1})\}, \tag{4.20}$$

with  $m_K = \min_{i=1, \dots, d} \inf_{\mathbf{x} \in \Omega_p} K_i(\mathbf{x}) > 0$ . Finally, since  $W^0 \subset W$ , the thesis follows.

(ii) Concerning the continuity, thanks to the Cauchy–Schwarz inequality, we have

$$|\mathcal{B}(\underline{w}, q)| \leq \|q\|_0 \|\underline{w}\|_W \quad \forall \underline{w} \in W, q \in Q.$$

Moreover, thanks to (4.6), there exists a constant  $\beta_* > 0$  such that

$$\forall q \in Q \quad \exists \mathbf{w} \in H_f, \mathbf{w} \neq \mathbf{0} : - \int_{\Omega_f} q \nabla \cdot \mathbf{w} \geq \beta_* \|\mathbf{w}\|_1 \|q\|_0.$$

Then, considering  $\underline{w} = (\mathbf{w}, 0) \in H_f \times H_p$ , the result follows with  $\beta = \beta_* > 0$ .

(iii) Thanks to the Cauchy–Schwarz inequality and the continuity of the extension operators  $E_f$  and  $E_p$ , whose continuity constants are denoted hereafter by  $C_1$  and  $C_2$ , respectively, we have

$$\begin{aligned} |\langle \mathcal{F}, \underline{w} \rangle| &\leq \|\mathbf{f}\|_0 \|\mathbf{w}\|_1 + \nu C_1 \|\mathbf{u}_{in}\|_{H^{1/2}(\Gamma_f^{in})} \|\mathbf{w}\|_1 \\ &\quad + g \max_j \|K_j\|_{\infty} C_2 \|\psi\|_1 \|\varphi\|_{H^{1/2}(\Gamma_p^b)} \\ &\leq C_{\mathcal{F}} (\|\mathbf{w}\|_1 + \|\varphi\|_1) \leq \sqrt{2} C_{\mathcal{F}} \|\underline{w}\|_W, \end{aligned}$$

where

$$C_{\mathcal{F}} = \max\{\|\mathbf{f}\|_0 + C_1 \nu \|\mathbf{u}_{in}\|_{H^{1/2}(\Gamma_f^{in})}, g C_2 \max_j \|K_j\|_{\infty} \|\varphi_p\|_{H^{1/2}(\Gamma_p^b)}\}. \tag{4.21}$$

(iv) The continuity of the functional  $\mathcal{G}$  follows from the Cauchy-Schwarz inequality and from the continuity of the extension operator  $E_f$ ; in fact it holds:

$$|\langle \mathcal{G}, q \rangle| \leq C_G \|q\|_0, \tag{4.22}$$

with  $C_G = C_1 \|\mathbf{u}_{in}\|_{H^{1/2}(\Gamma^{in})}$ .

□

We can now prove the main result of this Section.

**Proposition 4.3.** *The Stokes/Darcy coupled problem (4.13)–(4.14) admits a unique solution  $(\mathbf{u}_f^0, p_f, \varphi_0) \in H_f \times Q \times H_p$  which satisfies the following a-priori estimates:*

$$\begin{aligned} \|(\mathbf{u}_f^0, \varphi_0)\|_W &\leq \frac{1}{\alpha} \left( \sqrt{2}C_{\mathcal{F}} + \frac{\alpha + 2\gamma}{\beta} C_G \right), \\ \|p_f\|_0 &\leq \frac{1}{\beta} \left[ \left( 1 + \frac{2\gamma}{\alpha} \right) \sqrt{2}C_{\mathcal{F}} + \frac{2\gamma(\alpha + 2\gamma)}{\alpha\beta} C_G \right], \end{aligned}$$

where  $\beta, \gamma, \alpha, C_{\mathcal{F}}$  and  $C_G$  are the constants defined in (4.15), (4.18), (4.20), (4.21) and (4.22), respectively.

*Proof.* This is a straightforward consequence of the existence and uniqueness theorem of Brezzi (see [29, 33]), whose hypotheses are satisfied thanks to Lemma 4.2. □

*Remark 4.4.* From Proposition 4.3 it follows in particular that  $-\mathcal{K}\partial_n\varphi|_{\Gamma} \in \Lambda$ , since  $\mathbf{u}_f \cdot \mathbf{n}|_{\Gamma} \in \Lambda$ . Then, on  $\Gamma$ ,  $\varphi$  has a higher regularity than one might have expected.

#### 4.2. Mixed formulation of Darcy’s equation

In the analysis presented so far we have chosen to rewrite Darcy’s equation in form of the Poisson problem (3.15). Should we keep the mixed formulation (2.5)–(2.6) a well-posedness analysis can be developed as well; we refer to [88]. In this reference a Stokes/Darcy coupling analogous to the one of Section 4.1 is considered. Still adopting the interface conditions proposed by Jäger and Mikelić, a mixed form of Darcy’s equations is used; the coupling is realized via Lagrange multipliers. In particular, the following Lagrange multiplier

$$\ell \in \Lambda, \quad \ell = -\mathbf{n} \cdot \mathbb{T}(\mathbf{u}_f, p_f) \cdot \mathbf{n} = p_p \quad \text{on } \Gamma,$$

and the dual pairing

$$b_{\Gamma} : (H_f \times X_2) \times \Lambda \rightarrow \mathbb{R}, \quad b_{\Gamma}(\underline{v}, \ell) = \langle \mathbf{v}_1 \cdot \mathbf{n} + \mathbf{v}_2 \cdot \mathbf{n}, \ell \rangle$$

are introduced, where  $X_2$  is a suitable subspace of  $H(\text{div}; \Omega_p)$  accounting for the boundary conditions and where we have denoted  $\underline{v} = (\mathbf{v}_1, \mathbf{v}_2)$ .

Then, existence and uniqueness of the solution of the following global mixed problem is proved:

find  $\underline{u} = (\mathbf{u}_f, \mathbf{u}_p) \in H_f \times X_2, \underline{p} = (p_f, p_p) \in M, \ell \in \Lambda$ :

$$a(\underline{u}, \underline{v}) + b(\underline{v}, \underline{p}) + b_\Gamma(\underline{v}, \ell) = f(\underline{v}) \quad \forall \underline{v} \in H_f \times X_2, \tag{4.23}$$

$$b(\underline{u}, \underline{q}) = g(\underline{q}) \quad \forall \underline{q} \in M, \tag{4.24}$$

$$b_\Gamma(\underline{u}, \sigma) = 0 \quad \forall \sigma \in \Lambda, f \tag{4.25}$$

with

$$a(\underline{u}, \underline{v}) = a_f(\mathbf{u}_f, \mathbf{v}_f) + \int_\Gamma \sum_{j=1}^{d-1} \frac{\nu^{\alpha_{BJ}}}{\sqrt{K}} (\mathbf{u}_f \cdot \boldsymbol{\tau}_j)(\mathbf{v}_f \cdot \boldsymbol{\tau}_j) + \int_{\Omega_p} \mathbf{K}^{-1} \mathbf{u}_p \mathbf{v}_p,$$

$$b(\underline{v}, \underline{p}) = b_f(\mathbf{v}_f, p_f) - \int_{\Omega_p} p_p \nabla \cdot \mathbf{v}_p,$$

where  $f, g$  are suitably defined linear continuous functionals. Finally,  $M$  is a subspace of  $Q \times L^2(\Omega_p)$ .

If the computational domain is such that  $\bar{\Gamma} \cap \partial\Omega = \emptyset$ , i.e., if the porous medium is entirely enclosed in the fluid region, then (4.23)–(4.25) can be equivalently restated on the subspace of  $H_f \times X_2$  with trace continuous normal velocities:

$$\{\underline{v} \in H_f \times X_2 : b_\Gamma(\underline{v}, \sigma) = 0, \forall \sigma \in \Lambda\} \subset H_f \times X_2.$$

A study of the Stokes/Darcy problem in mixed form can also be found in [69, 72]. In particular, in [69] different possible weak formulations are studied.

### 4.3. Time-dependent Stokes/Darcy model

The analysis of a time-dependent Stokes/Darcy system has been recently carried out in [43]. In particular, equation (2.6) has been replaced by the saturated flow model:

$$s\partial_t\varphi + \nabla \cdot \mathbf{u}_p = 0 \quad \text{in } \Omega_p, \tag{4.26}$$

where  $s$  denotes the mass storativity coefficient which gives the mass of water added to storage (or released from it) in the porous medium depending on the rise (or decline) of the potential  $\varphi$ . Combining (4.26) and (2.5), the following time-dependent equation for the piezometric head is obtained:

$$s\partial_t\varphi - \nabla \cdot (\mathbf{K}\nabla\varphi) = 0 \quad \text{in } \Omega_p.$$

The Beavers-Joseph condition without Saffman’s simplification is used for the coupling, i.e.,

$$-\boldsymbol{\tau}_j \cdot \mathbb{T}(\mathbf{u}_f, p_f) \cdot \mathbf{n} = \frac{\nu^{\alpha_{BJ}}}{\sqrt{K}} (\mathbf{u}_f - \mathbf{u}_p) \cdot \boldsymbol{\tau}_j \quad \text{on } \Gamma.$$

Consider now the bilinear form  $\mathcal{A}_\eta(\underline{v}, \underline{w}) : W \times W \rightarrow \mathbb{R}$ ,

$$\begin{aligned} \mathcal{A}_\eta(\underline{v}, \underline{w}) &= a_f(\mathbf{v}, \mathbf{w}) + \frac{\eta}{s} a_p(\varphi, \psi) + \int_\Gamma g \varphi(\mathbf{w} \cdot \mathbf{n}) - \frac{\eta}{s} \int_\Gamma \psi(\mathbf{v} \cdot \mathbf{n}) \\ &\quad + \int_\Gamma \sum_{j=1}^{d-1} \frac{\nu \alpha_{BJ}}{\sqrt{K}} ((\mathbf{v} + \mathbf{K} \nabla \varphi) \cdot \boldsymbol{\tau}_j)(\mathbf{w} \cdot \boldsymbol{\tau}_j), \end{aligned}$$

for all  $\underline{v} = (\mathbf{v}, \varphi)$ ,  $\underline{w} = (\mathbf{w}, \psi) \in W$ , where  $\eta$  is a suitable scaling parameter, and the following duality pairing associated with the time derivative:

$$\langle \underline{v}_t, \underline{w} \rangle = \langle \partial_t \mathbf{v}, \mathbf{w} \rangle + \eta \langle \partial_t \varphi, \psi \rangle.$$

Then, we can write the weak form of the coupled time-dependent Stokes/Darcy problem as:

find  $\underline{u} = (\mathbf{u}_f, \varphi)$  and  $p_f$  such that

$$\begin{aligned} \langle \underline{u}_t, \underline{v} \rangle + \mathcal{A}_\eta(\underline{u}, \underline{v}) + \mathcal{B}(\underline{u}, p_f) &= \langle \widetilde{\mathcal{F}}, \underline{v} \rangle & \forall \underline{v} = (\mathbf{v}, \psi) \in W, \\ \mathcal{B}(\underline{u}, q) &= 0 & \forall q \in Q, \end{aligned}$$

where  $\widetilde{\mathcal{F}}$  is a linear continuous functional defined similarly to (4.10) and  $\mathcal{B}$  is the bilinear form (4.10).

The problem is studied firstly in the steady case showing its well-posedness for small enough values of the coefficient  $\alpha_{BJ}$ . Then, a backward-Euler discretization in time is introduced and the convergence to the continuous solution as the time step tends to zero is proved. Finally, the convergence of the fully discretized system is guaranteed.

These results rely on the choice of a suitably large parameter  $\eta$ . Notice that the choice of a large rescaling parameter  $\eta$  makes sense since the flow in porous media evolves on a relatively slow time scale compared to that of the flow in the conduit, and the re-scaling essentially brings them to the same time scale.

### 5. Multi-domain formulation of the Stokes/Darcy problem

Another possible approach to study the Navier-Stokes/Darcy problem is to exploit its naturally decoupled structure keeping separated the fluid and the porous media parts and exchanging information between surface and groundwater flows only through boundary conditions at the interface. From the computational point of view, this strategy is useful at the stage of setting up effective methods to solve the problem numerically. As we shall illustrate in Section 7, a discretization of this problem using, e.g., finite elements leads to a large sparse ill-conditioned linear system which requires a suitable preconditioning strategy to be solved. We would like to exploit the intrinsic decoupled structure of the problem at hand to design an iterative procedure requiring

at each step to compute independently the solution of the fluid and of the groundwater problems.

Therefore, in the next sections we shall apply a domain decomposition technique at the differential level to study the Navier-Stokes/Darcy coupled problem. Our aim will be to introduce and analyze a generalized Steklov-Poincaré interface equation (see [110]) associated to our problem, in order to reformulate it solely in terms of interface unknowns. This re-interpretation will be crucial to set up iterative procedures between the subdomains  $\Omega_f$  and  $\Omega_p$ , that will be later replicated at the discrete level.

In this section we start by considering the Stokes/Darcy problem, while Section 6 concerns the Navier-Stokes/Darcy coupling.

The Stokes/Darcy problem can be rewritten in a multi-domain formulation and, in particular, we prove the following result.

**Proposition 5.1.** *Let  $\Lambda$  be the space of traces introduced in Section 4. Problem (4.11)–(4.12) can be reformulated in an equivalent way as follows:*

*find  $\mathbf{u}_f^0 \in H_f$ ,  $p_f \in Q$ ,  $\varphi_0 \in H_p$  such that*

$$a_f(\mathbf{u}_f^0 + E_f \mathbf{u}_{in}, \mathbf{w}) + b_f(\mathbf{w}, p_f) + \int_{\Gamma} \sum_{j=1}^{d-1} \frac{\nu \alpha_{BJ}}{\sqrt{K}} (\mathbf{u}_f^0 \cdot \boldsymbol{\tau}_j) (R_1 \mu \cdot \boldsymbol{\tau}_j) = \int_{\Omega_f} \mathbf{f} \cdot \mathbf{w} \quad \forall \mathbf{w} \in H_f^0, \tag{5.1}$$

$$b_f(\mathbf{u}_f^0 + E_f \mathbf{u}_{in}, q) = 0 \quad \forall q \in Q, \tag{5.2}$$

$$a_p(\varphi_0 + E_p \varphi_p, \psi) = 0 \quad \forall \psi \in H_p^0, \tag{5.3}$$

$$\int_{\Gamma} (\mathbf{u}_f^0 \cdot \mathbf{n}) \mu = a_p(\varphi_0 + E_p \varphi_p, R_2 \mu) \quad \forall \mu \in \Lambda, \tag{5.4}$$

$$\int_{\Gamma} g \varphi_0 \mu = \int_{\Omega_f} \mathbf{f} (R_1 \mu) - a_f(\mathbf{u}_f^0 + E_f \mathbf{u}_{in}, R_1 \mu) - b_f(R_1 \mu, p_f) - \int_{\Gamma} \sum_{j=1}^{d-1} \frac{\nu \alpha_{BJ}}{\sqrt{K}} (\mathbf{u}_f^0 \cdot \boldsymbol{\tau}_j) (R_1 \mu \cdot \boldsymbol{\tau}_j) \quad \forall \mu \in \Lambda, \tag{5.5}$$

where  $R_1$  is any possible extension operator from  $\Lambda$  to  $H_f$ , i.e., a continuous operator from  $\Lambda$  to  $H_f$  such that  $(R_1 \mu) \cdot \mathbf{n} = \mu$  on  $\Gamma$  for all  $\mu \in \Lambda$ , and  $R_2$  is any possible continuous extension operator from  $H^{1/2}(\Gamma)$  to  $H_p$  such that  $R_2 \mu = \mu$  on  $\Gamma$  for all  $\mu \in H^{1/2}(\Gamma)$ .

*Proof.* Let  $(\underline{u}, p) \in W \times Q$  be the solution of (4.11)–(4.12). Considering in (4.11) as test functions  $(\underline{w}, \psi) \in H_f^0 \times H_p^0$ , we obtain (5.1) and (5.3). Moreover, (4.12) implies (5.2).

Now let  $\mu \in \Lambda$ ,  $R_1\mu \in H_f$ , and  $R_2\mu \in H_p$ . From (4.11) we have:

$$\begin{aligned} & a_f(\mathbf{u}_f^0 + E_f \mathbf{u}_{in}, R_1\mu) - \int_{\Omega_f} \mathbf{f}(R_1\mu) + g a_p(\varphi_0 + E_p \varphi_p, R_2\mu) - \int_{\Gamma} g(\mathbf{u}_f^0 \cdot \mathbf{n})\mu \\ & + b_f(R_1\mu, p_f) + \int_{\Gamma} \sum_{j=1}^{d-1} \frac{\nu \alpha_{BJ}}{\sqrt{K}} (\mathbf{u}_f^0 \cdot \boldsymbol{\tau}_j)(R_1\mu \cdot \boldsymbol{\tau}_j) = - \int_{\Gamma} g \varphi_0 \mu, \end{aligned}$$

so that (5.4) and (5.5) are satisfied.

Consider now two arbitrary functions  $\mathbf{w} \in H_f$ ,  $\psi \in H_p$  and let us indicate by  $\mu$  the normal trace of  $\mathbf{w}$  on  $\Gamma$ , i.e.,  $\mathbf{w} \cdot \mathbf{n}|_{\Gamma} = \mu \in \Lambda$ , and by  $\eta$  the trace of  $\psi$  on  $\Gamma$ , that is  $\psi|_{\Gamma} = \eta \in H^{1/2}(\Gamma)$ . Then  $(\mathbf{w} - R_1\mu) \in H_f^0$  and  $(\psi - R_2\eta) \in H_p^0$ . Setting  $\underline{u} = (\mathbf{u}_f^0, \varphi_0)$  and  $\underline{v} = (\mathbf{w}, \psi)$  we have:

$$\begin{aligned} \mathcal{A}(\underline{u}, \underline{v}) + \mathcal{B}(\underline{v}, p) &= a_f(\mathbf{u}_f^0, \mathbf{w} - R_1\mu) + b_f(\mathbf{w} - R_1\mu, p_f) \\ &+ \int_{\Gamma} \sum_{j=1}^{d-1} \frac{\nu \alpha_{BJ}}{\sqrt{K}} (\mathbf{u}_f^0 \cdot \boldsymbol{\tau}_j)((\mathbf{w} - R_1\mu) \cdot \boldsymbol{\tau}_j) \\ &+ g a_p(\varphi_0, \psi - R_2\eta) + \int_{\Gamma} g \varphi_0 (\mathbf{w} - R_1\mu) \cdot \mathbf{n} \\ &- \int_{\Gamma} g(\psi - R_2\eta)(\mathbf{u}_f^0 \cdot \mathbf{n}) \\ &+ a_f(\mathbf{u}_f^0, R_1\mu) + b_f(R_1\mu, p_f) \\ &+ \int_{\Gamma} \sum_{j=1}^{d-1} \frac{\nu \alpha_{BJ}}{\sqrt{K}} (\mathbf{u}_f^0 \cdot \boldsymbol{\tau}_j)(R_1\mu \cdot \boldsymbol{\tau}_j) \\ &+ \int_{\Gamma} g \varphi_0 (R_1\mu \cdot \mathbf{n}) + g a_p(\varphi_0 + E_p \varphi_p, R_2\eta) \\ &- g a_p(E_p \varphi_p, R_2\mu) - \int_{\Gamma} g(R_2\eta)(\mathbf{u}_f^0 \cdot \mathbf{n}). \end{aligned}$$

Then, using (5.1) and (5.3)–(5.5) we obtain:

$$\begin{aligned} \mathcal{A}(\underline{u}, \underline{v}) + \mathcal{B}(\underline{v}, p) &= \int_{\Omega_f} \mathbf{f}(\mathbf{w} - R_1\mu) - a_f(E_f \mathbf{u}_{in}, \mathbf{w} - R_1\mu) \\ &- g a_p(E_p \varphi_p, \psi - R_2\eta) + \int_{\Omega_f} \mathbf{f}(R_1\mu) - a_f(E_f \mathbf{u}_{in}, R_1\mu) \\ &+ \int_{\Gamma} g(\mathbf{u}_f^0 \cdot \mathbf{n})\eta - \int_{\Gamma} g(\mathbf{u}_f^0 \cdot \mathbf{n})\eta - g a_p(E_p \varphi_p, R_2\eta) \end{aligned}$$

and, recalling the definition (4.10) of the functional  $\mathcal{F}$ , we find that  $\underline{u} = (\mathbf{u}_f^0, \varphi_0)$  and  $p_f$  satisfy (4.11), for all  $\mathbf{w} \in H_f$ ,  $\psi \in H_p$ .

The proof is completed by observing that (4.12) follows from (5.2). □



### 5.1. The interface equation associated to the Stokes/Darcy problem

We choose now a suitable governing variable on the interface  $\Gamma$ . Considering the interface conditions (3.16) and (3.17), we can foresee two different strategies to select the interface variable:

- (i) we can set the interface variable  $\lambda$  as the trace of the normal velocity on the interface:

$$\lambda = \mathbf{u}_f \cdot \mathbf{n} = -K\partial_n\varphi; \quad (5.6)$$

- (ii) we can define the interface variable  $\sigma$  as the trace of the piezometric head on  $\Gamma$ :

$$\sigma = \varphi = -\frac{1}{g} \mathbf{n} \cdot \mathbb{T}(\mathbf{u}_f, p_f) \cdot \mathbf{n}.$$

Both choices are suitable from the mathematical viewpoint since they guarantee well-posed subproblems in the fluid and the porous medium part. We shall analyze here the interface equation corresponding to  $\lambda$ . We refer the reader to [53] for the study of the equation associated to  $\sigma$ .

*Remark 5.2.* The role played in this context by the interface variables  $\lambda$  and  $\sigma$  is quite different than the classical cases encountered in domain decomposition. We clarify this point on a test example.

Consider the Poisson problem  $-\Delta u = f$  on a domain split into two non-overlapping subdomains. The interface conditions are

$$u_1 = u_2 \quad \text{and} \quad \partial_n u_1 = \partial_n u_2 \quad \text{on the interface.}$$

We have therefore two possible choices of the interface variable, say  $\tilde{\lambda}$ :

1.  $\tilde{\lambda} = u_1 = u_2$  on the interface: this is the classical approach (see [110, Chapter 1]) which gives the usual Steklov-Poincaré equation in  $\tilde{\lambda}$  featuring the so-called Dirichlet-to-Neumann maps. Note that  $\tilde{\lambda}$  provides a Dirichlet boundary condition on the interface for both subproblems.
2.  $\tilde{\lambda} = \partial_n u_1 = \partial_n u_2$ : this is the so-called FETI approach (see [119, Chapters 1, 6]) which can be seen as dual to the one recalled in 1. In this case the value of  $\tilde{\lambda}$  provides a Neumann boundary condition on the interface for the two subproblems.

After computing  $\tilde{\lambda}$ , we have to solve in both cases the same kind of boundary value problem in the subdomains to recover the global solution.

For the Stokes/Darcy problem this is no longer true: in fact, should we know  $\lambda$  on  $\Gamma$ , then we would have to solve a “Dirichlet” problem in  $\Omega_f$  and a Neumann problem in  $\Omega_p$ . On the other hand, choosing  $\sigma$  as interface variable would lead to consider a Stokes problem in  $\Omega_f$  with a Neumann boundary condition on  $\Gamma$ , and a Darcy problem in  $\Omega_p$  with a Dirichlet boundary condition on  $\Gamma$ .

This behavior is due to the heterogeneity of the coupling itself and it will strongly influence the construction of the Steklov-Poincaré operators that will not play the role of Dirichlet-to-Neumann maps for both subdomains as in the Laplace case.

An analogous asymmetry can be encountered in other heterogeneous problems, e.g., in the interface conditions when dealing with an heterogeneous fluid-structure coupling (see [52]).

We consider as governing variable on the interface  $\Gamma$  the normal component of the velocity field  $\lambda = \mathbf{u}_f \cdot \mathbf{n}$  as indicated in (5.6).

Should we know a priori the value of  $\lambda$  on  $\Gamma$ , from (5.6) we would obtain a Dirichlet boundary condition for the Stokes system in  $\Omega_f$  ( $\mathbf{u}_f \cdot \mathbf{n} = \lambda$  on  $\Gamma$ ) and a Neumann boundary condition for the Darcy equation in  $\Omega_p$  ( $-\mathcal{K}\partial_n\varphi = \lambda$  on  $\Gamma$ ).

Joint with (3.18) for the fluid problem, these conditions allow us to recover (independently) the solutions  $(\mathbf{u}_f, p_f)$  of the Stokes problem in  $\Omega_f$  and the solution  $\varphi$  of the Darcy problem in  $\Omega_p$ .

For simplicity, from now on we consider the following condition on the interface:

$$\mathbf{u}_f \cdot \boldsymbol{\tau}_j = 0 \quad \text{on } \Gamma, \tag{5.7}$$

instead of (3.18). This simplification is acceptable from the physical viewpoint as discussed in Section 3 and it does not dramatically influence the coupling of the two subproblems since, as we have already pointed out, condition (3.18) is not strictly a coupling condition but only a boundary condition for the fluid problem in  $\Omega_f$ .

Remark that using the simplified condition (5.7), the multi-domain formulation of the Stokes/ Darcy problem (5.1)–(5.2) becomes:

find  $\mathbf{u}_f^0 \in H_f^r$ ,  $p_f \in Q$ ,  $\varphi_0 \in H_p$  such that

$$a_f(\mathbf{u}_f^0 + E_f \mathbf{u}_{in}, \mathbf{w}) + b_f(\mathbf{w}, p_f) = \int_{\Omega_f} \mathbf{f} \cdot \mathbf{w} \quad \forall \mathbf{w} \in (H_0^1(\Omega_f))^d, \tag{5.8}$$

$$b_f(\mathbf{u}_f^0 + E_f \mathbf{u}_{in}, q) = 0 \quad \forall q \in Q, \tag{5.9}$$

$$a_p(\varphi_0 + E_p \varphi_p, \psi) = 0 \quad \forall \psi \in H_p^0, \tag{5.10}$$

$$\int_{\Gamma} (\mathbf{u}_f^0 \cdot \mathbf{n}) \mu = a_p(\varphi_0 + E_p \varphi_p, R_2 \mu) \quad \forall \mu \in \Lambda, \tag{5.11}$$

$$\int_{\Gamma} g \varphi_0 \mu = \int_{\Omega_f} \mathbf{f} \cdot (R_1^r \mu) - a_f(\mathbf{u}_f^0 + E_f \mathbf{u}_{in}, R_1^r \mu) - b_f(R_1^r \mu, p_f) \quad \forall \mu \in \Lambda, \tag{5.12}$$

with  $R_2$  defined as in Proposition 5.1, and  $R_1^r : \Lambda \rightarrow H_f^r$  is any possible continuous extension operator from  $\Lambda$  to  $H_f^r$  such that  $R_1^r \mu \cdot \mathbf{n} = \mu$  on  $\Gamma$  for all  $\mu \in \Lambda$ , with

$$H_f^r = \{\mathbf{v} \in H_f : \mathbf{v} \cdot \boldsymbol{\tau}_j = 0 \text{ on } \Gamma\}.$$

We define the continuous extension operator

$$E_\Gamma : H^{1/2}(\Gamma) \rightarrow H_f^\tau, \quad \eta \rightarrow E_\Gamma \eta \quad \text{such that} \quad E_\Gamma \eta \cdot \mathbf{n} = \eta \quad \text{on } \Gamma.$$

We consider the (unknown) interface variable  $\lambda = \mathbf{u}_f \cdot \mathbf{n}$  on  $\Gamma$ ,  $\lambda \in \Lambda$ , and we split it as  $\lambda = \lambda_0 + \lambda_*$  where  $\lambda_* \in \Lambda$  depends on the inflow data and satisfies

$$\int_\Gamma \lambda_* = - \int_{\Gamma_f^{in}} \mathbf{u}_{in} \cdot \mathbf{n}, \tag{5.13}$$

whereas  $\lambda_0 \in \Lambda_0$ , with

$$\Lambda_0 = \{ \mu \in \Lambda : \int_\Gamma \mu = 0 \} \subset \Lambda.$$

Then, we introduce two auxiliary problems whose solutions (which depend on the problem data) are related to that of the global problem (5.8)–(5.12), as we will see later on:

(P1) Find  $\omega_0^* \in (H_0^1(\Omega_f))^d$ ,  $\pi^* \in Q_0$  such that

$$\begin{aligned} a_f(\omega_0^* + E_f \mathbf{u}_{in} + E_\Gamma \lambda_*, \mathbf{v}) + b_f(\mathbf{v}, \pi^*) &= \int_{\Omega_f} \mathbf{f} \cdot \mathbf{v} \quad \forall \mathbf{v} \in (H_0^1(\Omega_f))^d, \\ b_f(\omega_0^* + E_f \mathbf{u}_{in} + E_\Gamma \lambda_*, q) &= 0 \quad \forall q \in Q_0. \end{aligned}$$

(P2) Find  $\varphi_0^* \in H_p$  such that

$$a_p(\varphi_0^* + E_p \varphi_p, \psi) = \int_\Gamma \lambda_* \psi \quad \forall \psi \in H_p.$$

Now we define the following extension operators:

$$R_f : \Lambda_0 \rightarrow H_f^\tau \times Q_0, \quad \eta \rightarrow R_f \eta = (R_f^1 \eta, R_f^2 \eta)$$

such that  $(R_f^1 \eta) \cdot \mathbf{n} = \eta$  on  $\Gamma$  and

$$a_f(R_f^1 \eta, \mathbf{v}) + b_f(\mathbf{v}, R_f^2 \eta) = 0 \quad \forall \mathbf{v} \in (H_0^1(\Omega_f))^d, \tag{5.14}$$

$$b_f(R_f^1 \eta, q) = 0 \quad \forall q \in Q_0; \tag{5.15}$$

$$R_p : \Lambda \rightarrow H_p, \quad \eta \rightarrow R_p \eta$$

such that

$$a_p(R_p \eta, R_2 \mu) = \int_\Gamma \eta \mu \quad \forall \mu \in H^{1/2}(\Gamma). \tag{5.16}$$

We define the *Steklov-Poincaré* operator  $S$  as follows: for all  $\eta \in \Lambda_0$ ,  $\mu \in \Lambda$ ,

$$\langle S\eta, \mu \rangle = a_f(R_f^1\eta, R_1^\tau\mu) + b_f(R_1^\tau\mu, R_f^2\eta) + \int_\Gamma g(R_p\eta)\mu,$$

which can be split as the sum of two sub-operators  $S = S_f + S_p$ :

$$\langle S_f\eta, \mu \rangle = a_f(R_f^1\eta, R_1^\tau\mu) + b_f(R_1^\tau\mu, R_f^2\eta), \tag{5.17}$$

$$\langle S_p\eta, \mu \rangle = \int_\Gamma g(R_p\eta)\mu, \tag{5.18}$$

for all  $\eta \in \Lambda_0$  and  $\mu \in \Lambda$ .

Moreover, we define the functional  $\chi : \Lambda_0 \rightarrow \mathbb{R}$ ,

$$\begin{aligned} \langle \chi, \mu \rangle &= \int_{\Omega_f} \mathbf{f}(R_1^\tau\mu) - a_f(\omega_0^* + E_f \mathbf{u}_{in} + E_\Gamma \lambda_*, R_1^\tau\mu) \\ &\quad - b_f(R_1^\tau\mu, \pi^*) - \int_\Gamma g \varphi_0^* \mu \quad \forall \mu \in \Lambda. \end{aligned} \tag{5.19}$$

Now we can express the solution of the coupled problem in terms of the interface variable  $\lambda_0$ ; precisely, we can prove the following result.

**Theorem 5.3.** *The solution to (5.8)–(5.12) can be characterized as follows:*

$$\mathbf{u}_f^0 = \omega_0^* + R_f^1\lambda_0 + E_\Gamma \lambda_*, \quad p_f = \pi^* + R_f^2\lambda_0 + \hat{p}_f, \quad \varphi_0 = \varphi_0^* + R_p\lambda_0, \tag{5.20}$$

where  $\hat{p}_f = (\text{meas}(\Omega_f))^{-1} \int_{\Omega_f} p_f$  and  $\lambda_0 \in \Lambda_0$  is the solution of the following *Steklov-Poincaré* problem:

$$\langle S\lambda_0, \mu_0 \rangle = \langle \chi, \mu_0 \rangle \quad \forall \mu_0 \in \Lambda_0. \tag{5.21}$$

Moreover,  $\hat{p}_f$  can be obtained from  $\lambda_0$  by solving the algebraic equation

$$\hat{p}_f = \frac{1}{\text{meas}(\Gamma)} \langle S\lambda_0 - \chi, \zeta \rangle, \tag{5.22}$$

where  $\zeta \in \Lambda$  is a fixed function such that

$$\frac{1}{\text{meas}(\Gamma)} \int_\Gamma \zeta = 1.$$

*Proof.* Thanks to the divergence theorem, for all constant functions  $c$ ,

$$b_f(\mathbf{w}, c) = c \int_{\partial\Omega_f} \mathbf{w} \cdot \mathbf{n} = 0 \quad \forall \mathbf{w} \in (H_0^1(\Omega_f))^d.$$

Then, by direct inspection, the functions defined in (5.20) satisfy (5.8), (5.10) and (5.11). Moreover (5.9) is satisfied too. Indeed,  $\forall q \in Q$

$$b_f(\boldsymbol{\omega}_0^* + R_f^1 \lambda_0 + E_\Gamma \lambda_* + E_f \mathbf{u}_{in}, q) = b_f(\boldsymbol{\omega}_0^* + R_f^1 \lambda_0 + E_\Gamma \lambda_* + E_f \mathbf{u}_{in}, q - \bar{q}) + b_f(\boldsymbol{\omega}_0^* + R_f^1 \lambda_0 + E_\Gamma \lambda_* + E_f \mathbf{u}_{in}, \bar{q}),$$

where  $\bar{q}$  is the constant  $\bar{q} = (\text{meas}(\Omega_f))^{-1} \int_{\Omega_f} q$ . Still using the divergence theorem,

$$b_f(\boldsymbol{\omega}_0^* + R_f^1 \lambda_0 + E_\Gamma \lambda_* + E_f \mathbf{u}_{in}, \bar{q}) = \bar{q} \int_\Gamma \lambda_0 + \bar{q} \int_\Gamma \lambda_* + \bar{q} \int_{\Gamma_f^{in}} \mathbf{u}_{in} \cdot \mathbf{n}_f.$$

The right hand side is null thanks to (5.13) and since  $\lambda_0 \in \Lambda_0$ .

We now consider (5.12). Using (5.20) we obtain,  $\forall \mu \in \Lambda$ ,

$$\int_\Gamma g(R_p \lambda_0) \mu + a_f(R_f^1 \lambda_0, R_1^\tau \mu) + b_f(R_1^\tau \mu, R_f^2 \lambda_0) = \int_{\Omega_f} \mathbf{f}(R_1^\tau \mu) - \int_\Gamma g \varphi_0^* \mu - a_f(\boldsymbol{\omega}_0^* + E_f \mathbf{u}_{in} + E_\Gamma \lambda_*, R_1^\tau \mu) - b_f(R_1^\tau \mu, \pi^*) - b_f(R_1^\tau \mu, \hat{p}_f),$$

that is,

$$\langle S \lambda_0, \mu \rangle = \langle \chi, \mu \rangle - b_f(R_1^\tau \mu, \hat{p}_f) \quad \forall \mu \in \Lambda. \tag{5.23}$$

In particular, if we take  $\mu \in \Lambda_0 \subset \Lambda$ , we can invoke the divergence theorem and conclude that  $\lambda_0$  is the solution to the Steklov-Poincaré equation (5.21).

Now any  $\mu \in \Lambda$  can be decomposed as  $\mu = \mu_0 + \mu_\Gamma \zeta$ , with  $\mu_\Gamma = (\text{meas}(\Gamma))^{-1} \int_\Gamma \mu$ , so that  $\mu_0 \in \Lambda_0$ .

From (5.23) we obtain

$$\langle S \lambda_0, \mu_0 \rangle + \langle S \lambda_0, \mu_\Gamma \zeta \rangle = \langle \chi, \mu_0 \rangle + \langle \chi, \mu_\Gamma \zeta \rangle + \hat{p}_f \int_\Gamma \mu \quad \forall \mu \in \Lambda.$$

Therefore, thanks to (5.21), we have

$$\mu_\Gamma \langle S \lambda_0 - \chi, \zeta \rangle = \hat{p}_f \int_\Gamma \mu \quad \forall \mu \in \Lambda.$$

Since  $\int_\Gamma \mu = \mu_\Gamma \text{meas}(\Gamma)$ , we conclude that (5.22) holds. □

In next section we prove that (5.21) has a unique solution.

### 5.2. Analysis of the Steklov-Poincaré operators $S_f$ and $S_p$

We shall now prove some properties of the Steklov-Poincaré operators  $S_f$ ,  $S_p$  and  $S$ .

**Lemma 5.4.** *The Steklov-Poincaré operators enjoy the following properties:*

1.  $S_f$  and  $S_p$  are linear continuous operators on  $\Lambda_0$  (i.e.,  $S_f\eta \in \Lambda'_0$ ,  $S_p\eta \in \Lambda'_0$ ,  $\forall \eta \in \Lambda_0$ );
2.  $S_f$  is symmetric and coercive;
3.  $S_p$  is symmetric and positive.

*Proof.* 1.  $S_f$  and  $S_p$  are obviously linear. Next we observe that for every  $\mu \in \Lambda_0$  we can make the special choice  $R_1^T \mu = R_f^1 \mu$ . Consequently, from (5.17) and (5.15) it follows that  $S_f$  can be characterized as:

$$\langle S_f \eta, \mu \rangle = a_f(R_f^1 \eta, R_f^1 \mu) \quad \forall \eta, \mu \in \Lambda_0. \tag{5.24}$$

To prove continuity, we introduce the vector operator  $\mathcal{H}: \Lambda_0 \rightarrow H_f$ ,  $\mu \rightarrow \mathcal{H}\mu$ , such that

$$\begin{aligned} \int_{\Omega_f} \nabla(\mathcal{H}\mu) \cdot \nabla \mathbf{v} &= 0 \quad \forall \mathbf{v} \in (H_0^1(\Omega_f))^d, \\ (\mathcal{H}\mu) \cdot \mathbf{n} &= \mu \quad \text{on } \Gamma, \\ (\mathcal{H}\mu) \cdot \boldsymbol{\tau}_j &= 0 \quad \text{on } \Gamma, \quad j = 1, \dots, d-1, \\ \mathcal{H}\mu &= 0 \quad \text{on } \partial\Omega_f \setminus \Gamma. \end{aligned} \tag{5.25}$$

By comparison with the operator  $R_f^1$  introduced in (5.14)–(5.15), we see that, for all  $\mu \in \Lambda_0$ , the vector function

$$\mathbf{z}(\mu) = R_f^1 \mu - \mathcal{H}\mu \tag{5.26}$$

satisfies  $\mathbf{z}(\mu) = 0$  on  $\Gamma$ ; therefore  $\mathbf{z}(\mu) \in (H_0^1(\Omega_f))^d$ . By taking  $\mathbf{v} = \mathbf{z}(\mu)$  in (5.14), in view of the definition (5.26) we have

$$|a_f(R_f^1 \mu, \mathbf{z}(\mu))| = |b_f(\mathcal{H}\mu, R_f^2 \mu)| \leq \|R_f^2 \mu\|_0 \|\mathcal{H}\mu\|_1. \tag{5.27}$$

We now consider the function  $R_f^2 \mu$ . Since it belongs to  $Q_0$ , there exists  $\mathbf{w} \in (H_0^1(\Omega_f))^d$ ,  $\mathbf{w} \neq \mathbf{0}$ , such that

$$\beta^0 \|R_f^2 \mu\|_0 \|\mathbf{w}\|_1 \leq b_f(\mathbf{w}, R_f^2 \mu),$$

where  $\beta^0 > 0$  is the inf-sup constant, independent of  $\mu$  (see, e.g., [33]). Since  $\mathbf{w} \in (H_0^1(\Omega_f))^d$ , we can use (5.14) and obtain:

$$\beta^0 \|R_f^2 \mu\|_0 \|\mathbf{w}\|_1 \leq |a_f(R_f^1 \mu, \mathbf{w})| \leq 2\nu \|R_f^1 \mu\|_1 \|\mathbf{w}\|_1.$$

The last inequality follows from the Cauchy–Schwarz inequality. Therefore

$$\|R_f^2 \mu\|_0 \leq \frac{2\nu}{\beta^0} \|R_f^1 \mu\|_1 \quad \forall \mu \in \Lambda_0. \tag{5.28}$$

Now, using the Poincaré inequality (see, e.g., [109, page 11])

$$\exists C_{\Omega_f} > 0 : \quad \|\mathbf{v}\|_0 \leq C_{\Omega_f} \|\mathbf{v}\|_1 \quad \forall \mathbf{v} \in H_f, \tag{5.29}$$

and relations (5.26)–(5.28), we obtain:

$$\begin{aligned} \|R_f^1 \mu\|_1^2 &\leq \frac{1 + C_{\Omega_f}}{\nu} a_f(R_f^1 \mu, R_f^1 \mu) \\ &= \frac{1 + C_{\Omega_f}}{\nu} [a_f(R_f^1 \mu, \mathbf{z}(\mu)) + a_f(R_f^1 \mu, \mathcal{H}\mu)] \\ &\leq \frac{1 + C_{\Omega_f}}{\nu} [\|R_f^2 \mu\|_0 \|\mathcal{H}\mu\|_1 + 2\nu \|R_f^1 \mu\|_1 \|\mathcal{H}\mu\|_1] \\ &\leq 2(1 + C_{\Omega_f}) \left(1 + \frac{1}{\beta^0}\right) \|R_f^1 \mu\|_1 \|\mathcal{H}\mu\|_1 \end{aligned}$$

for all  $\mu \in \Lambda_0$ . Therefore

$$\begin{aligned} \|R_f^1 \mu\|_1 &\leq 2(1 + C_{\Omega_f}) \left(1 + \frac{1}{\beta^0}\right) \|\mathcal{H}\mu\|_1 \\ &\leq 2\alpha^*(1 + C_{\Omega_f}) \left(1 + \frac{1}{\beta^0}\right) \|\mu\|_\Lambda . \end{aligned} \tag{5.30}$$

The last inequality follows from the observation that  $\mathcal{H}\mu$  is a harmonic extension of  $\mu$ ; then there exists a positive constant  $\alpha^* > 0$  (independent of  $\mu$ ) such that

$$\|\mathcal{H}\mu\|_1 \leq \alpha^* \|\mathcal{H}\mu|_\Gamma\|_\Lambda = \alpha^* \|\mu\|_\Lambda$$

(see, e.g., [110]).

Thanks to (5.30) we can now prove the continuity of  $S_f$ ; in fact, for all  $\mu, \eta \in \Lambda_0$ , we have

$$|\langle S_f \mu, \eta \rangle| = |a_f(R_f^1 \mu, R_f^1 \eta)| \leq \beta_f \|\mu\|_\Lambda \|\eta\|_\Lambda ,$$

where  $\beta_f$  is the positive continuity constant

$$\beta_f = 2\nu \left[ \alpha^*(1 + C_{\Omega_f}) \left(1 + \frac{1}{\beta^0}\right) \right]^2 .$$

We now turn to the issue of continuity of  $S_p$ . Let  $m_K$  be the positive constant introduced in (4.20). Thanks to the Poincaré inequality and to (5.16) we have:

$$\|R_p \mu\|_1^2 \leq (1 + C_{\Omega_p}) \|\nabla R_p \mu\|_0^2 \leq \frac{1 + C_{\Omega_p}}{m_K} a_p(R_p \mu, R_p \mu) = \frac{1 + C_{\Omega_p}}{m_K} \int_\Gamma (R_p \mu)|_\Gamma \mu .$$

Finally, the Cauchy–Schwarz inequality and the trace inequality (4.17) allow us to deduce that

$$\|R_p \mu\|_1 \leq \frac{(1 + C_{\Omega_p})}{m_K} C_p \|\mu\|_\Lambda \quad \forall \mu \in \Lambda_0 .$$

Then, for all  $\mu, \eta \in \Lambda_0$ ,

$$\begin{aligned} |\langle S_p \mu, \eta \rangle| &\leq g \|R_p \mu|_{\Gamma}\|_{L^2(\Gamma)} \|\eta\|_{L^2(\Gamma)} \\ &\leq g C_p \|R_p \mu\|_1 \|\eta\|_{\Lambda} \leq \frac{g C_p^2 (1 + C_{\Omega_p})}{m_K} \|\mu\|_{\Lambda} \|\eta\|_{\Lambda}. \end{aligned}$$

Thus  $S_p$  is continuous, with continuity constant

$$\beta_p = \frac{g C_p^2 (1 + C_{\Omega_p})}{m_K}. \tag{5.31}$$

2.  $S_f$  is symmetric thanks to (5.24). Again using the Korn inequality and the trace inequality (4.16), for all  $\mu \in \Lambda_0$  we obtain

$$\langle S_f \mu, \mu \rangle \geq \frac{\nu \kappa_f}{2} \|R_f^1 \mu\|_1^2 \geq \frac{\nu \kappa_f}{2 C_f} \|(R_f^1 \mu \cdot \mathbf{n})|_{\Gamma}\|_{\Lambda}^2 = \alpha_f \|\mu\|_{\Lambda}^2;$$

thus  $S_f$  is coercive, with a coercivity constant given by

$$\alpha_f = \frac{\nu \kappa_f}{2 C_f}. \tag{5.32}$$

3.  $S_p$  is symmetric: for all  $\mu, \eta \in \Lambda$ :

$$\begin{aligned} \langle S_p \mu, \eta \rangle &= g \int_{\Gamma} (R_p \eta)|_{\Gamma} \mu = g a_p(R_p \mu, R_p \eta) \\ &= g a_p(R_p \eta, R_p \mu) = g \int_{\Gamma} \eta (R_p \mu)|_{\Gamma} = \langle S_p \eta, \mu \rangle. \end{aligned}$$

Moreover, thanks to (5.16),  $\forall \mu \in \Lambda_0$

$$\langle S_p \mu, \mu \rangle = \int_{\Gamma} g (R_p \mu) \mu = g a_p(R_p \mu, R_p \mu).$$

On the other hand, we have

$$\begin{aligned} \|\mu\|_{\Lambda'} &= \sup_{\eta \in \Lambda_0} \frac{\langle \mu, \eta \rangle}{\|\eta\|_{\Lambda}} = \sup_{\eta \in \Lambda_0} \frac{\langle -\mathbf{K} \partial_n (R_p \mu), \eta \rangle}{\|\eta\|_{\Lambda}} \\ &= \sup_{\eta \in \Lambda_0} \frac{a_p(R_p \mu, \mathcal{H}_p \eta)}{\|\eta\|_{\Lambda}} \leq \sup_{\eta \in \Lambda_0} \frac{\alpha_* a_p(R_p \mu, \mathcal{H}_p \eta)}{\|\mathcal{H}_p \eta\|_1} \\ &\leq \alpha_* \max_j \|\mathbf{K}_j\|_{\infty} \sup_{\eta \in \Lambda_0} \frac{\|R_p \mu\|_1 \|\mathcal{H}_p \eta\|_1}{\|\mathcal{H}_p \eta\|_1} \\ &= \alpha_* \max_j \|\mathbf{K}_j\|_{\infty} \|R_p \mu\|_1. \end{aligned}$$



We have denoted by  $\Lambda'$  the dual space of  $\Lambda_0$ , and by  $\langle \cdot, \cdot \rangle$  the duality pairing between  $\Lambda'$  and  $\Lambda_0$ . Moreover,  $\mathcal{H}_p\eta$  is the harmonic extension of  $\eta$  to  $H^1(\Omega_p)$ , i.e., the (weak) solution of the problem:

$$\begin{aligned} \nabla \cdot (\mathbf{K}\nabla(\mathcal{H}_p\eta)) &= 0 && \text{in } \Omega_p, \\ \mathbf{K}\nabla(\mathcal{H}_p\eta) \cdot \mathbf{n}_p &= 0 && \text{on } \Gamma_p, \\ \mathcal{H}_p\eta &= 0 && \text{on } \Gamma_p^b, \\ \mathcal{H}_p\eta &= \eta && \text{on } \Gamma, \end{aligned}$$

and we have used the equivalence of the norms (see, e.g., [99] or [110, Chapter 4])

$$\alpha_* \|\eta\|_\Lambda \leq \|\mathcal{H}_p\eta\|_1 \leq \alpha^* \|\eta\|_\Lambda.$$

We conclude that  $\langle S_p\mu, \mu \rangle \geq C\|\mu\|_\Lambda^2$  for a suitable constant  $C > 0$ . □

The following result is a straightforward consequence of Lemma 5.4.

**Corollary 5.5.** *The global Steklov-Poincaré operator  $S$  is symmetric, continuous and coercive. Moreover  $S$  and  $S_f$  are spectrally equivalent, i.e., there exist two positive constants  $k_1$  and  $k_2$  (independent of  $\eta$ ) such that*

$$k_1 \langle S_f\eta, \eta \rangle \leq \langle S\eta, \eta \rangle \leq k_2 \langle S_f\eta, \eta \rangle \quad \forall \eta \in \Lambda_0.$$

Before concluding this section, let us point out which differential problems correspond to the Steklov-Poincaré operators.

- (i) The operator  $S_f : \Lambda_0 \rightarrow \Lambda'_0$  maps

$$S_f : \{\text{normal velocities on } \Gamma\} \rightarrow \{\text{normal stresses on } \Gamma\}.$$

Computing  $S_f\lambda_0$  involves solving a Stokes problem in  $\Omega_f$  with the boundary conditions  $\mathbf{u}_f \cdot \mathbf{n} = \lambda_0$  and  $\mathbf{u}_f \cdot \boldsymbol{\tau}_j = 0$  on  $\Gamma$ , and then to compute the normal stress  $-\mathbf{n} \cdot \mathbb{T}(\mathbf{u}_f, p_f) \cdot \mathbf{n}$  on  $\Gamma$ . Moreover,  $S_f$  is spectrally equivalent to  $S$  and there exists  $S_f^{-1} : \Lambda'_0 \rightarrow \Lambda_0$ .

- (ii) The operator  $S_p : \Lambda_0 \rightarrow \Lambda'_0$  maps

$$S_p : \{\text{fluxes of } \varphi \text{ on } \Gamma\} \rightarrow \{\text{traces of } \varphi \text{ on } \Gamma\}.$$

Computing  $S_p\lambda_0$  corresponds to solve a Darcy problem in  $\Omega_p$  with the Neumann boundary condition  $-\mathbf{K}\partial_n\varphi = \lambda_0$  on  $\Gamma$  and to recover  $\varphi$  on  $\Gamma$ .

### 6. Multi-domain formulation and some non-linear extension operators associated to the Navier-Stokes/Darcy problem

In this section we apply domain decomposition techniques at the differential level to study the Navier-Stokes/Darcy problem (4.1), (3.6)–(3.11). In particular, we introduce and analyze some non-linear extension operators that will be used in Section 6.1 to write the Steklov-Poincaré interface equation associated to the coupled problem.

Due to the non-linearity of the problem, for the sake of simplicity we adopt in our analysis homogeneous boundary conditions, i.e., we will set  $\mathbf{u}_{in} = \mathbf{0}$  in (4.2) and  $\varphi_p = 0$  in (4.3).

We consider a linear continuous extension operator  $R_1 : \Lambda \rightarrow H_f$  such that  $R_1\mu \cdot \mathbf{n} = \mu$  on  $\Gamma$ , for all  $\mu \in \Lambda$ , while let  $R_2$  be the operator introduced in Proposition 5.1. Since there holds  $H_f = H_f^0 + \{R_1\mu : \mu \in \Lambda\}$ , we can prove the following result (see also [53]).

**Proposition 6.1.** *The coupled Navier-Stokes/Darcy problem (4.1), (3.6)–(3.11) can be equivalently reformulated in the multi-domain form:*

find  $\mathbf{u}_f \in H_f, p_f \in Q, \varphi \in H_p$  such that

$$a_f(\mathbf{u}_f, \mathbf{v}) + c_f(\mathbf{u}_f; \mathbf{u}_f, \mathbf{v}) + b_f(\mathbf{v}, p_f) + \int_{\Gamma} \sum_{j=1}^{d-1} \frac{\nu\alpha_{BJ}}{\sqrt{K}} (\mathbf{u}_f \cdot \boldsymbol{\tau}_j)(\mathbf{v} \cdot \boldsymbol{\tau}_j) = \int_{\Omega_f} \mathbf{f} \cdot \mathbf{v} \quad \forall \mathbf{v} \in H_f^0, \tag{6.1}$$

$$b_f(\mathbf{u}_f, q) = 0 \quad \forall q \in Q, \tag{6.2}$$

$$a_p(\varphi, \psi) = 0 \quad \forall \psi \in H_p^0, \tag{6.3}$$

$$\int_{\Gamma} (\mathbf{u}_f \cdot \mathbf{n})\mu = a_p(\varphi, R_2\mu) \quad \forall \mu \in \Lambda, \tag{6.4}$$

$$\int_{\Gamma} g \varphi \mu = \int_{\Omega_f} \mathbf{f}(R_1\mu) - a_f(\mathbf{u}_f, R_1\mu) - c_f(\mathbf{u}_f; \mathbf{u}_f, R_1\mu) - b_f(R_1\mu, p_f) - \int_{\Gamma} \sum_{j=1}^{d-1} \frac{\nu\alpha_{BJ}}{\sqrt{K}} (\mathbf{u}_f \cdot \boldsymbol{\tau}_j)(R_1\mu \cdot \boldsymbol{\tau}_j) \quad \forall \mu \in \Lambda. \tag{6.5}$$

In order to rewrite (6.1)–(6.5) as an interface equation in a scalar interface unknown defined on  $\Gamma$  corresponding to the trace of the fluid normal velocity  $\mathbf{u}_f \cdot \mathbf{n}$  on  $\Gamma$ , we need to introduce and analyze some further extension operators.

Similarly to the case of Stokes/Darcy (see Section 5.1), we consider the (unknown) interface variable  $\lambda = (\mathbf{u}_f \cdot \mathbf{n})|_{\Gamma}$ . Due to the incompressibility constraint in  $\Omega_f$  and to the boundary conditions imposed on  $\partial\Omega_f \setminus \Gamma$ , it must be  $\lambda \in \Lambda_0$ .

Let us define the *linear* extension operator:

$$\tilde{R}_f : \Lambda_0 \rightarrow H_f \times Q_0, \quad \eta \rightarrow \tilde{R}_f\eta = (\tilde{R}_f^1\eta, \tilde{R}_f^2\eta), \tag{6.6}$$

satisfying  $\widetilde{R}_f^1 \eta \cdot \mathbf{n} = \eta$  on  $\Gamma$ , and, for all  $\mathbf{v} \in H_f^0$ ,  $q \in Q_0$ ,

$$a_f(\widetilde{R}_f^1 \eta, \mathbf{v}) + b_f(\mathbf{v}, \widetilde{R}_f^2 \eta) + \int_{\Gamma} \sum_{j=1}^{d-1} \frac{\nu^{\alpha_{BJ}}}{\sqrt{K}} (\widetilde{R}_f^1 \eta \cdot \boldsymbol{\tau}_j)(\mathbf{v} \cdot \boldsymbol{\tau}_j) = 0, \tag{6.7}$$

$$b_f(\widetilde{R}_f^1 \eta, q) = 0. \tag{6.8}$$

Moreover, let  $R_p: \Lambda_0 \rightarrow H_p$  be the linear extension operator introduced in (5.16).

Finally, let us introduce the following non-linear extension operator:

$$\mathcal{R}_f: \Lambda_0 \rightarrow H_f \times Q_0, \quad \eta \rightarrow \mathcal{R}_f(\eta) = (\mathcal{R}_f^1(\eta), \mathcal{R}_f^2(\eta))$$

such that  $\mathcal{R}_f^1(\eta) \cdot \mathbf{n} = \eta$  on  $\Gamma$ , and, for all  $\mathbf{v} \in H_f^0$ ,  $q \in Q_0$ ,

$$a_f(\mathcal{R}_f^1(\eta), \mathbf{v}) + c_f(\mathcal{R}_f^1(\eta); \mathcal{R}_f^1(\eta), \mathbf{v}) + b_f(\mathbf{v}, \mathcal{R}_f^2(\eta)) + \int_{\Gamma} \sum_{j=1}^{d-1} \frac{\nu^{\alpha_{BJ}}}{\sqrt{K}} (\mathcal{R}_f^1(\eta) \cdot \boldsymbol{\tau}_j)(\mathbf{v} \cdot \boldsymbol{\tau}_j) = \int_{\Omega_f} \mathbf{f} \cdot \mathbf{v}, \tag{6.9}$$

$$b_f(\mathcal{R}_f^1(\eta), q) = 0. \tag{6.10}$$

In order to prove the existence and uniqueness of  $\mathcal{R}_f$ , we define the auxiliary non-linear operator

$$\begin{aligned} \mathcal{R}_0: \Lambda_0 \rightarrow H_f^0 \times Q_0, \quad \eta \rightarrow \mathcal{R}_0(\eta) &= (\mathcal{R}_0^1(\eta), \mathcal{R}_0^2(\eta)), \\ \text{with } \mathcal{R}_0^i(\eta) &= \mathcal{R}_f^i(\eta) - R_f^i \eta, \quad i = 1, 2. \end{aligned} \tag{6.11}$$

Clearly,  $\mathcal{R}_0^1(\eta) \cdot \mathbf{n} = 0$  on  $\Gamma$ , and it satisfies:

$$a_f(\mathcal{R}_0^1(\eta), \mathbf{v}) + c_f(\widetilde{R}_f^1 \eta + \mathcal{R}_0^1(\eta); \widetilde{R}_f^1 \eta + \mathcal{R}_0^1(\eta), \mathbf{v}) + b_f(\mathbf{v}, \mathcal{R}_0^2(\eta)) + \int_{\Gamma} \sum_{j=1}^{d-1} \frac{\nu^{\alpha_{BJ}}}{\sqrt{K}} (\mathcal{R}_0^1(\eta) \cdot \boldsymbol{\tau}_j)(\mathbf{v} \cdot \boldsymbol{\tau}_j) = \int_{\Omega_f} \mathbf{f} \cdot \mathbf{v}, \tag{6.12}$$

$$b_f(\mathcal{R}_0^1(\eta), q) = 0, \tag{6.13}$$

for all  $\mathbf{v} \in H_f^0$ ,  $q \in Q_0$ . Remark that problem (6.12)–(6.13) is analogous to (6.9)–(6.10), but here  $\mathcal{R}_0^1(\eta) \in H_f^0$ , while  $\mathcal{R}_f^1(\eta) \in H_f$ .

Moreover, given  $\eta \in \Lambda_0$ , we define the form

$$a(\mathbf{w}; \mathbf{z}, \mathbf{v}) = a_f(\mathbf{z}, \mathbf{v}) + c_f(\mathbf{w}; \mathbf{z}, \mathbf{v}) + c_f(\widetilde{R}_f^1 \eta; \mathbf{z}, \mathbf{v}) + c_f(\mathbf{z}; \widetilde{R}_f^1 \eta, \mathbf{v}) + \int_{\Gamma} \sum_{j=1}^{d-1} \frac{\nu^{\alpha_{BJ}}}{\sqrt{K}} (\mathbf{z} \cdot \boldsymbol{\tau}_j)(\mathbf{v} \cdot \boldsymbol{\tau}_j) \quad \forall \mathbf{w}, \mathbf{z}, \mathbf{v} \in (H^1(\Omega_f))^d,$$

and the functional

$$\langle \ell, \mathbf{v} \rangle = -c_f(\widetilde{R}_f^1 \eta; \widetilde{R}_f^1 \eta, \mathbf{v}) + \int_{\Omega_f} \mathbf{f} \cdot \mathbf{v} \quad \forall \mathbf{v} \in (H^1(\Omega_f))^d.$$

Thus, we can rewrite (6.12)–(6.13) as:

Given  $\eta \in \Lambda_0$ ,

$$\text{find } \mathcal{R}_0^1(\eta) \in V_f^0 : \quad a(\mathcal{R}_0^1(\eta); \mathcal{R}_0^1(\eta), \mathbf{v}) = \langle \ell, \mathbf{v} \rangle \quad \forall \mathbf{v} \in V_f^0. \quad (6.14)$$

Finally, let us recall the following inequality

$$\exists C_{\mathcal{N}} > 0 : \quad |c_f(\mathbf{w}; \mathbf{z}, \mathbf{v})| \leq C_{\mathcal{N}} |\mathbf{w}|_1 |\mathbf{z}|_1 |\mathbf{v}|_1 \quad \forall \mathbf{w}, \mathbf{z}, \mathbf{v} \in H_f, \quad (6.15)$$

which follows from the Poincaré inequality (5.29) and the inclusion  $(H^1(\Omega_f))^d \subset (L^4(\Omega_f))^d$  (for  $d = 2, 3$ ) due to the Sobolev embedding theorem (see [6]).

We can now state the following result.

**Proposition 6.2.** *Let  $\mathbf{f} \in L^2(\Omega_f)$  be such that*

$$C_{\mathcal{N}} C_{\Omega_f} \|\mathbf{f}\|_0 < \left( \frac{\kappa_f \nu}{2} \right)^2, \quad (6.16)$$

where  $\kappa_f$  is the constant in the Korn inequality (4.19) and  $C_{\mathcal{N}}$  is given in (6.15). If

$$\eta \in \left\{ \mu \in \Lambda_0 : |\widetilde{R}_f^1 \mu|_1 < \frac{\kappa_f \nu - \sqrt{\left(\frac{\kappa_f \nu}{2}\right)^2 + 3C_{\mathcal{N}} C_{\Omega_f} \|\mathbf{f}\|_0}}{3C_{\mathcal{N}}} \right\}, \quad (6.17)$$

then there exists a unique non-linear extension  $\mathcal{R}_f(\eta) = (\mathcal{R}_f^1(\eta), \mathcal{R}_f^2(\eta)) \in H_f \times Q_0$ .

*Remark 6.3.* Notice that (6.17) imposes a constraint on  $\eta$ . In particular, since the norms  $|\widetilde{R}_f^1 \eta|_1$  and  $\|\eta\|_{\Lambda}$  are equivalent (see [56, Lemma 4.1]), this condition implies that a unique extension  $\mathcal{R}_f(\eta)$  exists, provided the norm of  $\eta$  is small enough. In our specific case, this means that we would be able to consider an extension  $\mathcal{R}_f(\lambda)$  only if the normal velocity  $\lambda$  across the interface  $\Gamma$  is sufficiently small. Finally, remark that (6.16) guarantees that the radius of the ball in (6.17) is positive.

*Proof.* The proof is made of several steps and it is based on Theorems A.1–A.2.

1. Let  $\mathbf{v}, \mathbf{w} \in V_f^0$  and  $\eta \in \Lambda_0$ . Then, we have

$$\begin{aligned} a(\mathbf{w}; \mathbf{v}, \mathbf{v}) &= a_f(\mathbf{v}, \mathbf{v}) + c_f(\mathbf{w}; \mathbf{v}, \mathbf{v}) \\ &+ c_f(\widetilde{R}_f^1 \eta; \mathbf{v}, \mathbf{v}) + c_f(\mathbf{v}; \widetilde{R}_f^1 \eta, \mathbf{v}) + \int_{\Gamma} \sum_{j=1}^{d-1} \frac{\nu \alpha_{BJ}}{\sqrt{K}} (\mathbf{v} \cdot \boldsymbol{\tau}_j)(\mathbf{v} \cdot \boldsymbol{\tau}_j). \end{aligned} \quad (6.18)$$

Integrating by parts and recalling that  $\mathbf{w} \in V_f^0$ , then

$$c_f(\mathbf{w}; \mathbf{v}, \mathbf{v}) = \frac{1}{2} \int_{\partial\Omega_f} \mathbf{w} \cdot \mathbf{n} |\mathbf{v}|^2 - \frac{1}{2} \int_{\Omega_f} \nabla \cdot \mathbf{w} |\mathbf{v}|^2 = 0,$$

where  $|\mathbf{v}|$  is the Euclidean norm of the vector  $\mathbf{v}$ . Since

$$\int_{\Gamma} \sum_{j=1}^{d-1} \frac{\nu \alpha_{BJ}}{\sqrt{K}} (\mathbf{v} \cdot \boldsymbol{\tau}_j) (\mathbf{v} \cdot \boldsymbol{\tau}_j) \geq 0,$$

from (6.18) we get

$$a(\mathbf{w}; \mathbf{v}, \mathbf{v}) \geq a_f(\mathbf{v}, \mathbf{v}) + c_f(\widetilde{R}_f^1 \eta; \mathbf{v}, \mathbf{v}) + c_f(\mathbf{v}; \widetilde{R}_f^1 \eta, \mathbf{v}),$$

and using the inequalities (4.19) and (6.15) we obtain

$$a(\mathbf{w}; \mathbf{v}, \mathbf{v}) \geq \frac{\kappa_f \nu}{2} |\mathbf{v}|_1^2 - 2C_{\mathcal{N}} |\mathbf{v}|_1^2 |\widetilde{R}_f^1 \eta|_1.$$

Then, thanks to (6.17), the bilinear form  $a(\mathbf{w}; \cdot, \cdot)$  is uniformly elliptic on  $V_f^0$  with respect to  $\mathbf{w}$ , with constant  $\alpha_a$  (independent of  $\mathbf{w}$ )

$$\alpha_a = \frac{\kappa_f \nu}{2} - 2C_{\mathcal{N}} |\widetilde{R}_f^1 \eta|_1.$$

2. Still using (6.15), we easily obtain:

$$|a(\mathbf{w}_1; \mathbf{z}, \mathbf{v}) - a(\mathbf{w}_2; \mathbf{z}, \mathbf{v})| = |c_f(\mathbf{w}_1 - \mathbf{w}_2; \mathbf{z}, \mathbf{v})| \leq C_{\mathcal{N}} |\mathbf{w}_1 - \mathbf{w}_2|_1 |\mathbf{v}|_1 |\mathbf{z}|_1.$$

3. We have

$$\begin{aligned} \|\Pi \ell\|_{(V_f^0)'} &= \sup_{\mathbf{v} \in V_f^0, \mathbf{v} \neq 0} \frac{\left| -c_f(\widetilde{R}_f^1 \eta; \widetilde{R}_f^1 \eta, \mathbf{v}) + \int_{\Omega_f} \mathbf{f} \cdot \mathbf{v} \right|}{|\mathbf{v}|_1} \\ &\leq \sup_{\mathbf{v} \in V_f^0, \mathbf{v} \neq 0} \frac{C_{\mathcal{N}} |\widetilde{R}_f^1 \eta|_1^2 |\mathbf{v}|_1 + C_{\Omega_f} \|\mathbf{f}\|_0 |\mathbf{v}|_1}{|\mathbf{v}|_1} = C_{\mathcal{N}} |\widetilde{R}_f^1 \eta|_1^2 + C_{\Omega_f} \|\mathbf{f}\|_0. \end{aligned}$$

Conditions  $\alpha_a > 0$  and

$$C_{\mathcal{N}} \frac{\|\Pi \ell\|_{(V_f^0)'}}{\alpha_a^2} < 1$$

are equivalent to

$$C_{\mathcal{N}} |\widetilde{R}_f^1 \eta|_1 < \frac{1}{2} \frac{\kappa_f \nu}{2} \tag{6.19}$$

and

$$3 \left( C_{\mathcal{N}} |\widetilde{R}_f^1 \eta|_1 \right)^2 - 4 \frac{\kappa_f \nu}{2} C_{\mathcal{N}} |\widetilde{R}_f^1 \eta|_1 + \left( \frac{\kappa_f \nu}{2} \right)^2 - C_{\mathcal{N}} C_{\Omega_f} \|\mathbf{f}\|_0 > 0 \tag{6.20}$$

respectively. Condition (6.19) imposes  $(\kappa_f \nu / 2)^2 > C_{\mathcal{N}} C_{\Omega_f} \|\mathbf{f}\|_0$  in (6.20). This condition is (6.16), and, in this case, conditions (6.19) and (6.20) hold if (6.17) is satisfied.

4. Thanks to (6.17) and 1–3,  $a(\cdot; \cdot, \cdot)$  and  $\ell$  satisfy the hypotheses of Theorem A.1, which allows us to conclude that there exists a unique solution  $\mathcal{R}_0^1(\eta) \in V_f^0$  to (6.14).

5. Since the inf-sup condition is satisfied, Theorem A.2 guarantees that there exists a unique solution  $(\mathcal{R}_0^1(\eta), \mathcal{R}_0^2(\eta))$  to (6.12)–(6.13). The thesis follows from (6.11) and from the uniqueness of the operator  $\widetilde{R}_f$  (6.6).  $\square$

**6.1. The interface equation associated to the Navier-Stokes/Darcy problem**

In this section we reformulate the global coupled problem (6.1)–(6.5) as an interface equation depending solely on  $\lambda = (\mathbf{u}_f \cdot \mathbf{n})|_{\Gamma}$ .

We formally define the *non-linear* pseudo-differential operator  $\mathcal{S} : \Lambda_0 \rightarrow \Lambda'_0$ ,

$$\begin{aligned} \langle \mathcal{S}(\eta), \mu \rangle &= a_f(\mathcal{R}_f^1(\eta), R_1 \mu) + c_f(\mathcal{R}_f^1(\eta); \mathcal{R}_f^1(\eta), R_1 \mu) + b_f(R_1 \mu, \mathcal{R}_f^2(\eta)) \\ &+ \int_{\Gamma} \sum_{j=1}^{d-1} \frac{\nu \alpha_{BJ}}{\sqrt{K}} (\mathcal{R}_f^1(\eta) \cdot \boldsymbol{\tau}_j)(R_1 \mu \cdot \boldsymbol{\tau}_j) - \int_{\Omega_f} \mathbf{f} (R_1 \mu) \\ &+ \int_{\Gamma} g(R_p \eta) \mu \quad \forall \eta \in \Lambda_0, \forall \mu \in \Lambda. \end{aligned} \tag{6.21}$$

The operator  $\mathcal{S}$  is composed of two parts: a non-linear component associated to the fluid problem in  $\Omega_f$  (the terms in the first two lines), and the linear part  $S_p$  that we have already studied in Section 5.2 related to the problem in the porous media (corresponding to the last integral). The fluid part extends to the non-linear case the operator  $S_f$  of Section 5.2 and, similarly to  $S_f$ , it plays the role of a non-linear Dirichlet-to-Neumann map that associates at any given normal velocity  $\eta$  on  $\Gamma$  the normal component of the corresponding Cauchy stress tensor on  $\Gamma$ .

We have the following equivalence result, whose proof follows the guidelines of Theorem 5.3.

**Theorem 6.4.** *The solution of (6.1)–(6.5) can be characterized as follows:*

$$\mathbf{u}_f = \mathcal{R}_f^1(\lambda), \quad p_f = \mathcal{R}_f^2(\lambda) + \hat{p}_f, \quad \varphi = R_p \lambda,$$

where  $\hat{p}_f = (\text{meas}(\Omega_f))^{-1} \int_{\Omega_f} p_f$ , and  $\lambda \in \Lambda_0$  is the solution of the non-linear interface problem:

$$\langle \mathcal{S}(\lambda), \mu \rangle = 0 \quad \forall \mu \in \Lambda_0. \tag{6.22}$$

Moreover,  $\hat{p}_f$  can be obtained from  $\lambda$  by solving the algebraic equation

$$\hat{p}_f = (\text{meas}(\Gamma))^{-1} \langle \mathcal{S}(\lambda), \varepsilon \rangle,$$

where  $\varepsilon \in \Lambda$  is a fixed function such that

$$\frac{1}{\text{meas}(\Gamma)} \int_{\Gamma} \varepsilon = 1.$$

Notice that a more useful characterization of the operator  $\mathcal{S}$  can be provided. Indeed, with the special choice  $R_1 = \tilde{R}_f^1$  in (6.21), thanks to (6.7), we obtain

$$b_f(\tilde{R}_f^1 \mu, \mathcal{R}_f^2(\eta)) = 0 \quad \forall \eta, \mu \in \Lambda_0.$$

Moreover, owing to (6.11), for  $\eta, \mu \in \Lambda_0$ , we have

$$\begin{aligned} \langle \mathcal{S}(\eta), \mu \rangle &= a_f(\mathcal{R}_0^1(\eta) + \tilde{R}_f^1 \eta, \tilde{R}_f^1 \mu) + c_f(\mathcal{R}_0^1(\eta) + \tilde{R}_f^1 \eta; \mathcal{R}_0^1(\eta) + \tilde{R}_f^1 \eta, \tilde{R}_f^1 \mu) \\ &\quad + \int_{\Gamma} \sum_{j=1}^{d-1} \frac{\nu \alpha_{BJ}}{\sqrt{K}} ((\mathcal{R}_0^1(\eta) + \tilde{R}_f^1 \eta) \cdot \tau_j) (\tilde{R}_f^1 \mu \cdot \tau_j) \\ &\quad - \int_{\Omega_f} \mathbf{f}(\tilde{R}_f^1 \mu) + \int_{\Gamma} g(R_p \eta) \mu. \end{aligned}$$

By taking  $\mathcal{R}_0^1(\eta) \in H_f^0$  as test function in (6.7), we obtain:

$$a_f(\tilde{R}_f^1 \mu, \mathcal{R}_0^1(\eta)) + b_f(\mathcal{R}_0^1(\eta), R_f^2 \mu) + \int_{\Gamma} \sum_{j=1}^{d-1} \frac{\nu \alpha_{BJ}}{\sqrt{K}} (\tilde{R}_f^1 \mu \cdot \tau_j) (\mathcal{R}_0^1(\eta) \cdot \tau_j) = 0.$$

Finally, since  $R_f^2 \mu \in Q_0$ , owing to (6.12)–(6.13) it follows that

$$a_f(\tilde{R}_f^1 \mu, \mathcal{R}_0^1(\eta)) + \int_{\Gamma} \sum_{j=1}^{d-1} \frac{\nu \alpha_{BJ}}{\sqrt{K}} (\tilde{R}_f^1 \mu \cdot \tau_j) (\mathcal{R}_0^1(\eta) \cdot \tau_j) = 0,$$

so that, for all  $\eta, \mu \in \Lambda_0$ , the operator  $\mathcal{S}$  can be characterized as

$$\begin{aligned} \langle \mathcal{S}(\eta), \mu \rangle &= a_f(\tilde{R}_f^1 \eta, \tilde{R}_f^1 \mu) + c_f(\mathcal{R}_0^1(\eta) + \tilde{R}_f^1 \eta; \mathcal{R}_0^1(\eta) + \tilde{R}_f^1 \eta, \tilde{R}_f^1 \mu) \\ &\quad + \int_{\Gamma} \sum_{j=1}^{d-1} \frac{\nu \alpha_{BJ}}{\sqrt{K}} (\tilde{R}_f^1 \eta \cdot \tau_j) (\tilde{R}_f^1 \mu \cdot \tau_j) - \int_{\Omega_f} \mathbf{f}(\tilde{R}_f^1 \mu) + \int_{\Gamma} g(R_p \eta) \mu. \end{aligned} \quad (6.23)$$

**6.2. Well-posedness of the non-linear interface problem**

We study now the well-posedness of the non-linear interface problem (6.22).

Note that in view of (6.23),  $\mathcal{S}(\lambda)$  is defined in terms of the operator  $\mathcal{R}_0^1(\lambda)$ , which, thanks to (6.12)–(6.13), satisfies in its turn the following problem:

$$a_f(\mathcal{R}_0^1(\lambda), \mathbf{v}) + c_f(\mathcal{R}_0^1(\lambda) + \widetilde{R}_f^1 \lambda; \mathcal{R}_0^1(\lambda) + \widetilde{R}_f^1 \lambda, \mathbf{v}) + \int_{\Gamma} \sum_{j=1}^{d-1} \frac{\nu}{\varepsilon} (\mathcal{R}_0^1(\lambda) \cdot \boldsymbol{\tau}_j)(\mathbf{v} \cdot \boldsymbol{\tau}_j) = \int_{\Omega_f} \mathbf{f} \cdot \mathbf{v} \quad \forall \mathbf{v} \in V_f^0. \quad (6.24)$$

Therefore, in order to prove the existence and uniqueness of the solution of the interface problem, we have to consider (6.22), with the characterization of  $\mathcal{S}$  given in (6.23), coupled with (6.24), i.e., we have to guarantee at once the existence and uniqueness of  $\lambda \in \Lambda_0$  and  $\mathcal{R}_0^1(\lambda) \in V_f^0$ . To this aim we apply Theorem A.1 considering the product space  $\mathcal{W} = \Lambda_0 \times V_f^0$  endowed with the norm:

$$\|\bar{v}\|_{\mathcal{W}} = (|\widetilde{R}_f^1 \mu|_1^2 + |\mathbf{v}|_1^2)^{1/2} \quad \forall \bar{v} = (\mu, \mathbf{v}) \in \mathcal{W}.$$

We introduce the trilinear form and the linear functional associated with our problem in the space  $\mathcal{W}$ . For any fixed  $(\eta, \mathbf{w}) \in \mathcal{W}$ , we define the following operator depending on  $\bar{w}$ :

$$\begin{aligned} \tilde{\mathcal{A}}(\eta, \mathbf{w}) : \mathcal{W} &\rightarrow \mathcal{W}', \\ \langle (\tilde{\mathcal{A}}(\eta, \mathbf{w}))(\xi, \mathbf{u}), (\mu, \mathbf{v}) \rangle &= \langle (\mathcal{A}_f(\eta, \mathbf{w}))(\xi, \mathbf{u}), \mu \rangle + \langle (\mathcal{A}_0(\eta, \mathbf{w}))(\xi, \mathbf{u}), \mathbf{v} \rangle \end{aligned}$$

where, for every test function  $\mu \in \Lambda_0$ ,

$$\begin{aligned} \langle (\mathcal{A}_f(\eta, \mathbf{w}))(\xi, \mathbf{u}), \mu \rangle &= a_f(\widetilde{R}_f^1 \xi, \widetilde{R}_f^1 \mu) + c_f(\mathbf{w} + \widetilde{R}_f^1 \eta; \mathbf{u} + \widetilde{R}_f^1 \xi, \widetilde{R}_f^1 \mu) \\ &+ \int_{\Gamma} \sum_{j=1}^{d-1} \frac{\nu \alpha_{BJ}}{\sqrt{K}} (\widetilde{R}_f^1 \xi \cdot \boldsymbol{\tau}_j)(\widetilde{R}_f^1 \mu \cdot \boldsymbol{\tau}_j) + \int_{\Gamma} g(R_p \xi) \mu, \end{aligned}$$

whereas for any test function  $\mathbf{v} \in V_f^0$ ,

$$\begin{aligned} \langle (\mathcal{A}_0(\eta, \mathbf{w}))(\xi, \mathbf{u}), \mathbf{v} \rangle &= a_f(\mathbf{u}, \mathbf{v}) + c_f(\mathbf{w} + \widetilde{R}_f^1 \eta; \mathbf{u} + \widetilde{R}_f^1 \xi, \mathbf{v}) \\ &+ \int_{\Gamma} \sum_{j=1}^{d-1} \frac{\nu \alpha_{BJ}}{\sqrt{K}} (\mathbf{u} \cdot \boldsymbol{\tau}_j)(\mathbf{v} \cdot \boldsymbol{\tau}_j). \end{aligned}$$

We indicate by  $\tilde{a}$  the form associated to the operator  $\tilde{\mathcal{A}}$ :

$$\tilde{a}(\bar{w}; \bar{u}, \bar{v}) = \langle (\tilde{\mathcal{A}}(\eta, \mathbf{w}))(\xi, \mathbf{u}), (\mu, \mathbf{v}) \rangle,$$

for all  $\bar{w} = (\eta, \mathbf{w}), \bar{u} = (\xi, \mathbf{u}), \bar{v} = (\mu, \mathbf{v}) \in \mathcal{W}$ .



Next, we define two functionals  $\ell_f : \Lambda_0 \rightarrow \mathbb{R}$  and  $\ell_0 : V_f^0 \rightarrow \mathbb{R}$  as:

$$\begin{aligned} \langle \ell_f, \mu \rangle &= \int_{\Omega_f} \mathbf{f} (\widetilde{R}_f^1 \mu) \quad \forall \mu \in \Lambda_0, \\ \langle \ell_0, \mathbf{v} \rangle &= \int_{\Omega_f} \mathbf{f} \mathbf{v} \quad \forall \mathbf{v} \in V_f^0, \end{aligned}$$

and denote

$$\langle \tilde{\ell}, \bar{v} \rangle = \langle \ell_f, \mu \rangle + \langle \ell_0, \mathbf{v} \rangle \quad \forall \bar{v} = (\mu, \mathbf{v}) \in \mathcal{W}.$$

Thus, the problem defined by (6.22) and (6.24) can be reformulated as:

$$\text{find } \bar{u} = (\lambda, \mathcal{R}_0^1(\lambda)) \in \mathcal{W} : \quad \tilde{a}(\bar{u}; \bar{u}, \bar{v}) = \langle \tilde{\ell}, \bar{v} \rangle \quad \forall \bar{v} = (\mu, \mathbf{v}) \in \mathcal{W}. \quad (6.25)$$

We shall prove the existence and uniqueness of the solution only in a closed convex subset of  $\mathcal{W}$ .

**Lemma 6.5.** *Let  $\mathbf{f} \in L^2(\Omega_f)$  be such that*

$$2(1 + \sqrt{2})\sqrt{2C_{\mathcal{N}}C_{\Omega_f}\|\mathbf{f}\|_0} \leq \kappa_f\nu, \quad (6.26)$$

and consider two constants

$$r_m = \frac{C_1 - \sqrt{C_1^2 - 4C_2}}{2} \quad \text{and} \quad r_M = C_1 - \sqrt{\sqrt{2}C_2}, \quad (6.27)$$

where

$$C_1 = \frac{\kappa_f\nu}{4C_{\mathcal{N}}} \quad \text{and} \quad C_2 = \frac{\sqrt{2}C_{\Omega_f}\|\mathbf{f}\|_0}{2C_{\mathcal{N}}}. \quad (6.28)$$

Notice that, thanks to (6.26), there holds

$$0 \leq r_m < r_M. \quad (6.29)$$

If we consider

$$\overline{B}_r = \{\bar{w} = (\eta, \mathbf{w}) \in \mathcal{W} : |\widetilde{R}_f^1 \eta|_1 \leq r\}, \quad (6.30)$$

with

$$r_m < r < r_M, \quad (6.31)$$

then, there exists a unique solution  $\bar{u} = (\lambda, \mathcal{R}_0^1(\lambda)) \in \overline{B}_r$  of (6.25).

*Remark 6.6.* Condition (6.26) is equivalent to

$$C_1^2 \geq \frac{3 + 2\sqrt{2}}{\sqrt{2}}C_2. \quad (6.32)$$

*Proof.* The proof is composed of several parts.

1. For each  $\bar{w} = (\eta, \mathbf{w}) \in \bar{B}_r$  the bilinear form  $\tilde{a}(\bar{w}; \cdot, \cdot)$  is uniformly coercive on  $\mathcal{W}$ .

By definition, for all  $\bar{v} = (\mu, \mathbf{v}) \in \mathcal{W}$  we have

$$\begin{aligned} \tilde{a}(\bar{w}; \bar{v}, \bar{v}) &= a_f(\tilde{R}_f^1 \mu, \tilde{R}_f^1 \mu) + a_f(\mathbf{v}, \mathbf{v}) + \int_{\Gamma} g(R_p \mu) \mu \\ &\quad + c_f(\mathbf{w} + \tilde{R}_f^1 \eta; \mathbf{v} + \tilde{R}_f^1 \mu, \mathbf{v} + \tilde{R}_f^1 \mu) \\ &\quad + \int_{\Gamma} \sum_{j=1}^{d-1} \frac{\nu \alpha_{BJ}}{\sqrt{K}} (\tilde{R}_f^1 \mu \cdot \boldsymbol{\tau}_j) (\tilde{R}_f^1 \mu \cdot \boldsymbol{\tau}_j) + \int_{\Gamma} \sum_{j=1}^{d-1} \frac{\nu \alpha_{BJ}}{\sqrt{K}} (\mathbf{v} \cdot \boldsymbol{\tau}_j) (\mathbf{v} \cdot \boldsymbol{\tau}_j). \end{aligned}$$

Thanks to (5.16), we have  $\int_{\Gamma} g(R_p \mu) \mu \geq 0$ . Using the inequalities (4.19) and (6.15) and the fact that  $\mathbf{w} \in V_f^0$ , we obtain

$$\tilde{a}(\bar{w}; \bar{v}, \bar{v}) \geq \frac{C_k \nu}{2} (|\tilde{R}_f^1 \mu|_1^2 + |\mathbf{v}|_1^2) - 2C_N |\tilde{R}_f^1 \eta|_1 (|\tilde{R}_f^1 \mu|_1^2 + |\mathbf{v}|_1^2).$$

Thus,

$$\tilde{a}(\bar{w}; \bar{v}, \bar{v}) \geq \alpha_{\bar{a}} (|\tilde{R}_f^1 \mu|_1^2 + |\mathbf{v}|_1^2),$$

having set

$$\alpha_{\bar{a}} = \frac{C_k \nu}{2} - 2C_N |\tilde{R}_f^1 \eta|_1. \tag{6.33}$$

Condition  $\alpha_{\bar{a}} > 0$  is equivalent to  $|\tilde{R}_f^1 \eta|_1 < C_1$ , which is satisfied in view of (6.29), (6.27) and (6.31). Thus, the bilinear form  $\tilde{a}(\bar{w}; \cdot, \cdot)$  is uniformly coercive with respect to any  $\bar{w} \in \bar{B}_r$ .

Thanks to the Lax-Milgram Lemma (see, e.g., [109, page 133]) the operator  $\tilde{\mathcal{A}}(\bar{w}) \in \mathcal{L}(\mathcal{W}; \mathcal{W}')$  is invertible for each  $\bar{w} \in \bar{B}_r$ . Moreover, the inverse  $\mathcal{T}(\bar{w}) = (\tilde{\mathcal{A}}(\bar{w}))^{-1}$  belongs to  $\mathcal{L}(\mathcal{W}'; \mathcal{W})$  and satisfies

$$\|\mathcal{T}(\bar{w})\|_{\mathcal{L}(\mathcal{W}'; \mathcal{W})} \leq \frac{1}{\alpha_{\bar{a}}}.$$

Now, we prove that there exists a unique  $\bar{u} \in \bar{B}_r$  such that  $\bar{u} = \mathcal{T}(\bar{u})\tilde{\ell}$ , i.e., (6.25) has a unique solution in  $\bar{B}_r$ .

2.  $\bar{v} \rightarrow \mathcal{T}(\bar{v})\tilde{\ell}$  maps  $\bar{B}_r$  into  $\bar{B}_r$  and is a strict contraction in  $\bar{B}_r$ .

For all  $\bar{v} = (\mu, \mathbf{v}) \in \bar{B}_r$  we have

$$\|\mathcal{T}(\bar{v})\tilde{\ell}\|_{\mathcal{W}} \leq \|\mathcal{T}(\bar{v})\|_{\mathcal{L}(\mathcal{W}'; \mathcal{W})} \|\tilde{\ell}\|_{\mathcal{W}'} \leq \frac{\|\tilde{\ell}\|_{\mathcal{W}'}}{\alpha_{\bar{a}}}.$$

Moreover,

$$\begin{aligned} \|\tilde{\ell}\|_{\mathcal{W}'} &= \sup_{\bar{v} \in \mathcal{W}, \bar{v} \neq 0} \frac{\left| \int_{\Omega_f} \mathbf{f} (\tilde{R}_f^1 \mu) + \int_{\Omega_f} \mathbf{f} \mathbf{v} \right|}{\|\bar{v}\|_{\mathcal{W}}} \\ &\leq C_{\Omega_f} \|\mathbf{f}\|_0 \sup_{\bar{v} \in \mathcal{W}, \bar{v} \neq 0} \frac{|\tilde{R}_f^1 \mu|_1 + |\mathbf{v}|_1}{\|\bar{v}\|_{\mathcal{W}}} \leq \sqrt{2} C_{\Omega_f} \|\mathbf{f}\|_0. \end{aligned} \tag{6.34}$$

From (6.34) and (6.33), corresponding to some  $\bar{w} = (\eta, \mathbf{w}) \in \bar{B}_r$ , condition

$$\frac{\|\tilde{\ell}\|_{\mathcal{W}'}}{\alpha_{\bar{a}}} \leq r$$

is equivalent to

$$r^2 - C_1 r + C_2 \leq 0, \tag{6.35}$$

that is  $r_{min} \leq r \leq r_{max}$  with

$$r_{min} = \frac{C_1 - \sqrt{C_1^2 - 4C_2}}{2} \quad \text{and} \quad r_{max} = \frac{C_1 + \sqrt{C_1^2 - 4C_2}}{2}.$$

Since  $C_1^2 - 4C_2 \geq 0$  from (6.32), for any  $\bar{v} \in \bar{B}_r$  with  $r$  satisfying (6.35),  $\mathcal{T}(\bar{v})\tilde{\ell}$  belongs to  $\bar{B}_r$ .

Finally, to find  $r$  such that the map  $\bar{v} \rightarrow \mathcal{T}(\bar{v})\tilde{\ell}$  is a strict contraction in  $\bar{B}_r$ , we should guarantee (see [74, page 282]) that for any  $\bar{w}_1, \bar{w}_2 \in \bar{B}_r$

$$\|(\mathcal{T}(\bar{w}_1) - \mathcal{T}(\bar{w}_2))\tilde{\ell}\|_{\mathcal{W}} \leq \frac{\|\tilde{\ell}\|_{\mathcal{W}'}}{\alpha_{\bar{a}}^2} L(r) \|\bar{w}_1 - \bar{w}_2\|_{\mathcal{W}} < \|\bar{w}_1 - \bar{w}_2\|_{\mathcal{W}},$$

$L(r)$  being the Lipschitz continuity constant associated to  $\tilde{\mathcal{A}}$ . However,

$$\begin{aligned} | \langle (\tilde{\mathcal{A}}(\bar{w}_1) - \tilde{\mathcal{A}}(\bar{w}_2))(\bar{u}), \bar{v} \rangle | &= |\tilde{a}(\bar{w}_1; \bar{u}, \bar{v}) - \tilde{a}(\bar{w}_2; \bar{u}, \bar{v})| \\ &= |c_f(\mathbf{w}_1 + \tilde{R}_f^1 \eta_1 - (\mathbf{w}_2 + \tilde{R}_f^1 \eta_2); \mathbf{u} + \tilde{R}_f^1 \lambda, \mathbf{v} + \tilde{R}_f^1 \mu)| \\ &\leq C_N |\mathbf{w}_1 + \tilde{R}_f^1 \eta_1 - \mathbf{w}_2 - \tilde{R}_f^1 \eta_2|_1 |\mathbf{u} + \tilde{R}_f^1 \lambda|_1 |\mathbf{v} + \tilde{R}_f^1 \mu|_1 \\ &\leq 2\sqrt{2} C_N \|\bar{w}_1 - \bar{w}_2\|_{\mathcal{W}} \|\bar{u}\|_{\mathcal{W}} \|\bar{v}\|_{\mathcal{W}}, \end{aligned}$$

so that  $L(r) = 2\sqrt{2} C_N$ . Thus, condition

$$\frac{\|\tilde{\ell}\|_{\mathcal{W}'}}{\alpha_{\bar{a}}^2} L(r) < 1$$

is equivalent to

$$r^2 - 2C_1 r + C_1^2 - \sqrt{2} C_2 > 0, \tag{6.36}$$

i.e.,

$$r < r_{MIN} = C_1 - \sqrt{\sqrt{2}C_2} \quad \text{or} \quad r > r_{MAX} = C_1 + \sqrt{\sqrt{2}C_2}.$$

It is easy to see that  $r_{max} < r_{MAX}$ . Consequently, there exists a  $r$  which satisfies (6.35) and (6.36) if and only if  $r_{min} \leq r_{MIN} \leq r_{max}$ , which is equivalent to condition (6.32) or to condition (6.26). Under this condition, any  $r$  in the interval (6.31) with  $r_m = r_{min}$  and  $r_M = r_{MIN}$ , will satisfy both (6.35) and (6.36).

3. The existence and uniqueness of the solution  $\bar{u} = (\lambda, \mathcal{R}_0^1(\lambda)) \in \bar{B}_r$  to (6.25) is now a simple consequence of the Banach contraction theorem (see, e.g., [123]).  $\square$

The following Theorem is a direct consequence of the previous Lemma 6.5.

**Theorem 6.7.** *If (6.26) holds, then problem (6.25) has a unique solution*

$$\bar{u} = (\lambda, \mathcal{R}_0^1(\lambda))$$

in the set

$$B_{r_M} = \{\bar{w} = (\eta, \mathbf{w}) \in W : |\widetilde{R}_f^1 \eta|_1 < r_M\},$$

and it satisfies  $|\widetilde{R}_f^1 \lambda|_1 \leq r_m$ , where  $r_m$  and  $r_M$  are defined in (6.27). In particular, it follows that (6.22) has a unique solution  $\lambda$  in the set  $S_{r_M} = \{\eta \in \Lambda_0 : |\widetilde{R}_f^1 \eta|_1 < r_M\} \subset \Lambda_0$  which indeed belongs to  $S_{r_m} = \{\eta \in \Lambda_0 : |\widetilde{R}_f^1 \eta|_1 \leq r_m\}$ .

*Proof.* Since problem (6.22) has a solution  $\lambda$  if and only if  $\bar{u} = (\lambda, \mathcal{R}_0^1(\lambda))$  is a solution of problem (6.25), we prove only the first part of theorem.

From Lemma 6.5, if (6.26) holds, (6.25) has at least a solution in  $B_{r_M}$  as it has a solution in  $\bar{B}_r \subset B_{r_M}$ , for any  $r_m < r < r_M$ . To prove the uniqueness, let us assume that (6.25) has two solutions  $\bar{u}_1 = (\lambda_1, (\mathcal{R}_0^1(\lambda))_1) \neq \bar{u}_2 = (\lambda_2, (\mathcal{R}_0^1(\lambda))_2)$  in  $B_{r_M}$ . Then,  $r_1 = |\widetilde{R}_f^1 \lambda_1|_1 < r_M$  and  $r_2 = |\widetilde{R}_f^1 \lambda_2|_1 < r_M$ . Therefore, any set  $\bar{B}_r$  with  $\max\{r_m, r_1, r_2\} < r < r_M$  contains two different solutions of problem (6.25). This contradicts the result of Lemma 6.5. Now, let  $\bar{u} = (\lambda, \mathcal{R}_0^1(\lambda))$  be the unique solution of problem (6.25) in  $B_{r_M}$ . According to Lemma 6.5, it belongs to each  $\bar{B}_r \subset B_{r_M}$  with  $r_m < r < r_M$ , and consequently  $|\widetilde{R}_f^1 \lambda|_1 \leq r_m$ .  $\square$

*Remark 6.8.* Notice that condition (6.26) is analogous to that usually required to prove existence and uniqueness of the solution of the Navier-Stokes equations. Moreover, we have proved that the solution is unique in  $S_{r_M}$ . Thus, in view of Remark 6.3, Theorem 6.7 states that the solution is unique only for sufficiently small normal velocities  $\lambda$  across the interface  $\Gamma$ . Finally, notice that (6.26) implies (6.16) and that  $S_{r_m}$  is included in the set (6.17), so that the existence and uniqueness of the non-linear extension  $\mathcal{R}_0^1(\lambda)$  is ensured as well.

*Remark 6.9.* The steady Navier-Stokes/Darcy problem has also been recently studied in [75]. In this case, no multi-domain approach is considered and the analysis of the problem is carried out following the classical theory for non-linear systems (see [74, 42, 35, 36, 37]).

## 7. Finite element approximation of free and groundwater flows

We consider a triangulation  $\mathcal{T}_h$  of the domain  $\bar{\Omega}_f \cup \bar{\Omega}_p$ , depending on a positive parameter  $h > 0$ , made up of triangles if  $d = 2$ , or tetrahedra in the three-dimensional case. As usual, we assume that:

- (i) each triangle or tetrahedra, say  $T$ , is such that  $\text{int}(T) \neq \emptyset$ ;
- (ii)  $\text{int}(T_1) \cap \text{int}(T_2) = \emptyset$  for each pair of different  $T_1, T_2 \in \mathcal{T}_h$ , and if  $T_1 \cap T_2 = F \neq \emptyset$ , then  $F$  is a common face or edge or vertex to  $T_1$  and  $T_2$ ;
- (iii)  $\text{diam}(T) \leq h$  for all  $T \in \mathcal{T}_h$ ;
- (iv)  $\mathcal{T}_h$  is *regular*, that is there exists a constant  $C_{reg} \geq 1$  such that

$$\max_{T \in \mathcal{T}_h} \frac{\text{diam}(T)}{\rho_T} \leq C_{reg} \quad \forall h > 0,$$

with  $\rho_T = \sup\{\text{diam}(B) : B \text{ is a ball contained in } T\}$ ;

- (v) the triangulations  $\mathcal{T}_{fh}$  and  $\mathcal{T}_{ph}$  induced on the subdomains  $\Omega_f$  and  $\Omega_p$  are compatible on  $\Gamma$ , that is they share the same edges (if  $d = 2$ ) or faces (if  $d = 3$ ) therein.

*Remark 7.1.* The case of non-matching grids across the interface  $\Gamma$  for the Stokes-Darcy coupling has been studied in [23, 49, 68, 69, 71, 112, 113]. For a more general overview on non-matching grids approximations see, e.g., the monographs [22, 76, 121].

We shall denote by  $\mathbb{P}_r$ , with  $r$  a non negative integer, the usual space of algebraic polynomials of degree less than or equal to  $r$ .

In the next section, we briefly discuss some possible choices of finite element spaces that may be adopted to compute the solution of the fluid and the porous media problems.

### 7.1. Overview on the classical finite element approximation techniques

The literature on finite elements methods for the (Navier-)Stokes equations is quite broad. The crucial issue concerning the finite dimensional spaces, say  $V_h$  and  $Q_h$ , approximating the spaces of velocity and pressure, respectively, is that they must

satisfy the discrete compatibility condition [29]: there exists a positive constant  $\beta^* > 0$ , independent of  $h$ , such that

$$\forall q_h \in Q_h, \quad \exists \mathbf{v}_h \in V_h, \mathbf{v}_h \neq \mathbf{0} : \quad b_f(\mathbf{v}_h, q_h) \geq \beta^* \|\mathbf{v}_h\|_1 \|q_h\|_0. \quad (7.1)$$

Spaces satisfying (7.1) are said *inf-sup stable*.

Several choices can be made in this direction featuring both discontinuous pressure finite elements (e.g., the  $\mathbb{P}_2 - \mathbb{P}_0$  elements or the Crouzeix-Raviart elements defined using cubic bubble functions) and continuous pressure finite elements: among the latter we recall the Taylor-Hood (or  $\mathbb{P}_2 - \mathbb{P}_1$ ) elements and the  $(\mathbb{P}_1 \text{iso} \mathbb{P}_2) - \mathbb{P}_1$  elements. See, e.g., [109, Chapter 9] or [33, Chapter VI].

Concerning the solution of the Darcy problem (2.5)–(2.6), currently used numerical methods are based on two different approaches that we will briefly discuss in the next sections.

### 7.1.1. DARCY EQUATION AS A SCALAR ELLIPTIC PROBLEM

The first approach that we consider to solve Darcy equations is based on the primal, single field formulation (3.12) for the piezometric head: it amounts to solving a Poisson problem in the unknown  $\varphi$  using classical finite elements spaces and then to recover the velocity field by numerically computing the gradient of  $\varphi$ . This approach may lead to a loss of accuracy, i.e., to lower-order approximations for fluxes than the primal variable; besides, mass conservation is not guaranteed.

However, post-processing techniques for the velocity field based on gradient super convergence phenomena, like those studied by Zienkiewicz and Zhu, have been successfully used to improve accuracy and enforce mass conservation. In [92] it is shown that these methods and their variants may provide higher rates of convergence if compared with the classical displacement or mixed methods.

Let us point out that, in general, the coefficients of the tensor  $\mathbf{K}$  in (3.12) can be oscillatory or discontinuous with large jumps. Indeed, as we have observed in Section 2,  $\mathbf{K}$  depends on the properties of the porous media which may strongly vary in space due to the heterogeneity of subsurface rock formations. The heterogeneity here is presented by the multiscale fluctuations in the permeability of the media. Problems of this kind are referred to as *multiscale problems* in the literature.

Multiscale problems pose several challenges for computational science and engineering. The smaller scales must be well resolved over the range of the larger scales. Multiscale objects must therefore be described by a very large set of unknowns. The larger the range of scales, the more unknowns are needed and the higher the computational costs. Many of these challenges can be met owing to the recent progress in multiscale computational techniques coupled to the capability of the latest generation of computer systems.

Computational multiscale methods can be classified under three different types. In the first class of methods the full multiscale problem is discretized and highly efficient

numerical methods are then applied to accurately compute the full range of scales. Multigrid [9, 28, 102] and multilevel domain decomposition methods [60, 93, 4, 1] are examples of such techniques.

In the second class of multiscale methods only a fraction of the “microscale” space is included in order to reduce the number of unknowns. The microscales and the macroscales are coupled in the same simulation exploiting special properties of the original problem. This means that the method can not be fully general but rather relies on special assumptions on the coefficients. Techniques of this type include variational multiscale methods [80, 81, 34, 116], multiscale finite element methods [78, 79, 65, 44] and heterogeneous multiscale methods [62, 64, 63].

In the last class of multiscale methods the initial elliptic operator is replaced by an upscaled or homogenized operator. These techniques can be understood as more or less sophisticated averaging procedures where small scale variations in the coefficients are replaced by some kind of effective properties in regions that correspond to a grid block in the numerical model [59, 61, 104, 10, 120].

In the following subsections we will give a brief overview of multiscale methods.

**Variational Multiscale Method.** The variational multiscale method was introduced by Hughes, Brezzi et al. in [80, 81, 34]. Let us briefly illustrate it considering the variational problem:

$$\text{find } u \in V : \int_{\Omega} \mathbb{K} \nabla u \cdot \nabla v = \int_{\Omega} f v \quad \forall v \in V, \quad (7.2)$$

where  $V = H_0^1(\Omega)$  and  $\Omega$  is a bounded domain in  $\mathbb{R}^d$  ( $d = 2, 3$ ) with smooth boundary. A conforming Galerkin finite element approximation of (7.2) reads:

$$\text{find } u_R \in V_h : \int_{\Omega} \mathbb{K} \nabla u_R \cdot \nabla v_R = \int_{\Omega} f v_R \quad \forall v_R \in V_h, \quad (7.3)$$

where  $V_h$  is a finite dimensional space  $V_h \subset V$  and  $u_R$  represents the resolvable part of the solution.

Let  $V^b$  be a closed subspace of  $H_0^1(\Omega)$  such that  $V_h \cap V^b = \{0\}$ . Further, we define

$$V^{\oplus} = V_h \oplus V^b. \quad (7.4)$$

This space can be considered as the augmented space of  $V_h$ . Using the decomposition (7.4), we can express any  $v^{\oplus} \in V^{\oplus}$  as the sum of a *resolvable part*  $v_R \in V_h$ , and an *unresolvable part*  $v_U \in V^b$  in a unique way:

$$v^{\oplus} = v_R + v_U \in V_h \oplus V^b.$$

The variational problem (7.3) can be re-formulated as follows:

find  $u_h = u_R + u_U \in V_h \oplus V^b$  such that

$$\int_{\Omega} \mathbb{K} \nabla(u_R + u_U) \cdot \nabla v_R = \int_{\Omega} f v_R \quad \forall v_R \in V_h, \tag{7.5}$$

$$\int_{\Omega} \mathbb{K} \nabla(u_R + u_U) \cdot \nabla v_U = \int_{\Omega} f v_U \quad \forall v_U \in V^b. \tag{7.6}$$

Equation (7.6) can be written as

$$\int_{\Omega} \mathbb{K} \nabla u_U \cdot \nabla v_U = - \int_{\Omega} \mathbb{K} \nabla u_R \cdot \nabla v_U + \int_{\Omega} f v_U \quad \forall v_U \in V^b. \tag{7.7}$$

Problem (7.7) can be “solved” for any  $u_R$  and the solution can be formally written as

$$u_U = \mathcal{L}(-\nabla \cdot (\mathbb{K} \nabla u_R) - f), \tag{7.8}$$

where  $\mathcal{L}$  is a linear solution operator from  $H^{-1}(\Omega)$  to  $H_0^1(\Omega)$  which can also be viewed as the fine grid solution operator (or the discrete Green function operator) acting on the unresolvable scales. Substituting the unresolvable part of the solution (7.8) into (7.5) for the resolvable part, we get

$$\int_{\Omega} \mathbb{K} \nabla u_R \cdot \nabla v_R + \int_{\Omega} \mathbb{K} (\mathcal{L}(-\nabla \cdot (\mathbb{K} \nabla u_R) - f)) \cdot \nabla v_R = \int_{\Omega} f v_R \quad \forall v_R \in V^h. \tag{7.9}$$

The second term on the left in (7.9) represents the contribution of small scales to large scales.

Solving  $u_U$  exactly would be as expensive as solving the fine grid solution globally. In order to localize the computation of  $u_U$ , in [80, 81, 34] it is assumed that

$$V^b = \bigoplus_T H_0^1(T).$$

In other words, only those unresolvable scales that vanish on the boundaries of the grid elements  $T$  are accounted for, in the hope that their effect on  $V_h$  can be representative enough of the effect of all unresolvable scales. This is a quite strong assumption which, however, gives good approximation schemes in many cases. In other cases, as shown by the analysis in [78, 65], this assumption can introduce an  $O(1)$  error, especially near the boundary of each coarse element. Using the assumption  $u_U|_{\partial T} = 0$ ,  $u_U$  can be uniquely decomposed among each element  $T$ :

$$u_U = \sum_T u_{U,T}, \quad u_{U,T} \in H_0^1(T).$$

The variational problem (7.3) then becomes:

find  $u^\oplus = u_R + u_U + \sum_T u_{U,T} \in V_h \oplus V^b$  such that

$$\begin{aligned} \int_{\Omega} \mathbb{K} \nabla(u_R + u_U) \cdot \nabla v_R &= \int_{\Omega} f v_R \quad \forall v_R \in V_h \\ \int_T \mathbb{K} \nabla(u_R + u_{U,T}) \cdot \nabla v_{U,T} &= \int_T f v_{U,T} \quad \forall u_{U,T} \in H_0^1(T), \forall T. \end{aligned}$$



**The multiscale finite element method.** The multiscale finite element method [78, 79, 65] is an extension of an early idea of Babuška [12], which incorporates the fine scale information into the basis functions by solving the original homogeneous fine-scale differential equations on each element with proper boundary conditions. The small scale information is then brought to the large scales through the coupling of the global stiffness matrix. Thus, the effect of the small scales on the large scales is correctly captured. As a consequence, the basis function are adapted to the local properties of the differential operator.

In practical computations a large amount of overhead time comes from constructing the basis functions. In general, these multiscale basis functions are constructed numerically, and since they are independent from each other, they can be constructed in parallel. In many applications it is important to obtain a scaled-up equation from the fine grid equation in order to perform many useful tests in the scale-up (coarse grid) model with different boundary conditions or source terms. The multiscale finite element method can be used for such a purpose [122]. While methods based on homogenization theory are usually limited by restrictive assumptions on the media such as scale separation and periodicity, besides being expensive to use for solving problems with many separate scales, the number of scales is irrelevant for the multiscale finite element method. It is worth to note that multiscale finite element methods have also been developed in their adaptive [2], discontinuous [3] and mixed [5] version.

**Heterogeneous multiscale methods.** There are two main components in the heterogeneous multiscale methods [62, 63, 64]: an overall macroscopic scheme for the macroscale variables on a macroscale grid and estimating the missing macroscopic data from the microscopic model. For (7.2) the macroscopic solver can be chosen simply as the standard piecewise linear finite element method over a macroscopic triangulation  $\mathcal{T}_H$  of mesh size  $H$ . The data that need to be estimated is the stiffness matrix on  $\mathcal{T}_H$ . This is equivalent to evaluating the effective quadratic form  $\int_{\Omega} \mathbf{K} \nabla v_H \cdot \nabla v_H$  for  $v_H \in V_H$ , where  $V_H$  is the macroscopic finite element space.

The heterogeneous multiscale method offers substantial saving of cost compared to solve the full fine scale problems for problems with scale separation.

### 7.1.2. DARCY EQUATION IN MIXED FORM

The second (and more popular) approach for the discretization of the Darcy problem is based on the mixed formulation (2.5)–(2.6), since the latter permits to recover simultaneously both the primal unknown and its gradient with the same order of convergence. Moreover, mass is locally conserved and the continuity of fluxes is preserved.

This approach comprises the so-called mixed (MFE) and mixed-hybrid (MHFE) finite elements, among which we recall the Raviart-Thomas (RT) elements, the Brezzi-Douglas-Marini (BDM) and the Brezzi-Douglas-Fortin-Marini (BDFM) elements, only

to quote the most classical ones (see [33, 111, 118, 100, 101, 30, 31, 32]). In this context we cite also the recent work [96] which presents a new stabilized MFE method without mesh-dependent parameters, and the comparative study [77] concerning the numerical reliability of MFE and MHFE methods applied to porous media flows under the influence of mesh parameters and medium heterogeneity.

Other approaches are based on the Discontinuous Galerkin (DG) methods (see [11, 47]) which are attractive for porous media flow due to their high order convergence property, local conservation of mass, flexibility with respect of meshing and  $hp$ -adaptive refinement, and their robustness with respect to strongly discontinuous coefficients. A numerical comparison between DG and MFE for porous media can be found in [19].

MFE and DG have been also adopted in the recent works [88, 112, 113, 72] for the Stokes/Darcy coupling, and in [75] for the Navier-Stokes/Darcy problem. In particular, in [88] a coupling between inf-sup-stable finite elements for Stokes and MFE for Darcy equations is realized using hanging nodes on the interface  $\Gamma$ . The analysis developed shows that optimal error bounds can be obtained in both the fluid and the porous region.

DG methods based on Interior Penalty are considered in [112, 75] for both the fluid and the groundwater problem, and all unknowns are approximated by totally discontinuous polynomials of different orders.

The two approaches are combined in [113] where the fluid velocity and pressure are obtained by MFE in the porous media region, while they are approximated by DG in the incompressible flow region. Error estimates are derived for two-dimensional problems and the authors point out that non-matching grids on the interface can be used, with the space of discrete normal velocities on  $\Gamma$  playing the role of a mortar space.

The issue of adopting different meshes in the two subdomains has been considered also in [40], where  $\mathbb{P}_1 - \mathbb{P}_0$  finite elements, stabilized through a generalization of the Brezzi-Pitkäranta penalization, have been used for both the fluid and the porous medium, realizing the coupling via a Nitsche method.

A finite element scheme for the approximation of multi-domain heterogeneous problems like Stokes/Darcy has been proposed in [49]. This approach exploits stabilized mixed finite elements together with Nitsche type matching conditions that automatically adapt to the coupling of different subproblem combinations. See also [39, 41, 125].

The original variational multiscale method introduced in [80] that we have recalled above can be extended to the mixed formulation (2.5)–(2.6) to obtain a stabilization technique leading to inf-sup stable velocity and pressure spaces. The key idea of the formulation is still a multiscale splitting of the variables of interest into resolved (grid) scale and unresolved (subgrid) scales. The variational multiscale method provides the theoretical foundation from which stabilization methods such as the algebraic subgrid scales [80] and the orthogonal subgrid scales [48] are derived. For further discussions

on these methods we refer to [107].

Stabilized finite element methods for both Stokes and Darcy problems based on the variational multiscale method can be found in [14].

**7.2. Galerkin finite-element approximation of the Stokes/Darcy problem**

In this section, we present a possible approximation of the Stokes/Darcy problem considering the single field formulation (3.15) for Darcy equation. This approach allows the treatment of the interface conditions as natural conditions for both the fluid and the porous media, as for the continuous case; moreover, this approach will perfectly serve our purpose to characterize iterative substructuring methods to solve the coupled problem.

The setting of the coupled problem is the same as in Section 4.1.

What matters for the analysis we are going to develop, is only to guarantee that the compatibility condition (7.1) holds. Therefore, in the following, for the sake of exposition, we will consider the special choice of piecewise quadratic elements for the velocity components and piecewise linear for the pressure in the fluid domain ( $\mathbb{P}_2 - \mathbb{P}_1$  finite elements), while we shall consider quadratic  $\mathbb{P}_2$  elements for the piezometric head in the porous media domain. For the sake of clarity let us illustrate the degrees of freedom we are considering and how they match across the interface  $\Gamma$ : in Figure 5 we sketch two triangles of a conforming regular mesh and we indicate the degrees of freedom corresponding to the velocity  $\mathbf{u}_f$  and the pressure  $p_f$  in  $\Omega_f$ , and to the piezometric head  $\varphi$  in  $\Omega_p$ .

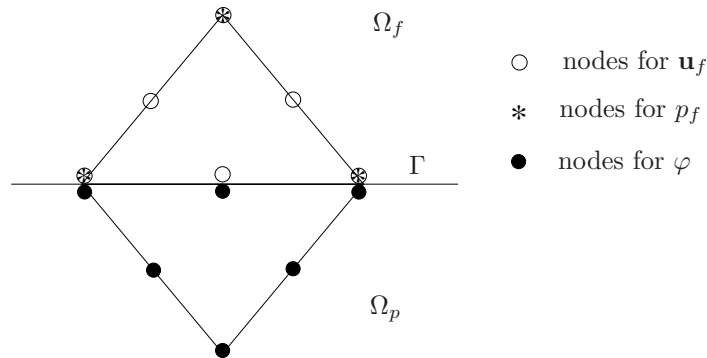


Figure 5 – Degrees of freedom of the finite elements used for approximating velocity, pressure and piezometric head.

We define the discrete spaces:

$$\begin{aligned} V_{fh} &= \{v_h \in X_{fh} : v_h = 0 \text{ on } \Gamma_f^{in}\}, & H_{fh} &= (V_{fh})^d, \quad d = 2, 3, \\ X_{fh} &= \{v_h \in C^0(\overline{\Omega}_f) : v_h = 0 \text{ on } \Gamma_f \text{ and } v_h|_K \in \mathbb{P}_2(K), \forall K \in \mathcal{T}_{fh}\}, \\ \widetilde{H}_{fh} &= (\widetilde{V}_{fh})^d, \quad d = 2, 3, \quad \text{where } \widetilde{V}_{fh} = \{v_h \in X_{fh} : v_h = 0 \text{ on } \Gamma\}, \\ H_{fh}^0 &= \{\mathbf{v}_h \in H_{fh} : \mathbf{v}_h \cdot \mathbf{n} = 0 \text{ on } \Gamma\}, \\ Q_h &= \{q_h \in C^0(\overline{\Omega}_f) : q_h|_K \in \mathbb{P}_1(K), \forall K \in \mathcal{T}_{fh}\}, \\ X_{ph} &= \{\psi_h \in C^0(\overline{\Omega}_p) : \psi_h|_K \in \mathbb{P}_2(K), \forall K \in \mathcal{T}_{ph}\}, \\ H_{ph} &= \{\psi_h \in X_{ph} : \psi_h = 0 \text{ on } \Gamma_p^b\}, & H_{ph}^0 &= \{\psi_h \in H_{ph} : \psi_h = 0 \text{ on } \Gamma\}, \\ W_h &= H_{fh} \times H_{ph}. \end{aligned}$$

Finally, we consider the spaces:

$$\Lambda_h = \{v_h|_\Gamma : v_h \in V_{fh}\} \quad \text{and} \quad \Lambda_{\dagger h} = \{\psi_h|_\Gamma : \psi_h \in X_{ph}\},$$

to approximate the trace spaces  $\Lambda$  and  $H^{1/2}(\Gamma)$  on  $\Gamma$ , respectively.

Now, let us consider the approximation of the boundary data. If we suppose that the Darcy datum  $\varphi_p$  on  $\Gamma_p^b$  belongs to  $\varphi_p \in H^{1/2}(\Gamma_p^b) \cap C^0(\Gamma_p^b)$ , we can take the quadratic interpolant  $\varphi_{ph}$  of its nodal values on  $\Gamma_p^b$ , and then the extension  $E_{ph}\varphi_{ph} \in X_{ph}$ , such that  $E_{ph}\varphi_{ph} = \varphi_{ph}$  at the nodes lying on  $\Gamma_p^b$  and  $E_{ph}\varphi_{ph} = 0$  at the nodes of  $\overline{\Omega}_p \setminus \Gamma_p^b$ .

We can proceed in the same way for the boundary datum  $\mathbf{u}_{in}$  for the Stokes problem, provided it belongs to  $(H^{1/2}(\Gamma_f^{in}))^d \cap (C^0(\Gamma_f^{in}))^d$ . We consider again its quadratic interpolant, say  $\mathbf{u}_{inh}$ , and then its extension

$$E_{fh}\mathbf{u}_{inh} \in \widetilde{H}_{fh}.$$

*Remark 7.2.* The discrete extension operator  $E_{fh}$  is the counterpart of the continuous operator  $E_f$  defined in (4.4). Note that also in this case we could have considered a discrete divergence free extension operator, say  $\widetilde{E}_{fh}$ , corresponding to  $\widetilde{E}_f$  that we have characterized in Remark 4.1. We point out that to define  $\widetilde{E}_{fh}$  we should consider the discrete counterpart of problem (4.5) whose solvability is now guaranteed thanks to (7.1).

The Galerkin approximation of the coupled Stokes/Darcy problem reads:

find  $\underline{\mathbf{u}}_h = (\mathbf{u}_{fh}^0, \varphi_{0h}) \in W_h$  and  $p_{fh} \in Q_h$ :

$$\mathcal{A}(\underline{\mathbf{u}}_h, \underline{\mathbf{v}}_h) + \mathcal{B}(\underline{\mathbf{v}}_h, p_{fh}) = \langle \mathcal{F}^*, \underline{\mathbf{v}}_h \rangle \quad \forall \underline{\mathbf{v}}_h \in W_h, \tag{7.10}$$

$$\mathcal{B}(\underline{\mathbf{u}}_h, q_h) = \langle \mathcal{G}^*, q_h \rangle \quad \forall q_h \in Q_h, \tag{7.11}$$

where

$$\begin{aligned} \langle \mathcal{F}^*, \underline{w} \rangle &= \int_{\Omega_f} \mathbf{f} \mathbf{w} - a_f(E_{fh} \mathbf{u}_{inh}, \mathbf{w}) - g a_p(E_{ph} \varphi_{ph}, \psi) \quad \forall \underline{w} = (\mathbf{w}, \psi) \in W, \\ \langle \mathcal{G}^*, q \rangle &= -b_f(E_{fh} \mathbf{u}_{inh}, q) \quad \forall q \in Q. \end{aligned}$$

The existence, uniqueness and stability of the discrete solution of (7.10)–(7.11) can be proved following the same steps of the continuous case, using in addition the fact that the spaces  $H_{fh}$  and  $Q_h$  satisfy the inf-sup condition (7.1).

The following error estimates hold. Let  $\underline{u} = (\mathbf{u}_f^0, \varphi_0) \in W$ ,  $p_f \in Q$  be the solutions to (4.13)–(4.14). Then, (see [29, 33])

$$\|\underline{u} - \underline{u}_h\|_W \leq \left(1 + \frac{\gamma}{\alpha}\right) \inf_{\underline{v}_h \in X_h^0} \|\underline{u} - \underline{v}_h\|_W + \frac{1}{\alpha} \inf_{q_h \in Q_h} \|p_f - q_h\|_0 \quad (7.12)$$

and

$$\|p_f - p_{fh}\|_0 \leq \frac{\gamma}{\beta^*} \left(1 + \frac{\gamma}{\alpha}\right) \inf_{\underline{v}_h \in X_h^0} \|\underline{u} - \underline{v}_h\|_W + \left(1 + \frac{1}{\beta^*} + \frac{\gamma}{\alpha\beta^*}\right) \|p - q_h\|_0, \quad (7.13)$$

where  $\gamma$  and  $\alpha$  are the  $h$ -independent continuity and coercivity constants of the bilinear form  $\mathcal{A}(\cdot, \cdot)$  defined in (4.18) and (4.20), respectively. Finally  $X_h^0$  is the discrete space

$$X_h^0 = \{\underline{v}_h \in W_h : \mathcal{B}(\underline{v}_h, q_h) = 0 \quad \forall q_h \in Q_h\}.$$

We remark that since constants  $\alpha$ ,  $\gamma$  and  $\beta^*$  are all independent of the discretization parameter  $h$ , (7.12) and (7.13) give optimal convergence estimates.

*Remark 7.3.* Notice that in addition to the discrete inf-sup condition (7.1), no further compatibility condition is required for the discrete spaces  $H_{fh}$  and  $H_{ph}$ . In fact, the mixed coupling terms on the interface appearing in the definition of the bilinear form  $\mathcal{A}(\cdot, \cdot)$ :

$$\int_{\Gamma} g \varphi_h(\mathbf{w}_h \cdot \mathbf{n}) - \int_{\Gamma} g \psi_h(\mathbf{v}_h \cdot \mathbf{n}),$$

give null contribution when we consider  $\mathbf{w}_h = \mathbf{v}_h$  and  $\psi_h = \varphi_h$ .

Finally, let us underline that in the finite-element approximation, the coupling condition (3.16), which imposes the continuity of normal velocity across the interface, has to be intended in the sense of the  $L^2(\Gamma)$ -projection on the finite element space  $H_{ph}$  on  $\Gamma$ . In fact, in (7.10) we are imposing

$$\int_{\Gamma} (-K \partial_n \varphi_h - \mathbf{u}_{fh} \cdot \mathbf{n}) \psi_h|_{\Gamma} = 0 \quad \forall \psi_h \in H_{ph}.$$

### 7.3. Algebraic formulation of the linear coupled problem

We introduce the following bases for the finite dimensional spaces  $H_{fh}$ ,  $Q_h$  and  $H_{ph}$ , respectively. Let  $N_f = \dim(H_{fh})$ ,  $N_q = \dim(Q_h)$  and  $N_p = \dim(H_{ph})$  and let  $N_\Gamma$  denote the number of nodes lying on the interface  $\Gamma$ . Then,

- (i)  $\{\omega_i\}_{i=1}^{N_f}$  is a basis for  $H_{fh}$ ;
- (ii)  $\{\pi_j\}_{j=1}^{N_q}$  is a basis for  $Q_h$ ;
- (iii)  $\{\phi_k\}_{k=1}^{N_p}$  is a basis for  $H_{ph}$ .

We can express the unknowns  $\mathbf{u}_{fh}^0$ ,  $p_{fh}$  and  $\varphi_{0h}$  as linear combinations with respect to these bases. In particular,

$$\mathbf{u}_{fh}^0 = \sum_{j=1}^{N_f} (\mathbf{u}_{fh}^0)^j \omega_j, \quad p_{fh} = \sum_{j=1}^{N_q} (p_{fh})^j \pi_j, \quad \varphi_{0h} = \sum_{j=1}^{N_p} (\varphi_{0h})^j \phi_j, \quad (7.14)$$

where  $(\mathbf{u}_{fh}^0)^j$ ,  $(p_{fh})^j$ ,  $(\varphi_{0h})^j$  denote the coefficients of the linear expansions.

Remark that  $(p_{fh})^j$ ,  $(\varphi_{0h})^j \in \mathbb{R}$ , while, for any fixed  $1 \leq j \leq N_f$ ,  $(\mathbf{u}_{fh}^0)^j$  is the  $d$ -uple of  $\mathbb{R}^d$ :  $((\mathbf{u}_{fh}^0)^j_1, \dots, (\mathbf{u}_{fh}^0)^j_d)^T$  such that  $(\mathbf{u}_{fh}^0)^j \omega_j$  is the vector  $((\mathbf{u}_{fh}^0)^j_1(\omega_j)_1, \dots, (\mathbf{u}_{fh}^0)^j_d(\omega_j)_d)^T$ ,  $(\omega_j)_i$  being the  $i$ -th component of  $\omega_j$ .

Now, we consider equation (7.10) and choose as test functions the basis functions of  $H_{fh}$  associated with the internal nodes of  $\Omega_f$ , say  $\omega_i$  for  $i = 1, \dots, N_f - N_\Gamma$ . We also suppose to have reordered these basis functions in such a way that the last  $N_\Gamma$  are associated to the nodes on  $\Gamma$ , and we distinguish them with the notation  $\omega_i^\Gamma$ . Therefore, thanks to (7.14), we have:

$$\begin{aligned} & \sum_{j=1}^{N_f - N_\Gamma} a_f(\omega_j, \omega_i) (\mathbf{u}_{fh}^0)^j + \sum_{j=1}^{N_\Gamma} \sum_{k=1}^{d-1} a_f((\omega_j^\Gamma \cdot \boldsymbol{\tau}_k), \omega_i) (\mathbf{u}_{fh}^0 \cdot \boldsymbol{\tau}_k)^j \\ & + \sum_{j=1}^{N_\Gamma} a_f((\omega_j^\Gamma \cdot \mathbf{n}), \omega_i) (\mathbf{u}_{fh}^0 \cdot \mathbf{n})^j + \sum_{j=1}^{N_q} b_f(\omega_i, \pi_j) (p_{fh})^j \\ & = \int_{\Omega_f} \mathbf{f} \omega_i - a_f(E_{fh} \mathbf{u}_{inh}, \omega_i), \quad i = 1, \dots, N_f - N_\Gamma. \end{aligned}$$

By  $\mathbf{u}_{int}$  we indicate the vector of the values of the unknown  $\mathbf{u}_{fh}^0$  at the nodes of  $\Omega_f \setminus \Gamma$  plus those of  $(\mathbf{u}_{fh}^0 \cdot \boldsymbol{\tau}_k)$  at the nodes lying on the interface  $\Gamma$ . Moreover,  $\mathbf{u}_\Gamma$  indicates the vector of the values of  $(\mathbf{u}_{fh}^0 \cdot \mathbf{n})$  at the nodes of  $\Gamma$ . Finally,  $\mathbf{p}$  is the vector of the values of the unknown pressure  $p_{fh}$  at the nodes of  $\Omega_f$ .

Then, we can write the following compact form (with obvious choice of notation for the matrices and the right hand side):

$$A_{ff} \mathbf{u}_{int} + A_{f\Gamma} \mathbf{u}_\Gamma + B^T \mathbf{p} = \mathbf{f}_f.$$

We consider again equation (7.10), however we choose as test functions  $\omega_i^\Gamma$ ,  $i = 1, \dots, N_\Gamma$ , associated to the nodes on  $\Gamma$ . Then, we obtain:

$$\begin{aligned} & \sum_{j=1}^{N_f - N_\Gamma} a_f(\omega_j, \omega_i^\Gamma)(\mathbf{u}_{fh}^0)^j + \sum_{j=1}^{N_\Gamma} \sum_{k=1}^{d-1} a_f((\omega_j^\Gamma \cdot \boldsymbol{\tau}_k), \omega_i^\Gamma)(\mathbf{u}_{fh}^0 \cdot \boldsymbol{\tau}_k)^j \\ & + \sum_{j=1}^{N_\Gamma} \int_\Gamma \left( \sum_{k=1}^{d-1} \frac{\nu \alpha_{BJ}}{\sqrt{K}} (\omega_i^\Gamma \cdot \boldsymbol{\tau}_k)(\omega_j^\Gamma \cdot \boldsymbol{\tau}_k) \right) (\mathbf{u}_{fh}^0)^j \\ & + \sum_{j=1}^{N_\Gamma} a_f(\omega_j^\Gamma \cdot \mathbf{n}, \omega_i^\Gamma)(\mathbf{u}_{fh}^0 \cdot \mathbf{n})^j \\ & + \sum_{j=1}^{N_q} b_f(\omega_i^\Gamma, \pi_j)(p_{fh})^j + \sum_{j=1}^{N_\Gamma} \left( \int_\Gamma g \phi_j^\Gamma(\omega_i^\Gamma \cdot \mathbf{n}) \right) (\varphi_{0h})^j \\ & = \int_{\Omega_f} \mathbf{f} \omega_i^\Gamma - a_f(E_{fh} \mathbf{u}_{inh}, \omega_i^\Gamma), \end{aligned}$$

where  $\phi_j^\Gamma$  denotes the functions of the basis of  $H_{ph}$  associated to the interface nodes.

In compact form we get:

$$A_{\Gamma f} \mathbf{u}_{int} + A_{\Gamma \Gamma}^f \mathbf{u}_\Gamma + B_{f\Gamma}^T \mathbf{p} + M_{\Gamma \Gamma} \boldsymbol{\phi} = \mathbf{f}_\Gamma.$$

Now, we consider for (7.10) the test functions  $\phi_i$ ,  $i = 1, \dots, N_p - N_\Gamma$ , associated to the internal nodes of domain  $\Omega_p$ . Again, we suppose the last  $N_\Gamma$  functions  $\{\phi_i^\Gamma\}_{i=1}^{N_\Gamma}$  to correspond to the nodes on  $\Gamma$ . We find:

$$\sum_{j=1}^{N_p - N_\Gamma} g a_p(\phi_j, \phi_i) (\varphi_{0h})^j + \sum_{j=1}^{N_\Gamma} g a_p(\phi_j^\Gamma, \phi_i) (\varphi_{0h})^j = -g a_p(E_{ph} \varphi_{ph}, \phi_i).$$

Let  $\boldsymbol{\phi}_{int}$  indicate the vector of the values of the piezometric head  $\varphi_{0h}$  at the nodes on  $\Omega_p \setminus \Gamma$ , and  $\boldsymbol{\phi}_\Gamma$  those at the nodes on  $\Gamma$ . Therefore, we have the compact form:

$$A_{pp} \boldsymbol{\phi}_{int} + A_{p\Gamma} \boldsymbol{\phi}_\Gamma = \mathbf{f}_p.$$

If we consider the test functions  $\phi_i^\Gamma$ , associated to the nodes on  $\Gamma$ , we have:

$$\begin{aligned} & \sum_{j=1}^{N_p - N_\Gamma} g a_p(\phi_j, \phi_i^\Gamma) (\varphi_{0h})^j + \sum_{j=1}^{N_\Gamma} g a_p(\phi_j^\Gamma, \phi_i^\Gamma) (\varphi_{0h})^j \\ & + \sum_{j=1}^{N_\Gamma} \left( - \int_\Gamma g \phi_i^\Gamma(\omega_j^\Gamma \cdot \mathbf{n}) \right) (\mathbf{u}_{fh}^0 \cdot \mathbf{n})^j = -g a_p(E_{ph} \varphi_{ph}, \phi_i^\Gamma), \end{aligned}$$

that in compact form becomes

$$A_{p\Gamma}^T \boldsymbol{\phi}_{int} + A_{\Gamma \Gamma}^p \boldsymbol{\phi}_\Gamma - M_{\Gamma \Gamma}^T \mathbf{u}_\Gamma = \mathbf{f}_{p\Gamma}.$$

Finally, we consider equation (7.11). Choosing the test functions  $\pi_i, i = 1, \dots, N_q$ , we have:

$$\sum_{j=1}^{N_f-N_\Gamma} b_f(\boldsymbol{\omega}_j, \pi_i)(\mathbf{u}_{fh}^0)^j + \sum_{j=1}^{N_\Gamma} \sum_{k=1}^{d-1} b_f(\boldsymbol{\omega}_j^\Gamma \cdot \boldsymbol{\tau}_k, \pi_i)(\mathbf{u}_{fh}^0 \cdot \boldsymbol{\tau}_k)^j + \sum_{j=1}^{N_\Gamma} b_f(\boldsymbol{\omega}_j^\Gamma \cdot \mathbf{n}, \pi_i)(\mathbf{u}_{fh}^0 \cdot \mathbf{n})^j = -b_f(E_{fh} \mathbf{u}_{inh}, \pi_i),$$

or in compact form:

$$\mathbf{B}_1 \mathbf{u}_{int} + \mathbf{B}_{f\Gamma} \mathbf{u}_\Gamma = \mathbf{f}_{in}.$$

Using the notation introduced above, we can then reformulate problem (7.10)–(7.11) in matrix form

$$\begin{pmatrix} A_{ff} & \mathbf{B}^T & A_{f\Gamma} & 0 & 0 \\ \mathbf{B}_1 & 0 & \mathbf{B}_{f\Gamma} & 0 & 0 \\ A_{\Gamma f} & \mathbf{B}_{f\Gamma}^T & A_{\Gamma\Gamma}^f & \mathbf{M}_{\Gamma\Gamma} & 0 \\ 0 & 0 & -\mathbf{M}_{\Gamma\Gamma}^T & A_{p\Gamma}^p & A_{p\Gamma}^T \\ 0 & 0 & 0 & A_{p\Gamma} & A_{pp} \end{pmatrix} \begin{pmatrix} \mathbf{u}_{int} \\ \mathbf{p} \\ \mathbf{u}_\Gamma \\ \phi_\Gamma \\ \phi_{int} \end{pmatrix} = \begin{pmatrix} \mathbf{f}_f \\ \mathbf{f}_{in} \\ \mathbf{f}_\Gamma \\ \mathbf{f}_{p\Gamma} \\ \mathbf{f}_p \end{pmatrix}. \tag{7.15}$$

The matrix of the linear system (7.15) is non-singular, and generally it is large and sparse. To effectively solve this system using an iterative method, a preconditioning strategy is thus in order. The characterization of suitable preconditioners will make the object of the next sections.

Remark that the coupling between Stokes and Darcy equations is realized at this algebraic stage through the third and the fourth rows of the global matrix. In particular, the submatrices  $\mathbf{M}_{\Gamma\Gamma}$  and  $-\mathbf{M}_{\Gamma\Gamma}^T$  impose the algebraic counterpart of the coupling conditions (3.17) and (3.16), respectively.

### 8. Iterative subdomain methods for the Stokes/Darcy problem

The theory developed for the Steklov-Poincaré operators associated to the exact Stokes/Darcy problem (see Sects. 5-5.2) can be adapted to investigate the Galerkin finite element approximation (7.10)–(7.11). This will allow us to characterize suitable discrete operators that are crucial to set up effective iterative schemes to solve (7.15).

#### 8.1. Interface problem for the discrete normal velocity

We follow the guidelines of Sects. 5 and 5.1 to derive the discrete interface equation corresponding to (5.21). Details can be found in [53].



First of all, we point out that the coupled problem (7.10)–(7.11) may be rewritten in the following multi-domain formulation.

**Proposition 8.1.** *Using the simplified condition  $\mathbf{u}_{fh} \cdot \boldsymbol{\tau}_j = 0$  on  $\Gamma$ , problem (7.10)–(7.11) can be formulated in an equivalent way as follows:*

find  $\mathbf{u}_{fh}^0 \in H_{fh}^\tau$ ,  $p_{fh} \in Q_h$ ,  $\varphi_{0h} \in H_{ph}$  such that

$$a_f(\mathbf{u}_{fh}^0 + E_{fh}\mathbf{u}_{inh}, \mathbf{w}_h) + b_f(\mathbf{w}_h, p_{fh}) = \int_{\Omega_f} \mathbf{f} \cdot \mathbf{w}_h \quad \forall \mathbf{w}_h \in \widetilde{H}_{fh}^0 \quad (8.1)$$

$$b_f(\mathbf{u}_{fh}^0 + E_{fh}\mathbf{u}_{inh}, q_h) = 0 \quad \forall q_h \in Q_h \quad (8.2)$$

$$a_p(\varphi_{0h} + E_{ph}\varphi_{ph}, \psi_h) = 0 \quad \forall \psi_h \in H_{ph}^0 \quad (8.3)$$

$$\int_{\Gamma} n(\mathbf{u}_{fh}^0 \cdot \mathbf{n})\mu_h = a_p(\varphi_{0h} + E_{ph}\varphi_{ph}, R_{2h}\mu_h) \quad \forall \mu_h \in \Lambda_h \quad (8.4)$$

$$\int_{\Gamma} g\varphi_{0h}\mu_h = \int_{\Omega_f} \mathbf{f} \cdot (R_{1h}^\tau\mu_h) - a_f(\mathbf{u}_{fh}^0 + E_{fh}\mathbf{u}_{inh}, R_{1h}^\tau\mu_h) - b_f(R_{1h}^\tau\mu_h, p_{fh}) \quad \forall \mu_h \in \Lambda_h, \quad (8.5)$$

where we have introduced the finite element spaces

$$H_{fh}^\tau = \{\mathbf{v}_h \in H_{fh} : \mathbf{v}_h \cdot \boldsymbol{\tau}_j = 0 \text{ on } \Gamma\} \text{ and } \widetilde{H}_{fh}^0 = \{\mathbf{v}_h \in H_{fh} : \mathbf{v}_h = \mathbf{0} \text{ on } \Gamma\}.$$

Moreover,  $R_{1h}^\tau$  can be any possible continuous extension operator from  $\Lambda_h$  to  $H_{fh}^\tau$  such that  $R_{1h}^\tau\mu_h \cdot \mathbf{n} = \mu_h$  on  $\Gamma$  for all  $\mu_h \in \Lambda_h$ , and  $R_{2h}$  can be any possible continuous extension operator from  $\Lambda_{\dagger h}$  to  $H_{ph}$  such that  $R_{2h}\mu_h = \mu_h$  on  $\Gamma$  for all  $\mu_h \in \Lambda_{\dagger h}$ .

*Proof.* The proof follows the same guidelines as in the continuous case, thus we refer the reader to Proposition 5.1. □

As done in the continuous case, let us choose as interface variable the trace  $\lambda_h$  of the normal velocity on  $\Gamma$ :

$$\lambda_h = \mathbf{u}_{fh} \cdot \mathbf{n} \text{ on } \Gamma.$$

Then, from (7.2) we obtain

$$\int_{\Gamma} (-K\partial_n\varphi_h - \lambda_h)\psi_h|_{\Gamma} = 0 \quad \forall \psi_h \in H_{ph}.$$

If  $\int_{\Gamma_f^{in}} \mathbf{u}_{inh} \cdot \mathbf{n} \neq 0$ , we introduce a function  $\lambda_{*h} \in \Lambda_h$ ,  $\lambda_{*h} = \tilde{c}_*\gamma_h$  where  $\gamma_h$  is a piecewise linear function on  $\Gamma$  such that  $\gamma_h(\mathbf{x}) = 0$  if  $\mathbf{x}$  is a node on  $\partial\Gamma$  and  $\gamma_h(\mathbf{x}) = 1$  if  $\mathbf{x}$  is a node on  $\Gamma \setminus \partial\Gamma$ , while  $\tilde{c}_* \in \mathbb{R}$  is defined as

$$\tilde{c}_* = - \frac{\int_{\Gamma_f^{in}} \mathbf{u}_{inh} \cdot \mathbf{n}_f}{\int_{\Gamma} \gamma_h}.$$

Then

$$\int_{\Gamma} \lambda_{*h} = - \int_{\Gamma_f^{in}} \mathbf{u}_{inh} \cdot \mathbf{n}_f . \tag{8.6}$$

We introduce the space

$$\Lambda_{0h} = \left\{ \mu_h \in \Lambda_h : \int_{\Gamma} \mu_h = 0 \right\} ,$$

and we define the following extension operators:

$$R_{fh} : \Lambda_{0h} \rightarrow H_{fh}^{\tau} \times Q_{0h}, \quad \eta_h \rightarrow R_{fh}\eta_h = (R_{fh}^1\eta_h, R_{fh}^2\eta_h),$$

such that  $(R_{fh}^1\eta_h) \cdot \mathbf{n} = \eta_h$  on  $\Gamma$  and

$$\begin{aligned} a_f(R_{fh}^1\eta_h, \mathbf{w}_h) + b_f(\mathbf{w}_h, R_{fh}^2\eta_h) &= 0 \quad \forall \mathbf{w}_h \in H_{fh}^0, \\ b_f(R_{fh}^1\eta_h, q_h) &= 0 \quad \forall q_h \in Q_{0h}, \end{aligned}$$

and

$$R_{ph} : \Lambda_{0h} \rightarrow H_{ph}, \quad \eta_h \rightarrow R_{ph}\eta_h,$$

such that

$$a_p(R_{ph}\eta_h, R_{2h}\mu_h) = \int_{\Gamma} n\eta_h\mu_h \quad \forall \mu_h \in \Lambda_{\dagger h}, \tag{8.7}$$

where  $R_{2h}$  is the extension operator introduced in Proposition 8.1.

Now we can define the *discrete Steklov-Poincaré* operator  $S_h : \Lambda_{0h} \rightarrow \Lambda'_h$ , for all  $\eta_h \in \Lambda_{0h}$  and for all  $\mu_h \in \Lambda_h$ , as follows:

$$\langle S_h\eta_h, \mu_h \rangle = a_f(R_{fh}^1\eta_h, R_{1h}^{\tau}\mu_h) + b_f(R_{1h}^{\tau}\mu_h, R_{fh}^2\eta_h) + \int_{\Gamma} g(R_{ph}\eta_h)\mu_h.$$

$S_h$  can be split as sum of two suboperators  $S_h = S_{fh} + S_{ph}$ , associated with the Stokes and Darcy problems, respectively, and defined respectively by

$$\langle S_{fh}\eta_h, \mu_h \rangle = a_f(R_{fh}^1\eta_h, R_{1h}^{\tau}\mu_h) + b_f(R_{1h}^{\tau}\mu_h, R_{fh}^2\eta_h), \tag{8.8}$$

$$\langle S_{ph}\eta_h, \mu_h \rangle = \int_{\Gamma} g(R_{ph}\eta_h)\mu_h,$$

for all  $\eta_h \in \Lambda_{0h}$ ,  $\mu_h \in \Lambda_h$ .

Finally, let  $\chi_h$  be the linear functional which represents the Galerkin counterpart of (5.19).

A reinterpretation of problem (8.1)–(8.5) in terms of a Steklov-Poincaré discrete interface problem is provided by the following result, which is the discrete counterpart of Theorem 5.3.

**Theorem 8.2.** *The solution to (8.1)–(8.5) can be characterized as follows:*

$$\begin{aligned} \mathbf{u}_{fh}^0 &= \boldsymbol{\omega}_{0h}^* + R_{fh}^1 \lambda_{0h} + E_{\Gamma h} \lambda_{*h}, & p_{fh} &= \pi_h^* + R_{fh}^2 \lambda_{0h} + \hat{p}_{fh}, \\ \varphi_{0h} &= \varphi_{0h}^* + R_{ph} \lambda_{0h}, \end{aligned}$$

where  $\hat{p}_{fh} = (\text{meas}(\Omega_f))^{-1} \int_{\Omega_f} p_h$ , and  $\lambda_{0h} \in \Lambda_{0h}$  is the solution of the discrete Steklov-Poincaré interface problem:

$$\langle S_h \lambda_{0h}, \mu_{0h} \rangle = \langle \chi_h, \mu_{0h} \rangle \quad \forall \mu_{0h} \in \Lambda_{0h}. \tag{8.9}$$

Moreover,  $\hat{p}_{fh}$  can be obtained from  $\lambda_{0h}$  by solving the algebraic equation

$$\hat{p}_{fh} = \frac{1}{\text{meas}(\Gamma)} \langle S_h \lambda_{0h} - \chi_h, \zeta_h \rangle,$$

where  $\zeta_h \in \Lambda_h$  is a given function that satisfies

$$\frac{1}{\text{meas}(\Gamma)} \int_{\Gamma} \zeta_h = 1.$$

**8.2. Analysis of the discrete Steklov-Poincaré operators  $S_{fh}$  and  $S_{ph}$**

Let us investigate some properties of the discrete Steklov-Poincaré operators  $S_{fh}$ ,  $S_{ph}$  and  $S_h$  that will allow us to prove existence and uniqueness for problem (8.9). Since their proof is similar to the one of the continuous case, we shall only sketch them, referring to Lemma 5.4 for more details.

**Lemma 8.3.** *The discrete Steklov–Poincaré operators enjoy the following properties:*

- (i)  $S_{fh}$  and  $S_{ph}$  are linear continuous operators on  $\Lambda_{0h}$ , i.e.,  $S_{fh} \eta_h \in \Lambda'_0$ ,  $S_{ph} \eta_h \in \Lambda'_0$ ,  $\forall \eta_h \in \Lambda_{0h}$ ;
- (ii)  $S_{fh}$  is symmetric and coercive;
- (iii)  $S_{ph}$  is symmetric and positive;
- (iv)  $S_h$  and  $S_{fh}$  are uniformly spectrally equivalent, i.e., there exist two constants  $\hat{k}_1$  and  $\hat{k}_2$  independent of  $h$ , such that  $\forall \eta_h \in \Lambda_h$ ,

$$\hat{k}_1 \langle S_{fh} \eta_h, \eta_h \rangle \leq \langle S_h \eta_h, \eta_h \rangle \leq \hat{k}_2 \langle S_{fh} \eta_h, \eta_h \rangle.$$

*Proof.* 1. Making the special choice  $R_{1h}^\tau = R_{fh}^1$ , the operator  $S_{fh}$  can be represented as follows

$$\langle S_{fh} \eta_h, \mu_h \rangle = a_f(R_{fh}^1 \eta_h, R_{fh}^1 \mu_h) \quad \forall \eta_h, \mu_h \in \Lambda_{0h}. \tag{8.10}$$

Now, proceeding as done at point 1. of Lemma 5.4, we can define the function  $\mathbf{z}_h(\mu_h) = R_{fh}^1 \mu_h - \mathcal{H}_h \mu_h \in \widehat{H}_{fh}^0$ ,  $\mathcal{H}_h$  being the Galerkin approximation of the harmonic extension operator defined in (5.25).

Using the inf-sup condition (5.3.43) of [109, page 173], we have for all  $\mu_h \in \Lambda_{0h}$

$$\|R_{fh}^2 \mu_h\|_0 \leq \frac{\nu}{\beta^*} \|R_{fh}^1 \mu_h\|_1,$$

and therefore

$$\|R_{fh}^1 \mu_h\|_1 \leq (1 + C_{\Omega_f}) \left(1 + \frac{1}{\beta^*}\right) \|\mathcal{H}_h \mu_h\|_1, \quad (8.11)$$

$C_{\Omega_f}$  being a positive constant due to the Poincaré inequality. Now, thanks to the Uniform Extension Theorem (see [109, Theorem 4.1.3] and [94]), there exists a positive constant  $C_{|\Omega_f|} > 0$ , depending on the measure of the subdomain  $\Omega_f$ , but independent of the parameter  $h$ , such that

$$\|\mathcal{H}_h \mu_h\|_1 \leq C_{|\Omega_f|} \|\mu_h\|_\Lambda \quad \forall \mu_h \in \Lambda_h.$$

Therefore, (8.11) yields  $\forall \mu_h \in \Lambda_{0h}$

$$\|R_{fh}^1 \mu_h\|_1 \leq C_{|\Omega_f|} (1 + C_{\Omega_f}) \left(1 + \frac{1}{\beta^*}\right) \|\mu_h\|_\Lambda. \quad (8.12)$$

From (8.12) we deduce the continuity of  $S_{fh}$ :

$$|\langle S_{fh} \mu_h, \eta_h \rangle| \leq \hat{\beta}_f \|\mu_h\|_\Lambda \|\eta_h\|_\Lambda,$$

where  $\hat{\beta}_f$  is the following positive constant, independent of  $h$ ,

$$\hat{\beta}_f = \nu \left[ C_{|\Omega_f|} (1 + C_{\Omega_f}) \left(1 + \frac{1}{\beta^*}\right) \right]^2. \quad (8.13)$$

Proceeding as for the continuous case, we can prove that  $S_{ph}$  is continuous with constant  $\beta_p$ , independent of  $h$ , defined in (5.31).

2.  $S_{fh}$  is symmetric thanks to (8.10) and the proof of its coercivity follows the one in the continuous case, the coercivity constant  $\alpha_f$  being the same (see (5.32)).
3. This property follows from point 3. of the proof of Lemma 5.4.  $\square$

*Remark 8.4.* Notice that the discrete operator  $S_{ph}$  is actually coercive (see, e.g., [45, 7]); however, its coercivity constant, say  $\alpha_{ph} > 0$  depends on  $h$  and, in particular, it vanishes as  $h \rightarrow 0$ . Since we are primarily looking for preconditioners for the interface problem (8.9) which are optimal with respect to  $h$ , we will not consider  $S_{ph}$  as a possible preconditioner any longer.

*Remark 8.5.* Thanks to Lax-Milgram Lemma (see, e.g., [109, page 133]), Lemma 8.3 guarantees that the discrete Steklov-Poincaré equation (8.9) has a unique solution.

**8.3. Algebraic formulation of the discrete Steklov-Poincaré operator  $S_h$**

We consider the linear system (7.15) and we set  $\mathbf{u}_f = (\mathbf{u}_{int}, \mathbf{p})^T$  and  $\phi = (\phi_\Gamma, \phi_{int})^T$ . Then, with obvious choice of notation, we can rewrite (7.15) in the following block form:

$$\begin{pmatrix} F & F_\Gamma^1 & 0 \\ F_\Gamma^2 & A_{\Gamma\Gamma}^f & M_1 \\ 0 & M_2 & D \end{pmatrix} \begin{pmatrix} \mathbf{u}_f \\ \mathbf{u}_\Gamma \\ \phi \end{pmatrix} = \begin{pmatrix} \mathbf{f}_1 \\ \mathbf{f}_\Gamma \\ \mathbf{f}_2 \end{pmatrix}. \tag{8.14}$$

By writing  $\mathbf{u}_\Gamma = \mathbf{u}_\Gamma^0 + \boldsymbol{\lambda}_*$ , where  $\boldsymbol{\lambda}_*$  is the vector whose components are the (known) values of  $\lambda_{*h}$  at the nodes on  $\Gamma$ , system (8.14) reduces to:

$$\begin{pmatrix} F & F_\Gamma^1 & 0 \\ F_\Gamma^2 & A_{\Gamma\Gamma}^f & M_1 \\ 0 & M_2 & D \end{pmatrix} \begin{pmatrix} \mathbf{u}_f \\ \mathbf{u}_\Gamma^0 \\ \phi \end{pmatrix} = \begin{pmatrix} \hat{\mathbf{f}}_1 \\ \hat{\mathbf{f}}_\Gamma \\ \hat{\mathbf{f}}_2 \end{pmatrix}$$

where  $\hat{\mathbf{f}}_1 = \mathbf{f}_1 - F_\Gamma^1 \boldsymbol{\lambda}_*$ ,  $\hat{\mathbf{f}}_\Gamma = \mathbf{f}_\Gamma - A_{\Gamma\Gamma}^f \boldsymbol{\lambda}_*$  and  $\hat{\mathbf{f}}_2 = \mathbf{f}_2 - M_2 \boldsymbol{\lambda}_*$ .

Upon eliminating the unknowns  $\mathbf{u}_f$  and  $\phi$ , we obtain the reduced Schur complement system:

$$\Sigma_h \mathbf{u}_\Gamma^0 = \boldsymbol{\chi}_h, \tag{8.15}$$

where we have defined

$$\Sigma_h = A_{\Gamma\Gamma}^f - F_\Gamma^2 F^{-1} F_\Gamma^1 - M_1 D^{-1} M_2 \tag{8.16}$$

and

$$\boldsymbol{\chi}_h = \hat{\mathbf{f}}_\Gamma - F_\Gamma^2 F^{-1} \hat{\mathbf{f}}_1 - M_1 D^{-1} \hat{\mathbf{f}}_2.$$

In (8.16) the first term

$$\Sigma_{fh} = A_{\Gamma\Gamma}^f - F_\Gamma^2 F^{-1} F_\Gamma^1 \tag{8.17}$$

arises from domain  $\Omega_f$ , whereas

$$\Sigma_{ph} = -M_1 D^{-1} M_2 \tag{8.18}$$

from  $\Omega_p$ . The matrices  $\Sigma_{fh}$  and  $\Sigma_{ph}$  are the algebraic counterparts of the operators  $S_{fh}$  and  $S_{ph}$ , respectively.

*Remark 8.6.* To be precise, notice that we are slightly abusing in notation, since for the algebraic system (7.15) we have considered the complete interface condition (3.18), while in order to characterize the discrete Steklov-Poincaré operators we have used its simplified form  $\mathbf{u}_{fh} \cdot \boldsymbol{\tau}_j = 0$  on  $\Gamma$ . Therefore, the exact algebraic counterpart of  $S_{fh}$  and  $S_{ph}$  should be obtained considering a basis of  $H_{fh}^\tau$  rather than  $H_{fh}$ .

Thanks to Lemma 8.3, the matrices  $\Sigma_{fh}$  and  $\Sigma_h$  are symmetric and positive definite. Moreover

$$[\Sigma_{fh}\boldsymbol{\mu}, \boldsymbol{\mu}] \leq [\Sigma_h\boldsymbol{\mu}, \boldsymbol{\mu}] \leq \left(1 + \frac{\beta_p}{\alpha_f}\right) [\Sigma_{fh}\boldsymbol{\mu}, \boldsymbol{\mu}] \quad \forall \boldsymbol{\mu} \in \mathbb{R}^{N_\Gamma},$$

where  $[\cdot, \cdot]$  is the Euclidean scalar product in  $\mathbb{R}^{N_\Gamma}$  and  $\alpha_f$  and  $\beta_p$  are the constants defined in (5.32) and (5.31), respectively.

Thus, the spectral condition number  $\chi_{sp}$  of the matrix  $\Sigma_{fh}^{-1}\Sigma_h$  is bounded independently of  $h$ :

$$\chi_{sp}(\Sigma_{fh}^{-1}\Sigma_h) \leq 1 + \frac{\beta_p}{\alpha_f},$$

and  $\Sigma_{fh}$  is an optimal preconditioner for  $\Sigma_h$ . Therefore, should we use  $\Sigma_{fh}$  as preconditioner to solve the symmetric linear system (8.15) using the preconditioned Richardson method

$$(\mathbf{u}_\Gamma^0)^{k+1} = (\mathbf{u}_\Gamma^0)^k + \Sigma_{fh}^{-1}(\boldsymbol{\chi}_h - \Sigma_h(\mathbf{u}_\Gamma^0)^k), \tag{8.19}$$

we would get convergence with a rate independent of  $h$ . Same conclusion if instead of (8.19) we would use a Krylov type method (e.g., the conjugate gradient method).

In the next section, we shall interpret (8.19) as a Dirichlet-Neumann substructuring scheme and we shall prove its convergence.

#### 8.4. A subdomain iterative method for the Stokes/Darcy problem

The iterative method we propose to compute the solution of the Stokes/Darcy problem (8.1)–(8.5) consists in solving first Darcy problem in  $\Omega_p$  imposing the continuity of the normal velocities across  $\Gamma$ . Then, we solve the Stokes problem in  $\Omega_f$  imposing the continuity of the normal stresses across the interface, using the value of  $\varphi_h$  on  $\Gamma$  that we have just computed in the porous media domain. Precisely, the iterative scheme reads as follows.

Given  $\mathbf{u}_{inh}$ , construct  $\lambda_{*h}$  as in (8.6). Then, let  $\lambda_h^0 \in \Lambda_{0h}$  be the initial guess, and, for  $k \geq 0$ :

- (i) Find  $\varphi_{0h}^{k+1} \in H_{ph}$  such that, for all  $\psi_h \in H_{ph}$ ,

$$a_p(\varphi_{0h}^{k+1}, \psi_h) - \int_\Gamma n \psi_h \lambda_{0h}^k = -a_p(E_{ph}\varphi_{ph}, \psi_h) + \int_\Gamma n \psi_h \lambda_{*h}. \tag{8.20}$$

(ii) Find  $(\mathbf{u}_{fh}^0)^{k+1} \in H_{fh}^\tau, p_{fh}^{k+1} \in Q_h$ :

$$\begin{aligned} & a_f((\mathbf{u}_{fh}^0)^{k+1}, \mathbf{w}_h) + b_f(\mathbf{w}_h, p_{fh}^{k+1}) + \int_\Gamma g\varphi_h^{k+1} \mathbf{w}_h \cdot \mathbf{n} \\ &= \int_{\Omega_f} \mathbf{f} \mathbf{w}_h - a_f(E_{fh} \mathbf{u}_{inh}, \mathbf{w}_h) \quad \forall \mathbf{w}_h \in H_{fh}^\tau, \end{aligned} \tag{8.21}$$

$$b_f((\mathbf{u}_{fh}^0)^{k+1}, q_h) = -b_f(E_{fh} \mathbf{u}_{inh}, q_h) \quad \forall q_h \in Q_h, \tag{8.22}$$

with  $\varphi_h^{k+1} = \varphi_{0h}^{k+1} + E_{ph} \varphi_{ph}$ .

(iii) Update  $\lambda_{0h}^k$ :

$$\lambda_{0h}^{k+1} = \theta(\mathbf{u}_{fh}^{k+1} \cdot \mathbf{n} - \lambda_{*h})|_\Gamma + (1 - \theta)\lambda_{0h}^k, \tag{8.23}$$

$\theta$  being a positive relaxation parameter and  $\mathbf{u}_{fh}^{k+1} = (\mathbf{u}_{fh}^0)^{k+1} + E_{fh} \mathbf{u}_{inh}$ .

*Remark 8.7.* Note that  $\lambda_{0h}^k \in \Lambda_{0h}$  for all  $k \geq 0$ . In fact,  $\lambda_{0h} \in \Lambda_{0h}$  given, suppose  $\lambda_{0h}^k \in \Lambda_0$ . Then

$$\int_\Gamma \lambda_{0h}^{k+1} = \theta \int_\Gamma (\mathbf{u}_{fh}^{k+1} \cdot \mathbf{n}|_\Gamma - \lambda_{*h}).$$

Now, since  $\int_{\Omega_f} \nabla \cdot \mathbf{u}_{fh}^{k+1} = 0$ , thanks to the divergence theorem we have

$$\int_\Gamma \mathbf{u}_{fh}^{k+1} \cdot \mathbf{n} = - \int_{\Gamma_f^{in}} \mathbf{u}_{inh} \cdot \mathbf{n}$$

and recalling (8.6) the thesis follows.

Following the general theory developed in [110], the above iterative method can be reinterpreted as a preconditioned Richardson method for the Steklov–Poincaré problem (8.9).

**Lemma 8.8.** *The iterative substructuring scheme (8.20)–(8.23) to compute the solution of the finite element approximation of the coupled problem Stokes/Darcy (8.1)–(8.5) is equivalent to a preconditioned Richardson method for the discrete Steklov–Poincaré equation (8.9), the preconditioner being the operator  $S_{fh}$  introduced in (8.8).*

*Proof.* Since  $E_{fh} \mathbf{u}_{inh} \cdot \mathbf{n} = 0$  on  $\Gamma$ , (8.23) reduces to:

$$\lambda_{0h}^{k+1} = \theta((\mathbf{u}_{fh}^0)^{k+1} \cdot \mathbf{n} - \lambda_{*h})|_\Gamma + (1 - \theta)\lambda_{0h}^k.$$

Let  $R_{1h}^\tau : \Lambda_h \rightarrow H_{fh}^\tau$  be the extension operator introduced in Proposition 8.1. For all  $\mu_h \in \Lambda_h$ , we can rewrite (8.21) as:

$$\begin{aligned} & a_f((\mathbf{u}_{fh}^0)^{k+1}, R_{1h}^\tau \mu_h) + b_f(R_{1h}^\tau \mu_h, p_{fh}^{k+1}) + \int_\Gamma g\varphi_h^{k+1} \mu_h \\ &= \int_{\Omega_f} \mathbf{f} (R_{1h}^\tau \mu_h) - a_f(E_{fh} \mathbf{u}_{inh}, R_{1h}^\tau \mu_h) \quad \forall \mu_h \in \Lambda_h. \end{aligned} \tag{8.24}$$

Let us define  $\hat{p}_{fh}^{k+1} = (\text{meas}(\Omega_f))^{-1} \int_{\Omega_f} p_{fh}^{k+1}$ ; then we set

$$p_{0h}^{k+1} = p_{fh}^{k+1} - \hat{p}_{fh}^{k+1},$$

and we note that  $p_{0h}^{k+1} \in Q_0$ . Then (8.24) gives:

$$\begin{aligned} & a_f((\mathbf{u}_{fh}^0)^{k+1}, R_{1h}^\tau \mu_h) + b_f(R_{1h}^\tau \mu_h, p_{0h}^{k+1}) + \int_{\Gamma} g \varphi_h^{k+1} \mu_h \\ &= \int_{\Omega_f} \mathbf{f}(R_{1h}^\tau \mu_h) + b_f(R_{1h}^\tau \mu_h, \hat{p}_{fh}^{k+1}) - a_f(E_{fh} \mathbf{u}_{inh}, R_{1h}^\tau \mu_h) \quad \forall \mu_h \in \Lambda_h. \end{aligned} \quad (8.25)$$

Let  $\omega_{0h}^*, \pi_h^*$  be the solution to the following problem:

find  $\omega_{0h}^* \in \widetilde{H}_{fh}^0, \pi_h^* \in Q_{0h}$  such that for all  $\mathbf{v}_h \in \widetilde{H}_{fh}^0, q_h \in Q_{0h}$

$$\begin{aligned} & a_f(\omega_{0h}^* + E_{fh} \mathbf{u}_{inh} + E_{\Gamma h} \lambda_{*h}, \mathbf{v}_h) + b_f(\mathbf{v}_h, \pi_h^*) = \int_{\Omega_f} \mathbf{f} \cdot \mathbf{v}_h, \\ & b_f(\omega_{0h}^* + E_{fh} \mathbf{u}_{inh} + E_{\Gamma h} \lambda_{*h}, q_h) = 0, \end{aligned}$$

where we have set  $Q_{0h} = \{q_h \in Q_h : \int_{\Omega_f} q_h = 0\}$  and  $E_{\Gamma h} \lambda_{*h} \in H_{fh}^\tau$  denotes a suitable discrete extension of  $\lambda_{*h}$ , such that  $E_{\Gamma h} \lambda_{*h} \cdot \mathbf{n} = \lambda_{*h}$  on  $\Gamma$ . Moreover, let  $\varphi_{0h}^* \in H_{ph}$  be such that

$$a_p(\varphi_{0h}^* + E_{ph} \varphi_{ph}, \psi_h) = \int_{\Gamma} n \lambda_{*h} \psi_h \quad \forall \psi_h \in H_{ph}. \quad (8.26)$$

Subtracting from both members in (8.25) the following terms:

$$a_f(\omega_{0h}^* + E_{\Gamma h} \lambda_{*h}, R_{1h}^\tau \mu_h) + b_f(R_{1h}^\tau \mu_h, \pi_h^*) + \int_{\Gamma} g \varphi_{0h}^* \mu_h,$$

we have, for all  $\mu_h \in \Lambda_h$ ,

$$\begin{aligned} & a_f((\mathbf{u}_{fh}^0)^{k+1} - \omega_{0h}^* - E_{\Gamma h} \lambda_{*h}, R_{1h}^\tau \mu_h) + b_f(R_{1h}^\tau \mu_h, p_{0h}^{k+1} - \pi_h^*) \\ & \quad + \int_{\Gamma} g(\varphi_h^{k+1} - \varphi_{0h}^*) \mu_h \\ &= \int_{\Omega_f} \mathbf{f}(R_{1h}^\tau \mu_h) - b_f(R_{1h}^\tau \mu_h, \pi_h^*) \\ & \quad - a_f(\omega_{0h}^* + E_{\Gamma h} \lambda_{*h} \\ & \quad + E_{fh} \mathbf{u}_{inh}, R_{1h}^\tau \mu_h) - \int_{\Gamma} g \varphi_{0h}^* \mu_h + b_f(R_{1h}^\tau \mu_h, \hat{p}_{fh}^{k+1}). \end{aligned} \quad (8.27)$$

Since

$$\int_{\Omega_f} \nabla \cdot (\omega_{0h}^* + E_{\Gamma h} \lambda_{*h} + E_{fh} \mathbf{u}_{inh}) = 0$$



and

$$\int_{\Omega_f} \nabla \cdot ((\mathbf{u}_{fh}^0)^{k+1} + E_{fh} \mathbf{u}_{inh}) = 0,$$

we obtain

$$\int_{\Omega} \nabla \cdot ((\mathbf{u}_{fh}^0)^{k+1} - \boldsymbol{\omega}_0^* - E_{\Gamma h} \lambda_{*h}) = 0.$$

Now, if we apply the divergence theorem and recall that  $(\mathbf{u}_{fh}^0)^{k+1} \in H_{fh}^\tau$ ,  $\boldsymbol{\omega}_{0h}^* \in \widetilde{H}_{fh}^0$  and  $E_{\Gamma h} \lambda_{*h} \in H_{fh}^\tau$ , we see that  $[(\mathbf{u}_{fh}^0)^{k+1} - E_{\Gamma h} \lambda_{*h}] \cdot \mathbf{n}|_\Gamma \in \Lambda_{0h}$ . Therefore, using the definition (8.8) of  $S_{fh}$ , we have:

$$\begin{aligned} a_f((\mathbf{u}_{fh}^0)^{k+1} - \boldsymbol{\omega}_{0h}^* - E_{\Gamma h} \lambda_{*h}, R_{1h}^\tau \mu_h) + b_f(R_{1h}^\tau \mu_h, p_{0h}^{k+1} - \pi_h^*) \\ = \langle S_{fh}(((\mathbf{u}_{fh}^0)^{k+1} - E_{\Gamma h} \lambda_{*h}) \cdot \mathbf{n})|_\Gamma, \mu_h \rangle \end{aligned}$$

for all  $\mu_h \in \Lambda_h$ .

Moreover, if we subtract (8.26) from (8.20), we obtain

$$a_p(\varphi_{0h}^{k+1} - \varphi_{0h}^*, \psi_h) = \int_{\Gamma} n \lambda_{0h}^k \psi_h \quad \forall \psi_h \in H_{ph},$$

whence, thanks to (8.7),  $\varphi_{0h}^{k+1} - \varphi_{0h}^* = R_{ph} \lambda_{0h}^k$ . Therefore

$$\int_{\Gamma} g(\varphi_h^{k+1} - \varphi_{0h}^*) \mu_h = \langle S_{ph} \lambda_{0h}^k, \mu_h \rangle \quad \forall \mu_h \in \Lambda_h.$$

Finally, if we apply the divergence theorem to the last term on the right hand side of (8.27) and we use the definition of  $\chi_h$ , we can rewrite the right hand side of (8.27) as

$$\langle \chi_h, \mu_h \rangle + \hat{p}_{fh}^{k+1} \int_{\Gamma} \mu_h \quad \forall \mu_h \in \Lambda_h.$$

Now, for all  $\mu_h \in \Lambda_{0h}$ , it follows:

$$\langle S_{fh}(((\mathbf{u}_{fh}^0)^{k+1} - E_{\Gamma h} \lambda_{*h}) \cdot \mathbf{n})|_\Gamma, \mu_h \rangle + \langle S_{ph} \lambda_{0h}^k, \mu_h \rangle = \langle \chi_h, \mu_h \rangle.$$

Therefore we can conclude that (8.20)–(8.23) is equivalent to the preconditioned Richardson scheme: let  $\lambda_{0h}^0 \in \Lambda_{0h}$  be given; for  $k \geq 0$ , find  $\lambda_{0h}^{k+1} \in \Lambda_{0h}$  s.t.

$$\lambda_{0h}^{k+1} = \lambda_{0h}^k + \theta_h S_{fh}^{-1}(\chi_h - S_h \lambda_{0h}^k). \tag{8.28}$$

□

*Remark 8.9.* The algorithm (8.20)–(8.23) does not feature the classical structure of a Dirichlet-Neumann method, which would require to solve one subproblem in the first subdomain with a Dirichlet boundary condition on the interface, and one problem

in the second subdomain with a Neumann boundary condition on the interface. As a matter of fact, the condition that we are imposing for the first subdomain  $\Omega_p$  is a Neumann (rather than a Dirichlet) natural condition on  $\Gamma$ . However, in view of (8.28), it shares with the Dirichlet-Neumann method the fact that the preconditioner of the Richardson iterations is the Steklov-Poincaré operator associated to the second subdomain  $\Omega_p$ .

The formulation (8.28) is very convenient for the analysis of convergence of the iterative scheme (8.20)–(8.23). Indeed, with this aim we can apply the following abstract convergence result (see [110, Theorem 4.2.2 and Remark 4.2.4]).

**Lemma 8.10.** *Let  $X$  be a (real) Hilbert space and  $X'$  be its dual. We consider a linear invertible continuous operator  $\mathcal{Q}: X \rightarrow X'$ , which can be split as  $\mathcal{Q} = \mathcal{Q}_1 + \mathcal{Q}_2$ , where both  $\mathcal{Q}_1$  and  $\mathcal{Q}_2$  are linear operators. Taken  $\mathcal{Z} \in X'$ , let  $x \in X$  be the unknown solution to the equation*

$$\mathcal{Q}x = \mathcal{Z}, \quad (8.29)$$

and consider for its solution the preconditioned Richardson method

$$\mathcal{Q}_2(x^{k+1} - x^k) = \theta(\mathcal{Z} - \mathcal{Q}x^k), \quad k \geq 0,$$

$\theta$  being a positive relaxation parameter. Suppose that the following conditions are satisfied:

- (i)  $\mathcal{Q}_2$  is symmetric, continuous with constant  $\beta_2$  and coercive with constant  $\alpha_2$ ;
- (ii)  $\mathcal{Q}_1$  is continuous with constant  $\beta_1$ ;
- (iii)  $\mathcal{Q}$  is coercive with constant  $\alpha_{\mathcal{Q}}$ .

Then, for any given  $x^0 \in X$  and for any  $0 < \theta < \theta_{max}$ , with

$$\theta_{max} = \frac{2\alpha_{\mathcal{Q}}\alpha_2^2}{\beta_2(\beta_1 + \beta_2)^2},$$

the sequence

$$x^{k+1} = x^k + \theta\mathcal{Q}_2^{-1}(\mathcal{Z} - \mathcal{Q}x^k)$$

converges in  $X$  to the solution of problem (8.29).

We can now prove the main result of this section.

**Theorem 8.11.** *For any choice of the initial guess  $\lambda_{0h}^0 \in \Lambda_{0h}$  and for suitable values of the relaxation parameter  $\theta$  the iterative method (8.20)–(8.23) converges to the solution  $(\mathbf{u}_{fh}^0, p_{fh}, \varphi_{0h}) \in H_{fh}^r \times Q_h \times H_{ph}$  of the coupled Stokes/Darcy problem (8.1)–(8.5).*

*Proof.* Upon setting  $X = \Lambda_{0h}$ ,  $\mathcal{Q} = S_h$ ,  $\mathcal{Q}_1 = S_{ph}$ ,  $\mathcal{Q}_2 = S_{fh}$  and  $\mathcal{Z} = \chi_h$ , the proof follows from Theorem 8.10, whose hypotheses are satisfied thanks to Lemma 8.3. In fact, for any initial guess  $\lambda_{0h}^0 \in \Lambda_{0h}$ , and any  $0 < \theta < \theta_{max}$  with

$$\theta_{max} = \frac{2\alpha_f^3}{\hat{\beta}_f(\hat{\beta}_f + \beta_p)^2},$$

the sequence defined in (8.28) converges to the solution of the Steklov–Poincaré equation (8.9). Taking the limit  $k \rightarrow \infty$  in the iterative procedure (8.20)–(8.23), it follows that  $\{((\mathbf{u}_{fh}^0)^k, p_{fh}^k, \varphi_{0h}^k)\}_k \rightarrow (\mathbf{u}_{fh}^0, p_{fh}, \varphi_{0h})$ .

The upper bound  $\theta_{max}$  is independent of  $h$  as such are the constants  $\alpha_f$ ,  $\hat{\beta}_f$  and  $\beta_p$ . (We recall that the constants  $\alpha_f$ ,  $\hat{\beta}_f$  and  $\beta_p$  are respectively the coercivity and the continuity constants of the operator  $S_{fh}$  and the continuity constant of  $S_{ph}$ , and they have been introduced in (5.32), (8.13) and (5.31), respectively. See also Lemma 8.3.) □

### 8.5. Matrix interpretation of the subdomain iterative method

The iterative scheme (8.20)–(8.23) corresponds to the following steps. Let  $\lambda_0^k \in \mathbb{R}^{N_\Gamma}$  be the vector of the values of  $\lambda_{0h}^k$  at the  $k$ -th step at the nodes of  $\Gamma$ .

Problem (8.20) yields the following algebraic system:

$$\begin{pmatrix} A_{p\Gamma}^p & A_{p\Gamma}^T \\ A_{p\Gamma} & A_{pp} \end{pmatrix} \begin{pmatrix} \phi_\Gamma^{k+1} \\ \phi_{int}^{k+1} \end{pmatrix} = \begin{pmatrix} \mathbf{f}_{p\Gamma} + M_\Gamma^T \lambda_0^k + M_\Gamma^T \lambda_* \\ \mathbf{f}_p \end{pmatrix}, \tag{8.30}$$

where  $\phi_\Gamma^{k+1}$  and  $\phi_{int}^{k+1}$  are the vectors of the nodal values of the solution  $\varphi_{0h}^{k+1}$  at the interface and internal nodes, respectively.

By formally eliminating  $\phi_{int}^{k+1}$  from (8.30), we obtain

$$(A_{p\Gamma}^p - A_{p\Gamma}^T A_{pp}^{-1} A_{p\Gamma}) \phi_\Gamma^{k+1} = \mathbf{f}_{p\Gamma} - A_{p\Gamma}^T A_{pp}^{-1} \mathbf{f}_p + M_\Gamma^T \lambda^k + M_\Gamma^T \lambda_*.$$

Now use  $\phi_\Gamma^{k+1}$  to compute the unknown vector  $\mathbf{u}_\Gamma^{k+1}$  by solving the following system, which corresponds to the Stokes problem (8.21)–(8.22):

$$\begin{pmatrix} A_{ff} & B^T & A_{f\Gamma} \\ B_1 & 0 & B_{f\Gamma} \\ A_{f\Gamma} & B_{f\Gamma}^T & A_{f\Gamma}^f \end{pmatrix} \begin{pmatrix} \mathbf{u}_{int}^{k+1} \\ \mathbf{p}^{k+1} \\ \mathbf{u}_\Gamma^{k+1} \end{pmatrix} = \begin{pmatrix} \mathbf{f}_f \\ \mathbf{f}_{in} \\ \mathbf{f}_\Gamma - M_\Gamma \phi_\Gamma^{k+1} \end{pmatrix}.$$

The vectors  $\mathbf{u}_{int}^{k+1}$  and  $\mathbf{p}^{k+1}$  contain respectively the nodal values of  $(\mathbf{u}_{fh}^0)^{k+1}$  and of the pressure  $p_{fh}^{k+1}$  at the internal points of  $\Omega_f$ , while  $\mathbf{u}_\Gamma^{k+1}$  the nodal values of the normal velocity  $\mathbf{u}_{fh}^{k+1} \cdot \mathbf{n}$  on  $\Gamma$ .

Finally, according to (8.23), we set

$$\lambda_0^{k+1} = \theta(\mathbf{u}_\Gamma^{k+1} - \lambda_*) + (1 - \theta)\lambda_0^k,$$

and we iterate restarting from (8.30) until the convergence test

$$\frac{\|\boldsymbol{\lambda}_0^{k+1} - \boldsymbol{\lambda}_0^k\|_{\mathbb{R}^{N_\Gamma}}}{\|\boldsymbol{\lambda}_0^{k+1}\|_{\mathbb{R}^{N_\Gamma}}} \leq \epsilon$$

is satisfied for a prescribed tolerance  $\epsilon$ ;  $\|\cdot\|_{\mathbb{R}^{N_\Gamma}}$  denotes the Euclidean norm in  $\mathbb{R}^{N_\Gamma}$ .

### 9. Some numerical results for the Stokes/Darcy coupling

For the sake of clarity, before presenting the numerical results, we give a schematic overview of the numerical algorithm we shall adopt, and we discuss the implementation of the preconditioned conjugate gradient (PCG) methods (see, e.g., [114]) which exploit the preconditioners  $\Sigma_{fh}$  of Section 8.3.

The method introduced in Sects. 8.4 and 8.5 can be written in the following pseudo-algorithmic form.

**Algorithm 1.** Choose an initial guess  $(\mathbf{u}_f^0) \cdot \mathbf{n}$  on  $\Gamma$ . Then, for  $k = 0, 1, \dots$  until convergence, do

1. Solve Darcy equation with boundary condition  $-\mathcal{K}\partial_n \varphi^{k+1} = \mathbf{u}_f^k \cdot \mathbf{n}$  on  $\Gamma$ .
2. Solve Stokes problem imposing  $-\mathbf{n} \cdot \mathbb{T}(\mathbf{u}_f^{k+\frac{1}{2}}, p_f^{k+\frac{1}{2}}) \cdot \mathbf{n} = g\varphi^{k+1}$  on  $\Gamma$ .
3. Update:  $\mathbf{u}_f^{k+1} \cdot \mathbf{n} = \theta \mathbf{u}_f^{k+\frac{1}{2}} \cdot \mathbf{n} + (1 - \theta) \mathbf{u}_f^k \cdot \mathbf{n}$  on  $\Gamma$ , with  $\theta \in (0, 1)$ .

On the other hand, the preconditioner  $\Sigma_{fh}$  can be used in the framework of PCG iterations to solve the symmetric positive definite Schur complement system (8.15). In this case, the algorithm reads as follows.

**Algorithm 2.** Given an initial guess  $(\mathbf{u}_\Gamma^0)^0$  for the fluid velocity on  $\Gamma$ , set  $\mathbf{r}^0 = \boldsymbol{\chi}_h - \Sigma_h(\mathbf{u}_\Gamma^0)^0$ , and  $\mathbf{w}^0 = \mathbf{z}^0 = \Sigma_{fh}^{-1}\mathbf{r}^0$ . Then, for  $k \geq 0$ :

$$\mathbf{v}^k = \Sigma_h \mathbf{w}^k, \tag{9.1}$$

$$\alpha_k = \frac{[\mathbf{w}^k, \mathbf{r}^k]}{[\mathbf{w}^k, \mathbf{v}^k]},$$

$$(\mathbf{u}_\Gamma^0)^{k+1} = (\mathbf{u}_\Gamma^0)^k + \alpha_k \mathbf{w}^k,$$

$$\mathbf{r}^{k+1} = \mathbf{r}^k - \alpha_k \mathbf{v}^k,$$

$$\text{solve } \Sigma_{fh} \mathbf{z}^{k+1} = \mathbf{r}^{k+1}, \tag{9.2}$$

$$\beta_k = \frac{[\mathbf{v}^k, \mathbf{z}^{k+1}]}{[\mathbf{w}^k, \mathbf{v}^k]},$$

$$\mathbf{w}^{k+1} = \mathbf{z}^{k+1} - \beta_k \mathbf{w}^k,$$

where  $[\cdot, \cdot]$  denotes the Euclidean scalar product in  $\mathbb{R}^{N_\Gamma}$ .

The most expensive steps in terms of computational effort are (9.1) and (9.2). Indeed, step (9.1) requires

- to compute  $\Sigma_{fh}\mathbf{w}^k$  which amounts to solving a Stokes problem in  $\Omega_f$  with a Dirichlet boundary condition on  $\Gamma$  (see the corresponding differential operator  $S_f$  in Section 5.2);
- to compute  $\Sigma_{ph}\mathbf{w}^k$  which amounts to solve a Darcy problem in  $\Omega_p$  with Neumann boundary condition on  $\Gamma$  (see the definition of the corresponding differential operator  $S_p$  in Section 5.2).

Step (9.2) demands to solve the linear system  $\Sigma_{fh}\mathbf{z}^{k+1} = \mathbf{r}^{k+1} \Leftrightarrow \mathbf{z}^{k+1} = \Sigma_{fh}^{-1}\mathbf{r}^{k+1}$  which amounts to solve a Stokes problem in  $\Omega_f$  with Neumann boundary condition on  $\Gamma$  (see also the definition of the differential operator  $S_f^{-1}$  in Section 5.2).

Each step of the PCG method requires therefore to solve one Darcy problem in  $\Omega_p$  and two Stokes problems in  $\Omega_f$ .

### 9.1. Numerical tests with respect to the grid parameter

We investigate the convergence properties of Algorithms 1 and 2 with respect to the grid parameter  $h$ . For the moment we set the physical parameters  $\nu$ ,  $K$ ,  $g$  to 1. We consider the computational domain  $\Omega \subset \mathbb{R}^2$  with  $\Omega_f = (0, 1) \times (1, 2)$ ,  $\Omega_p = (0, 1) \times (0, 1)$  and the interface  $\Gamma = (0, 1) \times \{1\}$ . We impose Dirichlet boundary conditions on the velocity on  $\partial\Omega_f \setminus \Gamma$ , while we consider a Dirichlet boundary condition  $\varphi = \varphi_p$  on the bottom boundary  $(0, 1) \times \{0\}$  and Neumann boundary conditions on the lateral boundaries  $\{0, 1\} \times (0, 1)$  of the domain  $\Omega_p$ . The boundary conditions and the forcing terms are chosen in such a way that the exact solution of the coupled Stokes/Darcy problem is

$$\begin{aligned} (\mathbf{u}_f)_1 &= -\cos\left(\frac{\pi}{2}y\right)\sin\left(\frac{\pi}{2}x\right), & (\mathbf{u}_f)_2 &= \sin\left(\frac{\pi}{2}y\right)\cos\left(\frac{\pi}{2}x\right) - 1 + x, \\ p_f &= 1 - x, & \varphi &= \frac{2}{\pi}\cos\left(\frac{\pi}{2}x\right)\cos\left(\frac{\pi}{2}y\right) - y(x - 1), \end{aligned}$$

where  $(\mathbf{u}_f)_1$  and  $(\mathbf{u}_f)_2$  are the components of the velocity field  $\mathbf{u}_f$ . Note in particular that  $\mathbf{u}_f \cdot \boldsymbol{\tau} = (\mathbf{u}_f)_1 = 0$  on  $\Gamma$  according to (5.7). Finally, remark that in Darcy equation a non null forcing term has been considered. This implies the presence of an additional term in the definition of the functional  $\mathcal{F}$  in (4.10), but it does not affect the theory we have developed.

In our computation, four different regular conforming meshes have been considered whose number of elements in  $\Omega$  and of nodes on  $\Gamma$  are reported in Table 2, together with the number of iterations to convergence obtained using Algorithms 1 and 2. The  $\mathbb{P}_2 - \mathbb{P}_1$  Taylor-Hood finite elements have been used for Stokes problem and  $\mathbb{P}_2$  elements for Darcy equation.

A tolerance  $10^{-10}$  has been prescribed for the convergence tests based on the relative residues. In Algorithm 1 we set the relaxation parameter  $\theta = 0.7$ .

Table 2 – Number of iterations obtained on different grids.

Number of mesh elements	Number of nodes on $\Gamma$	Algorithm 1 ( $\theta = 0.7$ )	Algorithm 2 (preconditioner $\Sigma_{fh}^{-1}$ )
172	13	18	5
688	27	18	5
2752	55	18	5
11008	111	18	5

Figure 6 shows the computed residues for the adopted iterative methods when using the finest mesh (logarithmic scale has been considered on the  $y$ -axis).

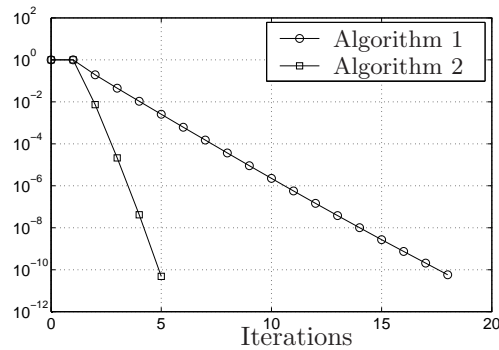


Figure 6 – Computed relative residues for the interface variable  $\lambda_h$  using Richardson and PCG iterations.

Table 3 reports the spectral condition numbers of the preconditioned Schur complement matrix  $\Sigma_{fh}^{-1}\Sigma_h$  illustrating the optimality of the preconditioner with respect to  $h$ .

Table 3 – Spectral condition numbers for the preconditioned Schur complement.

$h_{ \Gamma}$ approx.	$\chi_{sp}(\Sigma_{fh}^{-1}\Sigma_h)$
0.1429	1.083655
0.0714	1.083670
0.0357	1.083658
0.0179	1.083656

Finally, Figure 7 reports the errors with respect to the exact solution:

$$E_{Stokes}^h = \|\nabla \mathbf{u}_f - \nabla \mathbf{u}_{fh}\|_0 + \|p_f - p_{fh}\|_0, \quad E_{Darcy}^h = \|\varphi - \varphi_h\|_1$$

$$E_{\lambda_h} = \|\lambda - \lambda_h\|_0 \quad \text{and} \quad E_{\sigma_h} = \|\sigma - \sigma_h\|_0.$$

We recall that the following theoretical estimates hold (see, e.g., [109]):

$$E_{Darcy}^h \leq C_D h^{l+1} \|\varphi\|_l \quad C_D > 0,$$

with  $l = \min(2, s - 1)$  if  $\varphi \in H^s(\Omega_p)$  ( $s \geq 2$ ), and

$$E_{Stokes}^h \leq C_S h^r (\|\mathbf{u}_f\|_{r+1} + \|p_f\|_r) \quad C_S > 0,$$

with  $r = 1, 2$ , provided the solution  $(\mathbf{u}_f, p_f)$  is regular enough so that the norms at the right hand side make sense. The numerical results show that these theoretical estimates are fulfilled.

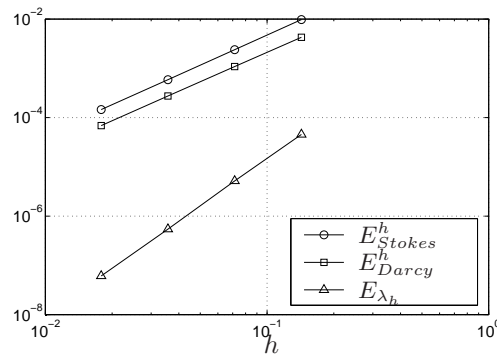


Figure 7 – Computed errors with respect to the exact solution versus  $h$  obtained using Algorithm 2.

The numerical tests we have presented show that, according to the theory developed in Section 8.3, the preconditioner  $\Sigma_{fh}$  is optimal with respect to the grid parameter  $h$  since the corresponding preconditioned substructuring methods yield convergence in a number of iterations independent of  $h$ .

### 9.2. The role of the physical parameters on the convergence behavior of the iterative methods

We consider now the influence of the physical parameters, which govern the coupled problem, on the convergence of the given algorithms. We use only Algorithm 2 as the PCG method embeds the choice of dynamic optimal acceleration parameters. We

take the same computational domain as in the test of Section 9.1 with the same kind of boundary conditions, but here the boundary data and the forcing terms are chosen in such a way that the exact solution of the coupled problem is

$$\begin{aligned}
 (\mathbf{u}_f)_1 &= y^2 - 2y + 1, & (\mathbf{u}_f)_2 &= x^2 - x, & p_f &= 2\nu(x + y - 1) + \frac{g}{3K}, \\
 \varphi &= \frac{1}{K} \left( x(1-x)(y-1) + \frac{y^3}{3} - y^2 + y \right) + \frac{2\nu}{g}x.
 \end{aligned}$$

The most relevant physical quantities for the coupling are the fluid viscosity  $\nu$  and the hydraulic conductivity  $K$ . Therefore, we test our algorithms with respect to different values of  $\nu$  and  $K$ , and set the other physical parameters to 1. We consider a convergence test based on the relative residue with tolerance  $10^{-10}$ .

In Table 4 we report the number of iterations necessary for several choices of  $\nu$  and  $K$  (the symbol # indicates that the method did not converge within 150 iterations), while in Figure 8 we show the spectral condition number  $\chi_{sp}(\Sigma_{fh}^{-1}\Sigma_h)$  versus  $h$  for the considered test cases.

We can see that the convergence of the algorithm is troublesome when the values of  $\nu$  and  $K$  decrease. In fact, in that case the method converges in a large number of iterations which increases when  $h$  decreases, losing its optimality properties. The subdomain iterative method that we have proposed is then effective only when the product  $\nu K$  is sufficiently large, while dealing with small values causes severe difficulties. (Remark that the latter are the very values of interest in real-life applications: see, for example, the values of  $K$  reported in Table 1 and recall that water has a kinematic viscosity  $\nu = 10^{-6} \text{ m}^2/\text{s}$ .)

Table 4 – Iterations using Algorithms 2 (preconditioner  $\Sigma_{fh}^{-1}$ ) with respect to several values of  $\nu$  and  $K$ .

	$\nu$	$K$	$h = 0.1428$	$h = 0.0714$	$h = 0.0357$	$h = 0.0178$
a)	1	1	5	5	5	5
b)	$10^{-1}$	$10^{-1}$	11	11	10	10
c)	$10^{-2}$	$10^{-1}$	15	19	18	17
d)	$10^{-3}$	$10^{-2}$	20	54	73	56
e)	$10^{-4}$	$10^{-3}$	20	59	#	#
f)	$10^{-6}$	$10^{-4}$	20	59	148	#

We introduce a formal argument for better understanding these results and to set up a more effective numerical scheme.

The source of trouble is represented by the very different structure of the Stokes equation (3.19) and of Darcy equations (2.5)–(2.6), which become even more dissimilar when  $\nu \ll 1$  and  $K \ll 1$ . In fact, in that case, under the physically reasonable



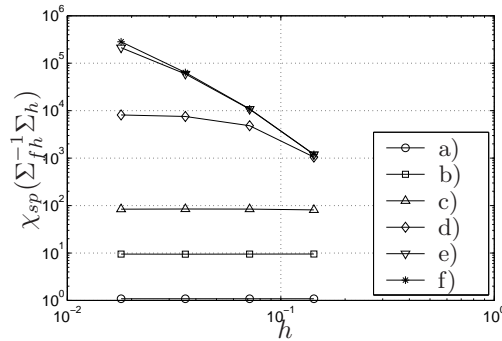


Figure 8 – Condition number  $\chi_{sp}(\Sigma_{fh}^{-1}\Sigma_h)$  versus  $h$  for the test cases reported in Table 4.

hypothesis that  $\nabla \mathbf{u}_f + \nabla^T \mathbf{u}_f$  and  $\nabla \varphi$  be sufficiently small, (3.19) reduces to

$$C_f \mathbf{I} + \nabla p_f \cong \mathbf{f},$$

while (2.5) becomes

$$\mathbf{u}_p + C_p \mathbf{I} \cong \mathbf{0},$$

where  $C_f$  and  $C_p$  denote two positive constants  $\ll 1$ . We rewrite (2.5) as

$$\mathbf{K}^{-1} \mathbf{u}_p + \nabla \varphi = \mathbf{0} \quad \text{in } \Omega_p, \tag{9.3}$$

and formally comparing (9.3) to (3.19), we are led to modify the latter by adding a mass term like  $\mathbf{K}^{-1} \mathbf{u}_p$  as follows:

$$\bar{\gamma} \mathbf{K}^{-1} \mathbf{u}_f - \nabla \cdot \mathbb{T}(\mathbf{u}_f, p_f) = \tilde{\mathbf{f}}, \quad \bar{\gamma} \in \mathbb{R}^+. \tag{9.4}$$

The right hand side has been modified accordingly. In this way we obtain a generalized Stokes momentum equation, and note that now (9.4) has the same behavior of (9.3) in the cases of our interest, that is when  $\nu \ll 1$  and  $\mathbf{K} \ll 1$ .

The mass term  $\bar{\gamma} \mathbf{K}^{-1} \mathbf{u}_f$  enhances the positivity of the discrete Steklov-Poincaré operator  $\Sigma_{fh}$  which acts as preconditioner in Algorithm 1 (or equivalently, Algorithm 2), thus enhancing the rate of convergence of the substructuring method. With this aim, we have carried out some numerical tests using the PCG Algorithm 2 to solve the modified problem Stokes/Darcy where (9.4) is considered instead of (3.19). The convergence results reported in Table 5 and the corresponding spectral condition numbers in Figure 9 show that the numerical scheme has improved substantially.

Table 5 – Number of iterations to solve the modified Stokes/Darcy problem using (9.4) for different values of  $\nu$ ,  $K$  and  $\bar{\gamma}$ .

$\nu$	$K$	$\bar{\gamma}$	Iterations on the mesh with grid size			
			$h = 0.1428$	$h = 0.0714$	$h = 0.0357$	$h = 0.0178$
$10^{-3}$	$10^{-2}$	0.1	15	24	28	28
		1	12	14	16	14
		10	8	9	9	8
$10^{-6}$	$10^{-4}$	0.1	15	23	28	33
		1	13	14	17	18
		10	8	9	9	9

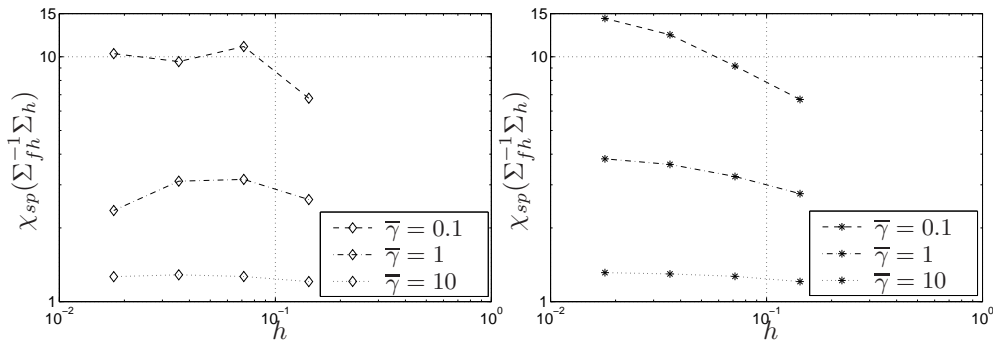


Figure 9 – Condition number  $\chi_{sp}(\Sigma_{fh}^{-1}\Sigma_h)$  for  $\nu = 10^{-3}$ ,  $K = 10^{-2}$  (left) and  $\nu = 10^{-6}$ ,  $K = 10^{-4}$  (right) versus  $h$  for different values of  $\bar{\gamma}$ .

### 9.3. A subdomain iterative method for a time-dependent problem

Equation (9.4) can be regarded as a discretization in time of the time-dependent Stokes momentum equation

$$\partial_t \mathbf{u}_f - \nabla \cdot \mathbb{T}(\mathbf{u}_f, p_f) = \mathbf{f} \quad \text{in } \Omega_f.$$

Precisely, if we consider

$$\bar{\gamma} K^{-1} \mathbf{u}_{f,n+1} - \nabla \cdot \mathbb{T}(\mathbf{u}_{f,n+1}, p_{f,n+1}) = \tilde{\mathbf{f}}_{n+1}, \quad n \geq 0,$$

with

$$\tilde{\mathbf{f}}_{n+1} = \mathbf{f}(\mathbf{x}, t_{n+1}) + \bar{\gamma} K^{-1} \mathbf{u}_{f,n},$$

we have a backward Euler discretization in time with  $\bar{\gamma} K^{-1}$  playing the role of the inverse of a time step (the subscript  $n$  refers to the  $n$ -th time level).

From the physical viewpoint, since the fluid velocities in  $\Omega_f$  are much higher than the ones through the porous medium (see [66]), a time-dependent model better represents the phenomena occurring during the filtration process.

Then, we can adopt the following algorithm.

**Algorithm 3.** Let  $[0, T]$  be a characteristic time interval. Consider for the sake of simplicity the first-order backward Euler scheme, and denote by  $\Delta t > 0$  the time step and  $N = T/\Delta t$ .

For  $n = 0, \dots, N - 1$ , do

- 0. Choose an initial guess  $(\mathbf{u}_f)_{n+1}^0 \cdot \mathbf{n}$  for the normal velocity on  $\Gamma$  at the  $(n + 1)$ -th time level.

For  $k \geq 0$  until convergence, do

- 1. Solve Darcy equation with boundary condition  $-\mathcal{K}\partial_n \varphi_{n+1}^{k+1} = (\mathbf{u}_f)_{n+1}^k \cdot \mathbf{n}$  on  $\Gamma$ .
- 2. Solve the Stokes problem

$$(\Delta t)^{-1} \mathbf{u}_{f,n+1}^{k+\frac{1}{2}} - \nabla \cdot \mathbb{T}(\mathbf{u}_{f,n+1}^{k+\frac{1}{2}}, p_{f,n+1}^{k+\frac{1}{2}}) = (\Delta t)^{-1} \mathbf{u}_{f,n} + \mathbf{f}_{n+1} \quad \text{in } \Omega_f,$$

$$\nabla \cdot \mathbf{u}_{f,n+1}^{k+\frac{1}{2}} = 0 \quad \text{in } \Omega_f,$$

$$\text{imposing } -\mathbf{n} \cdot \mathbb{T}(\mathbf{u}_{f,n+1}^{k+\frac{1}{2}}, p_{f,n+1}^{k+\frac{1}{2}}) \cdot \mathbf{n} = g\varphi_{n+1}^{k+1} \text{ on } \Gamma.$$

- 3. Update:  $(\mathbf{u}_f)_{n+1}^{k+1} \cdot \mathbf{n} = \theta (\mathbf{u}_f)_{n+1}^{k+\frac{1}{2}} \cdot \mathbf{n} + (1 - \theta) (\mathbf{u}_f)_{n+1}^k \cdot \mathbf{n}$  on  $\Gamma$ ,  $\theta \in (0, 1)$ .

To test this algorithm we consider the horizontal section of a channel 12 m long and 8 m wide which is partially occupied by a porous medium with discontinuous conductivity, as represented in Figure 10. A parabolic inflow profile is imposed on the left hand side boundary with maximal velocity equal to 0.1 m/s. On the right an outflow condition is imposed. The time interval is  $t \in [0, 0.5]$  and the time step  $\Delta t = 10^{-3}$  s; for space discretization three different computational meshes have been adopted. In a first case we have considered  $\nu = 10^{-5}$  m<sup>2</sup>/s and a discontinuous coefficient  $\mathcal{K} = 10^{-3}$  m/s in  $\Omega_p^{(1)}$ ,  $\mathcal{K} = 10^{-7}$  m/s in  $\Omega_p^{(2)}$ .

In Figure 11 we have represented the computed solution at time  $t = 0.05$  s, while in Figure 12 a zoom of the velocity field through the porous medium is shown; it can be seen that the velocity is almost null in the less permeable areas of the porous medium. Finally, Table 6 (left) reports the number of iterations obtained for three computational grids at different time levels, showing that the number of iterations is low and independent of  $h$ .

The same test has been performed considering different values of the parameters:  $\nu = 10^{-2}$  m<sup>2</sup>/s,  $\mathcal{K} = 10^{-1}$  m/s in  $\Omega_p^{(1)}$  and  $\mathcal{K} = 10^{-5}$  m/s in the less permeable part  $\Omega_p^{(2)}$  of the porous medium. The convergence results show that the number of

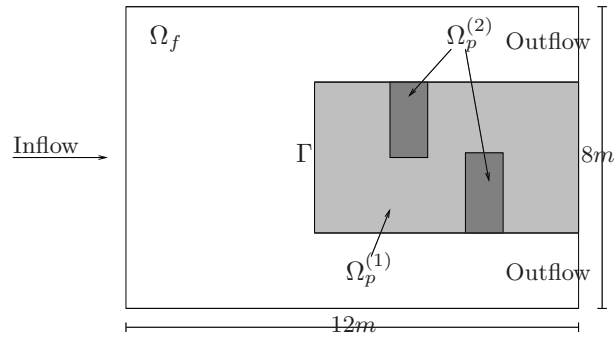


Figure 10 – Computational domain.

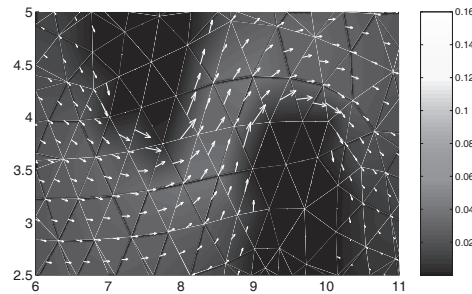


Figure 12 – Zoom of the velocity field through the porous medium.

iterations is essentially independent of these parameters, as it can be seen comparing the previous convergence results with those reported in Table 6 (right).

Table 6 – Number of iterations on different grids with  $\nu = 10^{-5} \text{ m}^2/\text{s}$ ,  $K = 10^{-3} \text{ m/s}$  and  $K = 10^{-7} \text{ m/s}$  (left); with  $\nu = 10^{-2} \text{ m}^2/\text{s}$ ,  $K = 10^{-1} \text{ m/s}$  and  $K = 10^{-5} \text{ m/s}$  (right).

Time level	Iterations on the mesh with			Time level	Iterations on the mesh with		
	232 el.	928 el.	3712 el.		232 el.	928 el.	3712 el.
0.001	21	21	21	0.001	22	22	22
0.003	20	19	19	0.003	20	20	20
0.006	12	11	11	0.006	15	15	15
0.009	10	10	10	0.009	15	15	15
0.01	10	10	10	0.01	15	15	15

The numerical results show that considering a time-dependent problem allows to

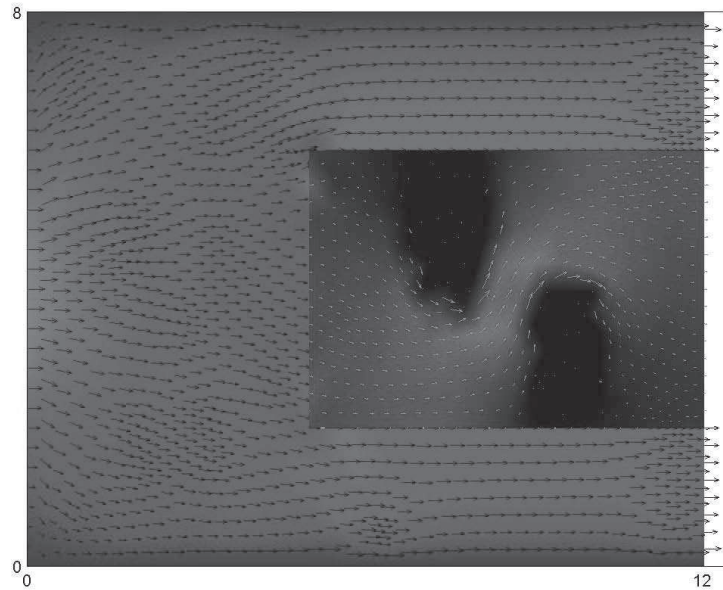


Figure 11 – Computed velocity field at  $t = 0.05$  s.

set up a far more efficient iterative method for problems with parameters in a range of physical interest. However, as we have pointed out in the preliminary tests of Section 9.2 (see Table 5), the value of  $\Delta t$  generally depends on  $\nu$  and  $K$ , and in some cases we could be forced to consider very small time steps  $\Delta t \ll 1$ . This could be quite annoying since one might be interested in considering long time scales, for example in modeling the filtration of pollutants in groundwater.

This limitation on  $\Delta t$  drives us to reconsider the steady coupled model. In fact, should we find an algorithm whose behavior were as much as possible independent of the physical parameters, then not only we would be able to solve the steady problem itself, but we could also use it in the framework of the time-dependent model where  $\Delta t$  would be chosen under the sole requirements of stability and accuracy.

*Remark 9.1.* An algorithm similar to Algorithm 3 has been adopted to simulate the coupling between free surface flows governed by the shallow water equations and groundwater flows. Theory and numerical results can be found in [97, 55].

## 10. Robin-Robin methods for the Stokes/Darcy coupling

In this section, we consider iterative methods to solve the Stokes/Darcy problem (4.13)–(4.14) based on Robin conditions across the interface  $\Gamma$ , i.e., proper linear combinations of the coupling conditions (3.16) and (3.17). These methods extend those illustrated in Section 8 and they are more robust giving a convergence rate that we observed numerically to be essentially independent of the grid parameter  $h$  and of the physical quantities characterizing the filtration.

We point out that these methods and their algebraic interpretation (see [53, 54]) have inspired algorithms featuring a similar structure in the context of fluid-structure interactions between blood flows and the poroelastic arterial wall. We refer the reader to [15] and also to [107, Chapter 6].

For the sake of simplicity, in the rest of this section we will consider the simplified condition on the interface  $\mathbf{u}_f \cdot \boldsymbol{\tau}_j = 0$  instead of (3.18). Moreover, we will use homogeneous boundary conditions, i.e., we will set  $\mathbf{u}_{in} = \mathbf{0}$  in (4.2) and  $\varphi_p = 0$  in (4.3).

### 10.1. A sequential Robin-Robin (sRR) method

We consider a sequential Robin-Robin (sRR) method which at each iteration requires to solve a Darcy problem in  $\Omega_p$  followed by a Stokes problem in  $\Omega_f$ , both with Robin conditions on  $\Gamma$ . Precisely, the algorithm reads as follows.

Having assigned a trace function  $\eta^0 \in L^2(\Gamma)$ , and two acceleration parameters  $\gamma_f \geq 0$  and  $\gamma_p > 0$ , for each  $k \geq 0$ :

- (i) Find  $\varphi^{k+1} \in H_p$  such that

$$\gamma_p a_p(\varphi^{k+1}, \psi) + \int_{\Gamma} g \varphi_{|\Gamma}^{k+1} \psi_{|\Gamma} = \int_{\Gamma} \eta^k \psi_{|\Gamma} \quad \forall \psi \in H_p. \quad (10.1)$$

This corresponds to imposing the following interface condition (in weak, or natural, form) for the Darcy problem:

$$-\gamma_p \mathbf{K} \partial_n \varphi^{k+1} + g \varphi_{|\Gamma}^{k+1} = \eta^k \quad \text{on } \Gamma. \quad (10.2)$$

- (ii) Then, find  $(\mathbf{u}_f^{k+1}, p_f^{k+1}) \in H_f^\tau \times Q$  such that

$$\begin{aligned} a_f(\mathbf{u}_f^{k+1}, \mathbf{v}) + b_f(\mathbf{v}, p_f^{k+1}) + \gamma_f \int_{\Gamma} (\mathbf{u}_f^{k+1} \cdot \mathbf{n})(\mathbf{v} \cdot \mathbf{n}) \\ = \int_{\Gamma} \left( \frac{\gamma_f}{\gamma_p} \eta^k - \frac{\gamma_f + \gamma_p}{\gamma_p} g \varphi_{|\Gamma}^{k+1} \right) (\mathbf{v} \cdot \mathbf{n}) + \int_{\Omega_f} \mathbf{f} \cdot \mathbf{v} \quad \forall \mathbf{v} \in H_f^\tau, \end{aligned} \quad (10.3)$$

$$b_f(\mathbf{u}_f^{k+1}, q) = 0 \quad \forall q \in Q. \quad (10.4)$$

This corresponds to imposing on the Stokes problem the following matching conditions on  $\Gamma$  (still in natural form):

$$\begin{aligned} \mathbf{n} \cdot \mathbb{T}(\mathbf{u}_f^{k+1}, p_f^{k+1}) \cdot \mathbf{n} + \gamma_f \mathbf{u}_f^{k+1} \cdot \mathbf{n} &= \frac{\gamma_f}{\gamma_p} \eta^k - \frac{\gamma_f + \gamma_p}{\gamma_p} g \varphi|_{\Gamma}^{k+1} \\ &= -g \varphi|_{\Gamma}^{k+1} - \gamma_f \mathbf{K} \partial_n \varphi^{k+1} \quad (10.5) \\ \mathbf{u}_f^{k+1} \cdot \boldsymbol{\tau}_j &= 0, \quad j = 1, \dots, d-1. \end{aligned}$$

(iii) Finally, set

$$\begin{aligned} \eta^{k+1} &= -\mathbf{n} \cdot \mathbb{T}(\mathbf{u}_f^{k+1}, p_f^{k+1}) \cdot \mathbf{n} + \gamma_p \mathbf{u}_f^{k+1} \cdot \mathbf{n} \\ &= (\gamma_f + \gamma_p)(\mathbf{u}_f^{k+1} \cdot \mathbf{n}) + \frac{\gamma_f + \gamma_p}{\gamma_p} g \varphi|_{\Gamma}^{k+1} - \frac{\gamma_f}{\gamma_p} \eta^k \in L^2(\Gamma). \quad (10.6) \end{aligned}$$

Concerning the solvability of problem (10.3)–(10.4), we note first that using the trace theorem and the Korn inequality (4.19), there exist two constants  $\kappa_1, \kappa_2 > 0$  such that

$$\int_{\Gamma} |\mathbf{u}_f \cdot \mathbf{n}|^2 \leq \kappa_1 \left( \int_{\Omega_f} (|\mathbf{u}_f|^2 + |\nabla \mathbf{u}_f|^2) \right) \leq \kappa_2 \int_{\Omega_f} |\nabla \mathbf{u}_f + \nabla^T \mathbf{u}_f|^2.$$

Therefore, the bilinear form

$$a_f(\mathbf{u}_f, \mathbf{v}) + \gamma_f \int_{\Gamma} (\mathbf{u}_f \cdot \mathbf{n})(\mathbf{v} \cdot \mathbf{n})$$

is continuous and coercive in  $H_f^r \times H_f^r$ . Moreover, the bilinear form  $b_f(\mathbf{v}, p)$  satisfies an inf–sup condition on the space  $H_f^r \times Q$  (see, e.g., [110, pages 157–158]). Then, for every  $\mathbf{f} \in (L^2(\Omega_f))^d$ ,  $\eta^k \in L^2(\Gamma)$  and  $\varphi|_{\Gamma}^{k+1} \in L^2(\Gamma)$ , there exists a unique solution of problem (10.3)–(10.4).

If the sRR method converges, in the limit we recover the solution  $(\mathbf{u}_f, p_f) \in H_f^r \times Q$  and  $\varphi \in H_p$  of the coupled Stokes/Darcy problem. Indeed, denoting by  $\varphi^*$  the limit of the sequence  $\varphi^k$  in  $H^1(\Omega_p)$  and by  $(\mathbf{u}_f^*, p_f^*)$  that of  $(\mathbf{u}_f^k, p_f^k)$  in  $(H^1(\Omega_f))^d \times Q$ , we obtain

$$-\gamma_p \mathbf{K} \nabla \varphi^* \cdot \mathbf{n} + g \varphi|_{\Gamma}^* = -\mathbf{n} \cdot \mathbb{T}(\mathbf{u}_f^*, p_f^*) \cdot \mathbf{n} + \gamma_p \mathbf{u}_f^* \cdot \mathbf{n} \quad \text{on } \Gamma, \quad (10.7)$$

so that, as a consequence of (10.5), we have

$$(\gamma_f + \gamma_p) \mathbf{u}_f^* \cdot \mathbf{n} = -(\gamma_f + \gamma_p) \mathbf{K} \nabla \varphi^* \cdot \mathbf{n} \quad \text{on } \Gamma,$$

yielding, since  $\gamma_f + \gamma_p \neq 0$ ,  $\mathbf{u}_f^* \cdot \mathbf{n} = -\mathbf{K} \partial_n \varphi^*$  on  $\Gamma$ , and also, from (10.7), that  $\mathbf{n} \cdot \mathbb{T}(\mathbf{u}_f^*, p_f^*) \cdot \mathbf{n} = -g \varphi|_{\Gamma}^*$  on  $\Gamma$ . Thus, the two interface conditions (3.16) and (3.17) are satisfied, and we can conclude that the limit functions  $\varphi^* \in H_p$  and  $(\mathbf{u}_f^*, p_f^*) \in H_f^r \times Q$  are the solutions of the coupled Stokes/Darcy problem.

We address the issue of convergence of the sRR method in Section 10.3.

**10.2. Interpretation of the sRR method as an alternating direction scheme**

The sRR method can be interpreted as an alternating direction scheme (see [8] and also [53]). For technical reasons, to make precise this statement let us assume that the flux boundary condition  $\mathbb{T}(\mathbf{u}_f, p_f) \cdot \mathbf{n} = \mathbf{0}$  is imposed on the top  $\Gamma_f^2$  (see Figure 1) of the fluid domain  $\Omega_f$ . This allows us to guarantee at each step the uniqueness of the pressure  $p_f$  in the space  $Q$ . Moreover, we assume that the interface  $\Gamma$  is smooth, say, a  $\mathcal{C}^2$ -manifold with boundary. Then, we introduce the spaces

$$\begin{aligned} \widehat{H}_f &= \{ \mathbf{v} \in (H^1(\Omega_f))^d : \mathbf{v} = \mathbf{0} \text{ on } \Gamma_f^1 \cup \Gamma_f^3 \}, \\ \widehat{H}_f^\tau &= \{ \mathbf{v} \in \widehat{H}_f : \mathbf{v} \cdot \boldsymbol{\tau}_j = 0 \text{ on } \Gamma, j = 1, \dots, d-1 \}, \\ \widehat{H}_f^{\tau, n} &= \{ \mathbf{v} \in \widehat{H}_f^\tau : \mathbf{v} \cdot \mathbf{n} = 0 \text{ on } \Gamma \}, \end{aligned}$$

and we define the operator  $\widehat{S}_f$  as

$$\widehat{S}_f : H_0^{1/2}(\Gamma) \rightarrow (H_0^{1/2}(\Gamma))', \quad \chi \rightarrow \widehat{S}_f \chi = \mathbf{n} \cdot (\mathbb{T}(\mathbf{u}_\chi, p_\chi) \cdot \mathbf{n}),$$

where  $(\mathbf{u}_\chi, p_\chi) \in \widehat{H}_f^\tau \times Q$  satisfies

$$\begin{aligned} a_f(\mathbf{u}_\chi, \mathbf{v}) + b_f(\mathbf{v}, p_\chi) &= 0 \quad \forall \mathbf{v} \in \widehat{H}_f^{\tau, n}(\Omega_f), \\ b_f(\mathbf{u}_\chi, q) &= 0 \quad \forall q \in Q, \end{aligned}$$

with  $\mathbf{u}_\chi \cdot \mathbf{n} = \chi$  on  $\Gamma$ .

Notice that  $\widehat{S}_f$  corresponds essentially to the operator  $S_f$  defined in (5.17) except for the boundary condition  $\mathbb{T}(\mathbf{u}_f, p_f) \cdot \mathbf{n} = \mathbf{0}$  on  $\Gamma_f^2$ . Indeed, in the definition of  $S_f$  only homogeneous Dirichlet boundary conditions on  $\partial\Omega_f \setminus \Gamma$  were imposed.

On the other hand, let  $S_p$  be the operator defined in (5.18). Let us recall that, for each  $\eta \in (H_0^{1/2}(\Gamma))'$ ,

$$S_p : (H_0^{1/2}(\Gamma))' \rightarrow H_0^{1/2}(\Gamma), \quad \eta \rightarrow S_p \eta = g\varphi_\eta|_\Gamma,$$

where  $\varphi_\eta \in H_p$  is the solution of

$$a_p(\varphi_\eta, \psi) = \langle \eta, \psi|_\Gamma \rangle_\Gamma \quad \forall \psi \in H_p,$$

and  $\langle \cdot, \cdot \rangle_\Gamma$  denotes the duality pairing between  $(H_0^{1/2}(\Gamma))'$  and  $H_0^{1/2}(\Gamma)$ . As a consequence, we have  $-\mathbf{K}\partial_n \varphi_\eta = \eta$  on  $\Gamma$ .

Since for each  $\varphi \in H_p$  we have  $S_p(-\mathbf{K}\partial_n \varphi) = g\varphi|_\Gamma$ , the first step (10.3)–(10.4) of our procedure corresponds to imposing on  $\Gamma$

$$\begin{aligned} -\gamma_p \mathbf{K}\partial_n \varphi^{k+1} + g\varphi|_\Gamma^{k+1} &= -\gamma_p \mathbf{K}\nabla \varphi^{k+1} \cdot \mathbf{n} + S_p(-\mathbf{K}\partial_n \varphi^{k+1}) \\ &= (\gamma_p I + S_p)(-\mathbf{K}\partial_n \varphi^{k+1}) = \eta^k, \end{aligned}$$



hence

$$-\mathbf{K}\partial_n\varphi^{k+1} = (\gamma_p I + S_p)^{-1}\eta^k .$$

On the other hand, the right hand side in (10.5) can be written as

$$\begin{aligned} -g\varphi_{|\Gamma}^{k+1} - \gamma_f \mathbf{K}\partial_n\varphi^{k+1} &= S_p(\mathbf{K}\partial_n\varphi^{k+1}) - \gamma_f \mathbf{K}\partial_n\varphi^{k+1} \\ &= -(\gamma_f I - S_p)\mathbf{K}\partial_n\varphi^{k+1} \\ &= (\gamma_f I - S_p)(\gamma_p I + S_p)^{-1}\eta^k . \end{aligned} \tag{10.8}$$

In an analogous way, still denoting by  $(\mathbf{u}_f^{k+1}, p_f^{k+1})$  the solution of (10.3)–(10.4) with  $\mathbf{f} = \mathbf{0}$  and  $H_f^\tau$  replaced by  $\widehat{H}_f^\tau$ , one has  $\widehat{S}_f(\mathbf{u}_f^{k+1} \cdot \mathbf{n}) = \mathbf{n} \cdot \mathbb{T}(\mathbf{u}_f^{k+1}, p_f^{k+1}) \cdot \mathbf{n}$ . Then, the left hand side in (10.5) can be written as

$$\begin{aligned} \mathbf{n} \cdot \mathbb{T}(\mathbf{u}^{k+1}, p^{k+1}) \cdot \mathbf{n} + \gamma_f \mathbf{u}^{k+1} \cdot \mathbf{n} &= \widehat{S}_f(\mathbf{u}^{k+1} \cdot \mathbf{n}) + \gamma_f \mathbf{u}^{k+1} \cdot \mathbf{n} \\ &= (\gamma_f I + \widehat{S}_f)(\mathbf{u}^{k+1} \cdot \mathbf{n}) . \end{aligned} \tag{10.9}$$

Using (10.8) and (10.9), the interface condition (10.5) becomes

$$\mathbf{u}^{k+1} \cdot \mathbf{n} = (\gamma_f I + \widehat{S}_f)^{-1}(\gamma_f I - S_p)(\gamma_p I + S_p)^{-1}\eta^k .$$

In conclusion, our iterative procedure (with  $\mathbf{f} = \mathbf{0}$ ) can be written as

$$\begin{aligned} \eta^{k+1} &= -\mathbf{n} \cdot \mathbb{T}(\mathbf{u}^{k+1}, p^{k+1}) \cdot \mathbf{n} + \gamma_p \mathbf{u}^{k+1} \cdot \mathbf{n} \\ &= -\widehat{S}_f(\mathbf{u}^{k+1} \cdot \mathbf{n}) + \gamma_p \mathbf{u}^{k+1} \cdot \mathbf{n} \\ &= (\gamma_p I - \widehat{S}_f)\mathbf{u}^{k+1} \cdot \mathbf{n} \\ &= (\gamma_p I - \widehat{S}_f)(\gamma_f I + \widehat{S}_f)^{-1}(\gamma_f I - S_p)(\gamma_p I + S_p)^{-1}\eta^k . \end{aligned} \tag{10.10}$$

This is an alternating direction scheme, *à la* Peaceman–Rachford (see [106]), that has been deeply analyzed in the literature. Sufficient conditions for convergence are that  $\gamma_f = \gamma_p$  and the operators  $\widehat{S}_f$  and  $S_p$  are bounded and strictly positive in a given Hilbert space. These do not apply in the present situation, as the operators  $\widehat{S}_f$  and  $S_p$  act from a space into its dual. In fact, we can only prove that the iteration operator is non-expansive, but not a contraction in  $(H_{00}^{1/2}(\Gamma))'$ .

On the other hand, it is worthy to note that the convergence of this alternating direction scheme can be easily proved in the discrete case, as the matrices that correspond to the finite dimensional Steklov–Poincaré operators  $\widehat{S}_f$  and  $S_p$  are in fact symmetric and positive definite. Indeed, the discrete counterpart of  $S_p$  is the local Schur complement  $\Sigma_p$  introduced in (8.18), while  $\widehat{S}_f$  corresponds to a slight modification of  $\Sigma_f$  in (8.17) to account for the boundary condition  $\mathbb{T}(\mathbf{u}_f, p_f) \cdot \mathbf{n} = \mathbf{0}$  instead of  $\mathbf{u}_f = \mathbf{0}$  on  $\Gamma_f^2$ .

The prove of convergence of (10.10) can be found in [57].

**10.3. Convergence of the sRR method**

We prove that the sequences  $\varphi^k$  and  $(\mathbf{u}_f^k, p_f^k)$  generated by the sRR method (10.1)–(10.6) converge in  $H^1(\Omega_p)$  and  $(H^1(\Omega_f))^d \times Q$ , respectively. As a consequence, the sequence  $\eta^k$  is convergent in the dual space  $H^{-1/2}(\Gamma)$  and weakly convergent in  $L^2(\Gamma)$ .

The proof of convergence that we are presenting follows the guidelines of the theory by P.-L. Lions [91] for the Robin-Robin method (see also [110, Section 4.5]).

We denote by  $\mathbf{e}_u^k = \mathbf{u}_f^k - \mathbf{u}_f$ ,  $e_p^k = p_f^k - p_f$  and  $e_\varphi^k = \varphi^k - \varphi$  the errors at the  $k$ -th step. Remark that, thanks to the linearity, the functions  $(\mathbf{e}_u^k, e_p^k)$  satisfy problem (10.3)–(10.4) with  $\mathbf{f} = \mathbf{0}$ , while  $e_\varphi^k$  is a solution to (10.3)–(10.4). Moreover, we assume that  $\gamma_p = \gamma_f$ , and we denote by  $\gamma$  their common value.

Finally, let us point out that the solutions  $(\mathbf{u}_f, p_f) \in H_f^r \times Q$  and  $\varphi \in H_p$  of the coupled Stokes/Darcy problem satisfy  $\mathbf{n} \cdot \mathbb{T}(\mathbf{u}_f, p_f) \cdot \mathbf{n} \in H^{1/2}(\Gamma)$  (as it is equal to  $-g\varphi|_\Gamma$  on  $\Gamma$ ), and  $\nabla\varphi \cdot \mathbf{n} \in L^2(\Gamma)$  (as it is equal to  $-\mathbf{K}^{-1}\mathbf{u}_f \cdot \mathbf{n}$  on  $\Gamma$ ), i.e., these functions enjoy a better regularity than one might usually expect. Therefore, the interface conditions (10.2) and (10.5) for the error functions hold in  $L^2(\Gamma)$ .

Let us come to the proof of convergence. Choosing  $\psi = e_\varphi^{k+1}$  in (10.1), and using the identity

$$AB = \frac{1}{4}[(A + B)^2 - (A - B)^2],$$

we have

$$\begin{aligned} g a_p(e_\varphi^{k+1}, e_\varphi^{k+1}) &= \frac{1}{\gamma} \int_\Gamma (\eta^k - g e_{\varphi|\Gamma}^{k+1}) g e_{\varphi|\Gamma}^{k+1} \\ &= \frac{1}{4\gamma} \int_\Gamma (\eta^k)^2 - \frac{1}{4\gamma} \int_\Gamma (\eta^k - 2g e_{\varphi|\Gamma}^{k+1})^2. \end{aligned} \tag{10.11}$$

Similarly, taking  $\mathbf{v} = \mathbf{e}_u^{k+1}$  in (10.3) and using (10.6) we have:

$$\begin{aligned} a_f(\mathbf{e}_u^{k+1}, \mathbf{e}_u^{k+1}) &= \frac{1}{\gamma} \int_\Gamma (\eta^k - 2g e_{\varphi|\Gamma}^{k+1} - \gamma \mathbf{e}_u^{k+1} \cdot \mathbf{n})(\gamma \mathbf{e}_u^{k+1} \cdot \mathbf{n}) \\ &= \frac{1}{4\gamma} \int_\Gamma (\eta^k - 2g e_{\varphi|\Gamma}^{k+1})^2 - \frac{1}{4\gamma} \int_\Gamma (\eta^k - 2g e_{\varphi|\Gamma}^{k+1} - 2\gamma \mathbf{e}_u^{k+1} \cdot \mathbf{n})^2 \\ &= \frac{1}{4\gamma} \int_\Gamma (\eta^k - 2g e_{\varphi|\Gamma}^{k+1})^2 - \frac{1}{4\gamma} \int_\Gamma (\eta^{k+1})^2. \end{aligned} \tag{10.12}$$

Adding (10.11) and (10.12) we find

$$g a_p(e_\varphi^{k+1}, e_\varphi^{k+1}) + a_f(\mathbf{e}_u^{k+1}, \mathbf{e}_u^{k+1}) + \frac{1}{4\gamma} \int_\Gamma (\eta^{k+1})^2 = \frac{1}{4\gamma} \int_\Gamma (\eta^k)^2.$$

Summing over  $k$  from  $k = 0$  to  $k = N$ , with  $N \geq 1$ , we finally obtain

$$\sum_{k=0}^N (g a_p(e_\varphi^{k+1}, e_\varphi^{k+1}) + a_f(\mathbf{e}_u^{k+1}, \mathbf{e}_u^{k+1})) + \frac{1}{4\gamma} \int_\Gamma (\eta^{N+1})^2 = \frac{1}{4\gamma} \int_\Gamma (\eta^0)^2.$$

Thus, the series

$$\sum_{k=0}^{\infty} (g a_p(e_\varphi^{k+1}, e_\varphi^{k+1}) + a_f(\mathbf{e}_u^{k+1}, \mathbf{e}_u^{k+1}))$$

is convergent, and the errors  $e_\varphi^k$  and  $\mathbf{e}_u^k$  tend to zero in  $H^1(\Omega_p)$  and  $(H^1(\Omega_f))^d$ , respectively. The convergence of the pressure error  $e_p^k$  to 0 in  $Q$  is then a well-known consequence of the convergence of the velocity.

**10.4. Some numerical results**

The sRR algorithm on the discrete problem (5.8)–(5.12) becomes: taking a trace function  $\eta_h^0 \in \Lambda_h$ , and considering two acceleration parameters  $\gamma_f \geq 0$  and  $\gamma_p > 0$ , for each  $k \geq 0$ ,

- (i) Find  $\varphi_h^{k+1} \in H_{ph}$  such that

$$\gamma_p a_p(\varphi_h^{k+1}, \psi_h) + \int_\Gamma g \varphi_{h|\Gamma}^{k+1} \psi_h = \int_\Gamma \eta_h^k \psi_h \quad \forall \psi_h \in H_{ph} . \quad (10.13)$$

- (ii) Then, find  $(\mathbf{u}_{fh}^{k+1}, p_{fh}^{k+1}) \in H_{fh}^\tau \times Q_h$  such that

$$\begin{aligned} & a_f(\mathbf{u}_{fh}^{k+1}, \mathbf{v}_h) + b_f(\mathbf{v}_h, p_{fh}^{k+1}) + \gamma_f \int_\Gamma (\mathbf{u}_{fh}^{k+1} \cdot \mathbf{n})(\mathbf{v}_h \cdot \mathbf{n}) \\ &= \int_\Gamma \left( \frac{\gamma_f}{\gamma_p} \eta_h^k - \frac{\gamma_f + \gamma_p}{\gamma_p} g \varphi_{h|\Gamma}^{k+1} \right) (\mathbf{v}_h \cdot \mathbf{n}) + \int_{\Omega_f} \mathbf{f} \cdot \mathbf{v}_h \quad \forall \mathbf{v}_h \in H_{fh}^\tau, \\ & b_f(\mathbf{u}_{fh}^{k+1}, q_h) = 0 \quad \forall q_h \in Q_h . \end{aligned} \quad (10.14)$$

- (iii) Finally, set

$$\eta_h^{k+1} = (\gamma_f + \gamma_p)(\mathbf{u}_{fh}^{k+1} \cdot \mathbf{n}) + \frac{\gamma_f + \gamma_p}{\gamma_p} g \varphi_{h|\Gamma}^{k+1} - \frac{\gamma_f}{\gamma_p} \eta_h^k \in \Lambda_h .$$

For  $\gamma_p = \gamma_f$ , the convergence of this algorithm can be proved as we did in Section 10.3 to show the convergence of (10.1)–(10.5). Moreover, it is also possible to prove the convergence of the alternating direction scheme (see Section 10.2), as the discrete Steklov–Poincaré operators are positive definite (however, in principle the proof of convergence cannot assure that the rate of convergence is independent of the mesh size  $h$ ).

For the numerical tests we have exploited the interpretation of the method in terms of alternating direction iterations (Section 10.2) in order to obtain some guidelines for the choice of the relaxation parameters, at least for the case of our interest, that is, when  $\nu$  and the entries of  $\mathbf{K}$  are very small (we recall that in this case the convergence rate of the Dirichlet-Neumann method deteriorates, see Section 9.2).

In particular, considering (10.10), we are led to investigate the behavior of the eigenvalues, say  $\delta_f^j$  and  $\delta_p^j$ , of the operators  $S_f$  and  $S_p$ , respectively; in fact, if we can estimate

$$\max_j \left| \frac{\gamma_p - \delta_f^j}{\gamma_f + \delta_f^j} \right| \cdot \max_j \left| \frac{\gamma_f - \delta_p^j}{\gamma_p + \delta_p^j} \right|, \tag{10.15}$$

this could be taken as a rough estimate of the convergence rate of the algorithm.

Assuming that  $K$  is a constant multiple of the identity, we proved that in the limit  $\nu \rightarrow 0$  and  $K \rightarrow 0$  (for a fixed mesh size  $h$ ),  $\delta_f^j \rightarrow 0$  while  $\delta_p^j \rightarrow \infty$  [53]. Thus, for small values of  $\nu$  and  $K$  the ratio (10.15) behaves like  $\gamma_p/\gamma_f$ . This provides a first indication for the choice of the relaxation parameters, i.e., one should take  $\gamma_f > \gamma_p > 0$ . Moreover,  $\gamma_f$  and  $\gamma_p$  should not be taken too large to avoid possible increases of the condition numbers of the Stokes and Darcy stiffness matrices in (10.13) and (10.14), respectively. A reasonable trade-off is to choose both parameters approximately equal to  $10^{-1}$ .

For the numerical tests, we take the same setting as in Section 9.2. In Table 7 we report the number of iterations obtained using the sRR method for some small values of  $\nu$  and  $K$  and for four different computational grids. A convergence test based on the relative increment of the trace of the discrete normal velocity on the interface  $\mathbf{u}_{fh}^k \cdot \mathbf{n}|_\Gamma$  has been considered with tolerance  $10^{-9}$ . In all computations we have taken  $\gamma_f = 0.3$  and  $\gamma_p = 0.1$ .

Table 7 – Number of iterations using the sRR method with respect to  $\nu$ ,  $K$  and four different grid sizes  $h$  ( $h_1 \approx 0.14$  and  $h_i = h_1/2^{i-1}$ ,  $i = 2, 3, 4$ ); the acceleration parameters are  $\gamma_f = 0.3$  and  $\gamma_p = 0.1$ .

$\nu$	$K$	$h_1$	$h_2$	$h_3$	$h_4$
$10^{-4}$	$10^{-3}$	19	19	19	19
$10^{-6}$	$10^{-4}$	20	20	20	20
$10^{-6}$	$10^{-7}$	20	20	20	20

Finally, we have considered the longitudinal section of a water channel 10 m long with a water depth of 1 m. At the inlet of the channel (see Figure 13) a parabolic inflow profile with maximal velocity 0.1 m/s is imposed, while on the other boundaries we impose  $\mathbf{u}_f = \mathbf{0}$ . The fluid is thus forced to filtrate through an homogeneous porous medium 10 m deep characterized by an hydraulic conductivity  $K = 10^{-3}$  m/s. The fluid has a density  $\nu = 10^{-6}$  m<sup>2</sup>/s. On the bottom of the porous media domain we impose  $\varphi = 0$  while on the lateral boundaries the impermeability condition  $K\partial_n\varphi = 0$  is assumed.

To compute the solution of the global problem we have considered the Algorithm 6.1 setting  $\gamma_f = 0.3$  and  $\gamma_p = 0.1$ . The tolerance on the relative increment has been set to  $10^{-5}$ . We have used three different computational meshes. The convergence

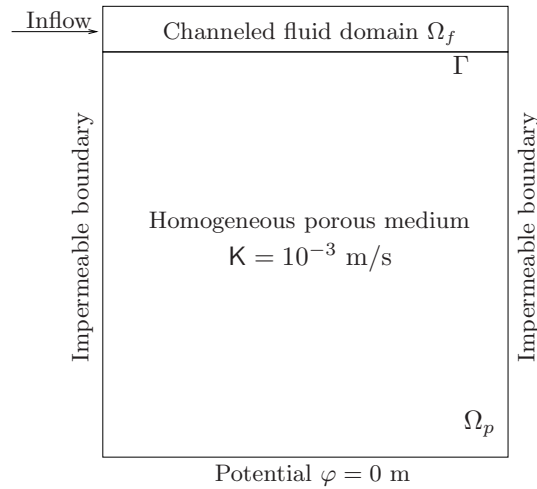


Figure 13 – Computational domain for the channeled fluid-porous media test case.

results are reported in table 8, while Figs. 14, 15 represents the computed velocity field and piezometric head.

Table 8 – Number of iterations obtained for three different computational meshes.

Mesh elements	Iterations
1272	6
5088	6
20352	6

The numerical results we have presented show that the alternating direction method sensibly improves the convergence behavior of the more classical Dirichlet-Neumann methods, specifically in presence of physically interesting parameters.

However, this method may still be improved by introducing a dynamic strategy to choose the acceleration parameters. Moreover, it would be interesting to apply the preconditioners issued by the alternating direction approach in the framework of the GMRES method.

*Remark 10.1.* A parallel variant of the sRR method presented in this section might also be considered. More precisely, the method would read as follows: let  $\mu^k \in L^2(\Gamma)$  be an assigned trace function on  $\Gamma$ , and  $\gamma_1, \gamma_2$  be two positive parameters; then, for  $k \geq 0$ ,

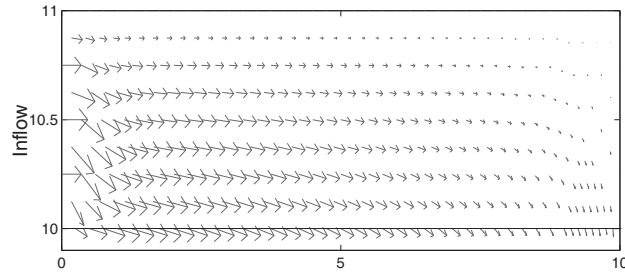


Figure 14 – Computed velocity field.

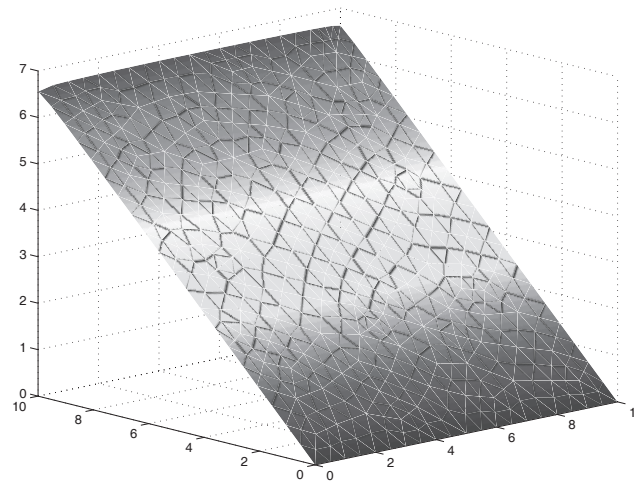


Figure 15 – Computed piezometric head.

(i) Find  $(\mathbf{u}_f^{k+1}, p_f^{k+1}) \in H_f^\tau \times Q$  such that

$$\begin{aligned}
 & a_f(\mathbf{u}_f^{k+1}, \mathbf{v}) + b_f(\mathbf{v}, p_f^{k+1}) - \gamma_1 \int_{\Gamma} (\mathbf{u}_f^{k+1} \cdot \mathbf{n})(\mathbf{v} \cdot \mathbf{n}) \\
 & = \int_{\Gamma} \mu^k (\mathbf{v} \cdot \mathbf{n}) + \int_{\Omega_f} \mathbf{f} \cdot \mathbf{v} \quad \forall \mathbf{v} \in H_f^\tau, \\
 & b_f(\mathbf{u}_f^{k+1}, q) = 0 \quad \forall q \in Q,
 \end{aligned}$$

and, at the same time, find  $\varphi^{k+1} \in H_p$  such that

$$a_p(\varphi^{k+1}, \psi) + \frac{1}{\gamma_1} \int_{\Gamma} g\varphi_{|\Gamma}^{k+1}\psi_{|\Gamma} = -\frac{1}{\gamma_1} \int_{\Gamma} \mu^k \psi_{|\Gamma} \quad \forall \psi \in H_p .$$

Remark that on the interface  $\Gamma$  we are imposing the matching conditions

$$\begin{aligned} \mathbf{n} \cdot \mathbb{T}(\mathbf{u}_f^{k+1}, p^{k+1}) \cdot \mathbf{n} - \gamma_1 \mathbf{u}_f^{k+1} \cdot \mathbf{n} &= \mu^k = -g\varphi_{|\Gamma}^{k+1} + \gamma_1 \mathbb{K}\partial_n \varphi^{k+1}, \\ \mathbf{u}_f^{k+1} \cdot \boldsymbol{\tau}_j &= 0, \quad j = 1, \dots, d-1. \end{aligned}$$

(ii) As a second step, find  $(\hat{\omega}^{k+1}, \hat{\pi}^{k+1}) \in H_f^r \times Q$  such that

$$\begin{aligned} a_f(\hat{\omega}^{k+1}, \mathbf{v}) + b_f(\mathbf{v}, \hat{\pi}^{k+1}) + \gamma_2 \int_{\Gamma} (\hat{\omega}^{k+1} \cdot \mathbf{n})(\mathbf{v} \cdot \mathbf{n}) \\ = \gamma_2 \int_{\Gamma} \hat{\sigma}^{k+1}(\mathbf{v} \cdot \mathbf{n}) \quad \forall \mathbf{v} \in H_f^r, \\ b_f(\hat{\omega}^{k+1}, q) = 0 \quad \forall q \in Q, \end{aligned}$$

and find  $\hat{\chi}^{k+1} \in H_p$  such that

$$a_p(\hat{\chi}^{k+1}, \psi) + \frac{1}{\gamma_2} \int_{\Gamma} g\hat{\chi}_{|\Gamma}^{k+1}\psi_{|\Gamma} = \int_{\Gamma} \hat{\sigma}^{k+1}\psi_{|\Gamma} \quad \forall \psi \in H_p ,$$

where

$$\hat{\sigma}^{k+1} = \mathbf{u}_f^{k+1} \cdot \mathbf{n} + \mathbb{K}\partial_n \varphi^{k+1} = \mathbf{u}_f^{k+1} \cdot \mathbf{n} + \frac{1}{\gamma_1}(g\varphi_{|\Gamma}^{k+1} + \mu^k) \in L^2(\Gamma) .$$

Note that on the interface  $\Gamma$  we are now imposing the matching conditions

$$\begin{aligned} \mathbf{n} \cdot \mathbb{T}(\hat{\omega}^{k+1}, \hat{\pi}^{k+1}) \cdot \mathbf{n} + \gamma_2 \hat{\omega}^{k+1} \cdot \mathbf{n} &= \gamma_2 \hat{\sigma}^{k+1} = g\hat{\chi}_{|\Gamma}^{k+1} - \gamma_2 \mathbb{K}\partial_n \hat{\chi}^{k+1}, \\ \hat{\omega}^{k+1} \cdot \boldsymbol{\tau}_j &= 0, \quad j = 1, \dots, d-1. \end{aligned}$$

(iii) Finally, set

$$\begin{aligned} \mu^{k+1} &= \mu^k - \theta[\mathbf{n} \cdot \mathbb{T}(\hat{\omega}^{k+1}, \hat{\pi}^{k+1}) \cdot \mathbf{n} + g\hat{\chi}_{|\Gamma}^{k+1}] \\ &= \mu^k - \theta[\gamma_2(\hat{\sigma}^{k+1} - \hat{\omega}^{k+1} \cdot \mathbf{n}) + g\hat{\chi}_{|\Gamma}^{k+1}] \in L^2(\Gamma) , \end{aligned}$$

where  $\theta > 0$  is a further acceleration parameter.

Although interesting from the theoretical point of view this algorithm unfortunately yields poor convergence results. We refer the reader to [57].

## 11. Iterative methods for the Navier-Stokes/Darcy problem

In this section, we introduce and analyze some iterative methods to compute the solution of a conforming finite element approximation of the non-linear Navier-Stokes/Darcy problem (4.11)–(4.12). For the easiness of notation, we will write our algorithms in continuous form. However, they can be straightforwardly translated into a discrete setting considering conforming internal Galerkin approximations of the spaces used hereafter.

Moreover, the convergence results that we will present hold in the discrete case (i.e., in the finite element spaces) without any dependence of the convergence rate on the grid parameter  $h$ , since they are established by using the properties of the operators in the continuous case.

Finally, for the sake of simplicity, we adopt homogeneous boundary conditions as already done in Section 6.

### 11.1. Fixed-point iterations

Fixed-point iterations to solve the coupled problem (4.11)–(4.12) can be written as follows. Given  $\mathbf{u}_f^0 \in H_f$ , for  $n \geq 1$ , find  $\mathbf{u}_f^n \in H_f$ ,  $p_f^n \in Q$ ,  $\varphi^n \in H_p$  such that

$$a_f(\mathbf{u}_f^n, \mathbf{v}) + c_f(\mathbf{u}_f^{n-1}; \mathbf{u}_f^n, \mathbf{v}) + b_f(\mathbf{v}, p_f^n) + \int_{\Gamma} g \varphi^n (\mathbf{v} \cdot \mathbf{n}) + \int_{\Gamma} \sum_{j=1}^{d-1} \frac{\nu \alpha_{BJ}}{\sqrt{K}} (\mathbf{u}_f^n \cdot \boldsymbol{\tau}_j) (\mathbf{v} \cdot \boldsymbol{\tau}_j) = \int_{\Omega_f} \mathbf{f} \cdot \mathbf{v}, \quad (11.1)$$

$$b_f(\mathbf{u}_f^n, q) = 0, \quad (11.2)$$

$$a_p(\varphi^n, \psi) = \int_{\Gamma} \psi (\mathbf{u}_f^n \cdot \mathbf{n}), \quad (11.3)$$

for all  $\mathbf{v} \in H_f$ ,  $q \in Q$ ,  $\psi \in H_p$ .

Algorithm (11.1)–(11.3) requires to solve at each iteration a linear coupled problem, and it can be reinterpreted as a fixed-point method to solve the interface problem (6.25). Indeed, let us first rewrite (11.1)–(11.2) in the equivalent form:

find  $\mathbf{u}_f^n \in V_f$  such that

$$a_f(\mathbf{u}_f^n, \mathbf{v}) + c_f(\mathbf{u}_f^{n-1}; \mathbf{u}_f^n, \mathbf{v}) + \int_{\Gamma} g \varphi^n (\mathbf{v} \cdot \mathbf{n}) + \int_{\Gamma} \sum_{j=1}^{d-1} \frac{\nu \alpha_{BJ}}{\sqrt{K}} (\mathbf{u}_f^n \cdot \boldsymbol{\tau}_j) (\mathbf{v} \cdot \boldsymbol{\tau}_j) = \int_{\Omega_f} \mathbf{f} \cdot \mathbf{v} \quad \forall \mathbf{v} \in V_f. \quad (11.4)$$

We denote  $\lambda^n = \mathbf{u}_f^n \cdot \mathbf{n}$  on  $\Gamma$  and we remark that  $\lambda^n \in \Lambda_0$ . Then, we consider  $\widetilde{R}_f^1 \lambda^n \in H_f$  and we set  $\mathbf{u}^n = \mathbf{u}_f^n - \widetilde{R}_f^1 \lambda^n$ . By definition,  $\mathbf{u}^n \cdot \mathbf{n} = 0$  on  $\Gamma$ . Moreover,



remark that for all  $\eta \in \Lambda_0$ , (6.8) implies that  $\nabla \cdot \widetilde{R}_f^1 \eta = 0$  in  $\Omega_f$  since we can choose  $q = \nabla \cdot \widetilde{R}_f^1 \eta$ . Thus,  $\mathbf{u}^n \in V_f^0$ .

From (11.3) it follows  $-\mathcal{K} \partial_n \varphi^n = \mathbf{u}_f^n \cdot \mathbf{n} = \lambda^n$  on  $\Gamma$ , so that by definition of  $R_p$ , we can write  $\varphi^n = R_p \lambda^n$ .

Finally, since  $\mathbf{v} \in V_f$ , proceeding as for  $\mathbf{u}_f^n$ , we can split  $\mathbf{v} = \mathbf{w} + \widetilde{R}_f^1 \mu$  with  $\mu = \mathbf{v} \cdot \mathbf{n}$  on  $\Gamma$  and  $\mathbf{w} \in V_f^0$ . Thus, (11.4) becomes

$$\begin{aligned} & a_f(\mathbf{u}^n + \widetilde{R}_f^1 \lambda^n, \mathbf{w} + \widetilde{R}_f^1 \mu) + c_f(\mathbf{u}^{n-1} + \widetilde{R}_f^1 \lambda^{n-1}; \mathbf{u}^n + \widetilde{R}_f^1 \lambda^n, \mathbf{w} + \widetilde{R}_f^1 \mu) \\ & + \int_{\Gamma} g(R_p \lambda^n) (\mathbf{w} + \widetilde{R}_f^1 \mu) \cdot \mathbf{n} + \int_{\Gamma} \sum_{j=1}^{d-1} \frac{\nu \alpha_{BJ}}{\sqrt{K}} ((\mathbf{u}^n + \widetilde{R}_f^1 \lambda^n) \cdot \boldsymbol{\tau}_j) ((\mathbf{w} + \widetilde{R}_f^1 \mu) \cdot \boldsymbol{\tau}_j) \\ & = \int_{\Omega_f} \mathbf{f}(\mathbf{w} + \widetilde{R}_f^1 \mu). \end{aligned}$$

Taking into account that  $\mathbf{w} \in V_f^0$  and the definition of  $\widetilde{R}_f^1$  (6.7)–(6.8), this corresponds to the fixed-point method:

Given  $\bar{u}^{n-1} = (\lambda^{n-1}, \mathbf{u}^{n-1}) \in \mathcal{W}$ , for  $n \geq 1$ ,

$$\text{find } \bar{u}^n = (\lambda^n, \mathbf{u}^n) \in \mathcal{W} : \quad \bar{a}(\bar{u}^{n-1}; \bar{u}^n, \bar{w}) = \langle \bar{\ell}, \bar{w} \rangle \quad \forall \bar{w} = (\mu, \mathbf{w}) \in \mathcal{W}.$$

(Recall that  $\mathcal{W} = \Lambda_0 \times V_f^0$ . See Section 6.2.)

Thanks to this equivalence, the convergence of (11.1)–(11.3) is a direct consequence of Lemma 6.5. We can state the following result which is a straightforward corollary of Theorem 6.7.

**Proposition 11.1.** *If (6.26) holds and if  $\mathbf{u}_f^0$  is such that the  $H^1$  seminorm in  $\Omega_f$   $|\widetilde{R}_f^1(\mathbf{u}_f^0 \cdot \mathbf{n})|_1 < r_M$  with  $r_M$  given in (6.27), then the sequence  $(\mathbf{u}_f^n, p_f^n, \varphi^n)$  converges for  $n \rightarrow \infty$  to the unique solution  $(\mathbf{u}_f, p_f, \varphi)$  of problem (4.11)–(4.12), and  $|\widetilde{R}_f^1(\mathbf{u}_f \cdot \mathbf{n})|_1 \leq r_m$ .*

### 11.2. Newton-like methods

Let us consider now the following Newton method to solve (the discrete form of) (4.11)–(4.12): let  $\mathbf{u}_f^0 \in H_f$  be given; then, for  $n \geq 1$ , find  $\mathbf{u}_f^n \in H_f, p_f^n \in Q, \varphi^n \in H_p$

such that, for all  $\mathbf{v} \in H_f$ ,  $q \in Q$ ,  $\psi \in H_p$ ,

$$a_f(\mathbf{u}_f^n, \mathbf{v}) + c_f(\mathbf{u}_f^n; \mathbf{u}_f^{n-1}, \mathbf{v}) + c_f(\mathbf{u}_f^{n-1}; \mathbf{u}_f^n, \mathbf{v}) + b_f(\mathbf{v}, p_f^n) + \int_{\Gamma} g \varphi^n (\mathbf{v} \cdot \mathbf{n}) \\ + \int_{\Gamma} \sum_{j=1}^{d-1} \frac{\nu \alpha_{BJ}}{\sqrt{K}} (\mathbf{u}_f^n \cdot \boldsymbol{\tau}_j) (\mathbf{v} \cdot \boldsymbol{\tau}_j) = c_f(\mathbf{u}_f^{n-1}; \mathbf{u}_f^{n-1}, \mathbf{v}) + \int_{\Omega_f} \mathbf{f} \cdot \mathbf{v}, \quad (11.5)$$

$$b_f(\mathbf{u}_f^n, q) = 0, \quad (11.6)$$

$$a_p(\varphi^n, \psi) = \int_{\Gamma} \psi (\mathbf{u}_f^n \cdot \mathbf{n}). \quad (11.7)$$

In order to reduce the computational cost, we might consider the modified Newton method:

find  $\mathbf{u}_f^n \in H_f$ ,  $p_f^n \in Q$ ,  $\varphi^n \in H_p$  such that, for all  $\mathbf{v} \in H_f$ ,  $q \in Q$ ,  $\psi \in H_p$ ,

$$a_f(\mathbf{u}_f^n, \mathbf{v}) + c_f(\mathbf{u}_f^n; \mathbf{u}_f^0, \mathbf{v}) + c_f(\mathbf{u}_f^0; \mathbf{u}_f^n, \mathbf{v}) + b_f(\mathbf{v}, p_f^n) + \int_{\Gamma} g \varphi^n (\mathbf{v} \cdot \mathbf{n}) \\ + \int_{\Gamma} \sum_{j=1}^{d-1} \frac{\nu \alpha_{BJ}}{\sqrt{K}} (\mathbf{u}_f^n \cdot \boldsymbol{\tau}_j) (\mathbf{v} \cdot \boldsymbol{\tau}_j) = c_f(\mathbf{u}_f^{n-1}; \mathbf{u}_f^0, \mathbf{v}) \\ + c_f(\mathbf{u}_f^0 - \mathbf{u}_f^{n-1}; \mathbf{u}_f^{n-1}, \mathbf{v}) + \int_{\Omega_f} \mathbf{f} \cdot \mathbf{v}, \quad (11.8)$$

$$b_f(\mathbf{u}_f^n, q) = 0, \quad (11.9)$$

$$a_p(\varphi^n, \psi) = \int_{\Gamma} \psi (\mathbf{u}_f^n \cdot \mathbf{n}). \quad (11.10)$$

Like for fixed-point iterations, we have to solve a linearized coupled problem at each iteration of the Newton algorithms.

This method corresponds to using an inexact Jacobian in which we have dropped the terms arising from the linearized trilinear convective terms. The matrix associated to this inexact Jacobian is now independent of the iteration level, hence it can be factorized once and for all (offline) at the very first iteration.

We would like to rewrite the Newton methods (11.5)–(11.7) and (11.8)–(11.10) as iterative schemes for the interface equation (6.25). Let us consider the exact Newton method first. First of all, notice that it can be expressed in the equivalent form:

find  $\mathbf{u}_f^n \in V_f$ ,  $\varphi^n \in H_p$  such that, for all  $\mathbf{v} \in V_f$ ,  $\psi \in H_p$ ,

$$\begin{aligned} & a_f(\mathbf{u}_f^n, \mathbf{v}) + c_f(\mathbf{u}_f^n; \mathbf{u}_f^{n-1}, \mathbf{v}) + c_f(\mathbf{u}_f^{n-1}; \mathbf{u}_f^n, \mathbf{v}) + \int_{\Gamma} g\varphi^n(\mathbf{v} \cdot \mathbf{n}) \\ & + \int_{\Gamma} \sum_{j=1}^{d-1} \frac{\nu\alpha_{BJ}}{\sqrt{K}} (\mathbf{u}_f^n \cdot \boldsymbol{\tau}_j)(\mathbf{v} \cdot \boldsymbol{\tau}_j) = c_f(\mathbf{u}_f^{n-1}; \mathbf{u}_f^{n-1}, \mathbf{v}) + \int_{\Omega_f} \mathbf{f} \cdot \mathbf{v}, \quad (11.11) \\ a_p(\varphi^n, \psi) & = \int_{\Gamma} \psi(\mathbf{u}_f^n \cdot \mathbf{n}). \end{aligned}$$

Furthermore, (11.11) can be equivalently restated as:

find  $\mathbf{u}_f^n \in V_f$  such that

$$\begin{aligned} & a_f(\mathbf{u}_f^n - \mathbf{u}_f^{n-1}, \mathbf{v}) + c_f(\mathbf{u}_f^n - \mathbf{u}_f^{n-1}; \mathbf{u}_f^{n-1}, \mathbf{v}) + c_f(\mathbf{u}_f^{n-1}; \mathbf{u}_f^n - \mathbf{u}_f^{n-1}, \mathbf{v}) \\ & + \int_{\Gamma} g(\varphi^n - \varphi^{n-1})(\mathbf{v} \cdot \mathbf{n}) + \int_{\Gamma} \sum_{j=1}^{d-1} \frac{\nu\alpha_{BJ}}{\sqrt{K}} ((\mathbf{u}_f^n - \mathbf{u}_f^{n-1}) \cdot \boldsymbol{\tau}_j)(\mathbf{v} \cdot \boldsymbol{\tau}_j) \\ & = -a_f(\mathbf{u}_f^{n-1}, \mathbf{v}) - c_f(\mathbf{u}_f^{n-1}; \mathbf{u}_f^{n-1}, \mathbf{v}) - \int_{\Gamma} g\varphi^{n-1}(\mathbf{v} \cdot \mathbf{n}) \\ & - \int_{\Gamma} \sum_{j=1}^{d-1} \frac{\nu\alpha_{BJ}}{\sqrt{K}} (\mathbf{u}_f^{n-1} \cdot \boldsymbol{\tau}_j)(\mathbf{v} \cdot \boldsymbol{\tau}_j) + \int_{\Omega_f} \mathbf{f} \cdot \mathbf{v} \quad \forall \mathbf{v} \in V_f. \quad (11.12) \end{aligned}$$

Let us now indicate by  $P(\bar{u})$  the operator associated to (6.25):  $P(\bar{u}) : \mathcal{W} \rightarrow \mathcal{W}'$ ,  $P(\bar{u}) = (\tilde{\mathcal{A}}\bar{u})\bar{u} - \tilde{\ell}$ ,  $\bar{u} = (\lambda, \mathbf{u}) \in \mathcal{W}$ ,  $\tilde{\mathcal{A}}$  and  $\tilde{\ell}$  being defined in Section 6.2. More precisely,

$$\begin{aligned} \langle P(\bar{u}), \bar{w} \rangle & = a_f(\tilde{R}_f^1 \lambda, \tilde{R}_f^1 \mu) + a_f(\mathbf{u}, \mathbf{w}) + c_f(\mathbf{u} + \tilde{R}_f^1 \lambda; \mathbf{u} + \tilde{R}_f^1 \lambda, \mathbf{w} + \tilde{R}_f^1 \mu) \\ & + \int_{\Gamma} \sum_{j=1}^{d-1} \frac{\nu\alpha_{BJ}}{\sqrt{K}} (\tilde{R}_f^1 \lambda \cdot \boldsymbol{\tau}_j)(\tilde{R}_f^1 \mu \cdot \boldsymbol{\tau}_j) + \int_{\Gamma} \sum_{j=1}^{d-1} \frac{\nu\alpha_{BJ}}{\sqrt{K}} (\mathbf{u} \cdot \boldsymbol{\tau}_j)(\mathbf{w} \cdot \boldsymbol{\tau}_j) \\ & + \int_{\Gamma} g(R_p \lambda)\mu - \int_{\Omega_f} \mathbf{f}(\mathbf{w} + \tilde{R}_f^1 \mu) \quad \forall \bar{w} = (\mu, \mathbf{w}) \in \mathcal{W}. \end{aligned}$$

The Gateaux derivative of the operator  $P$  in  $\bar{u}$  reads,  $\forall \bar{v} = (\eta, \mathbf{v}), \bar{w} = (\mu, \mathbf{w}) \in \mathcal{W}$ ,

$$\begin{aligned} \langle (P'(\bar{u}))(\bar{v}), \bar{w} \rangle &= a_f(\widetilde{R}_f^1 \eta, \widetilde{R}_f^1 \mu) + a_f(\mathbf{v}, \mathbf{w}) \\ &+ c_f(\mathbf{v} + \widetilde{R}_f^1 \eta; \mathbf{u} + \widetilde{R}_f^1 \lambda, \mathbf{w} + \widetilde{R}_f^1 \mu) \\ &+ c_f(\mathbf{u} + \widetilde{R}_f^1 \lambda; \mathbf{v} + \widetilde{R}_f^1 \eta, \mathbf{w} + \widetilde{R}_f^1 \mu) \\ &+ \int_{\Gamma} \sum_{j=1}^{d-1} \frac{\nu^{\alpha_{BJ}}}{\sqrt{K}} (\widetilde{R}_f^1 \eta \cdot \boldsymbol{\tau}_j) (\widetilde{R}_f^1 \mu \cdot \boldsymbol{\tau}_j) \\ &+ \int_{\Gamma} \sum_{j=1}^{d-1} \frac{\nu^{\alpha_{BJ}}}{\sqrt{K}} (\mathbf{v} \cdot \boldsymbol{\tau}_j) (\mathbf{w} \cdot \boldsymbol{\tau}_j) + \int_{\Gamma} g(R_p \eta) \mu. \end{aligned}$$

Notice also that, in view of the definition of  $\widetilde{R}_f^1$ , we have

$$\begin{aligned} \langle P(\bar{u}), \bar{w} \rangle &= a_f(\mathbf{u} + \widetilde{R}_f^1 \lambda, \mathbf{w} + \widetilde{R}_f^1 \mu) + c_f(\mathbf{u} + \widetilde{R}_f^1 \lambda; \mathbf{u} + \widetilde{R}_f^1 \lambda, \mathbf{w} + \widetilde{R}_f^1 \mu) \\ &+ \int_{\Gamma} \sum_{j=1}^{d-1} \frac{\nu^{\alpha_{BJ}}}{\sqrt{K}} ((\mathbf{u} + \widetilde{R}_f^1 \lambda) \cdot \boldsymbol{\tau}_j) ((\mathbf{w} + \widetilde{R}_f^1 \mu) \cdot \boldsymbol{\tau}_j) \\ &+ \int_{\Gamma} g(R_p \lambda) \mu - \int_{\Omega_f} \mathbf{f}(\mathbf{w} + \widetilde{R}_f^1 \mu), \end{aligned}$$

and

$$\begin{aligned} \langle (P'(\bar{u}))(\bar{v}), \bar{w} \rangle &= a_f(\mathbf{v} + \widetilde{R}_f^1 \eta, \mathbf{w} + \widetilde{R}_f^1 \mu) + c_f(\mathbf{v} + \widetilde{R}_f^1 \eta; \mathbf{u} + \widetilde{R}_f^1 \lambda, \mathbf{w} + \widetilde{R}_f^1 \mu) \\ &+ c_f(\mathbf{u} + \widetilde{R}_f^1 \lambda; \mathbf{v} + \widetilde{R}_f^1 \eta, \mathbf{w} + \widetilde{R}_f^1 \mu) \\ &+ \int_{\Gamma} \sum_{j=1}^{d-1} \frac{\nu^{\alpha_{BJ}}}{\sqrt{K}} ((\mathbf{v} + \widetilde{R}_f^1 \eta) \cdot \boldsymbol{\tau}_j) ((\mathbf{w} + \widetilde{R}_f^1 \mu) \cdot \boldsymbol{\tau}_j) + \int_{\Gamma} g(R_p \eta) \mu. \end{aligned}$$

Following the same argument used in Section 11.1, we can write in (11.12)  $\mathbf{u}_f^k = \mathbf{u}^k + \widetilde{R}_f^1 \lambda^k$  with  $\mathbf{u}^k \in V_f^0$  and  $\lambda^k = \mathbf{u}_f^k \cdot \mathbf{n}$  on  $\Gamma$ , and we can set  $\varphi^k = R_p \lambda^k$  ( $k = n-1, n$ ). Moreover, using again the fact that  $V_f = V_f^0 + \{\widetilde{R}_f^1 \mu : \mu \in \Lambda_0\}$ , we can write  $\mathbf{v} = \mathbf{w} + \widetilde{R}_f^1 \mu$  for  $\mathbf{w} \in V_f^0$  and  $\mu = \mathbf{v} \cdot \mathbf{n} \in \Lambda_0$  on  $\Gamma$ .

Substituting into (11.12), we can easily see that it corresponds to the following Newton method to solve (6.25): given  $\bar{u}^0 = (\lambda^0, \mathbf{u}^0) \in \mathcal{W}$ , for  $n \geq 1$ , find  $\bar{u}^n = (\lambda^n, \mathbf{u}^n) \in \mathcal{W}$  such that

$$\langle (P'(\bar{u}^{n-1}))(\bar{u}^n - \bar{u}^{n-1}), \bar{w} \rangle = -\langle P(\bar{u}^{n-1}), \bar{w} \rangle \quad \forall \bar{w} = (\mu, \mathbf{w}) \in \mathcal{W}. \quad (11.13)$$

Proceeding in an analogous way, one can show that algorithm (11.8)–(11.10) corresponds to the modified Newton method to solve (6.25): given  $\bar{u}^0 = (\lambda_0, \mathbf{u}^0) \in \mathcal{W}$ ,

for  $n \geq 1$ , find  $\bar{u}^n = (\lambda^n, \mathbf{u}^n) \in \mathcal{W}$  such that

$$\langle (P'(\bar{u}^0))(\bar{u}^n - \bar{u}^{n-1}), \bar{w} \rangle = -\langle P(\bar{u}^{n-1}), \bar{w} \rangle \quad \forall \bar{w} = (\mu, \mathbf{w}) \in \mathcal{W}. \quad (11.14)$$

Concerning the convergence of the Newton methods, we can prove the following result.

**Proposition 11.2.** *Let  $\mathbf{f} \in L^2(\Omega_f)$  and let*

$$\tilde{C}_1 = \frac{32C_{\mathcal{N}}C_{\Omega_f}\|\mathbf{f}\|_0}{(C_{\kappa\nu})^2}, \quad \tilde{C}_2 = \frac{2\sqrt{2}C_{\Omega_f}\|\mathbf{f}\|_0}{C_{\kappa\nu}}.$$

If

$$\tilde{C}_1 \leq \frac{1}{2}, \quad (11.15)$$

then, there exists a unique solution  $\bar{u} = (\lambda, \mathcal{R}_0^1(\lambda)) \in \bar{B}_{r_0}$  of (6.25), with

$$\bar{B}_{r_0} = \{\bar{w} = (\eta, \mathbf{w}) \in \mathcal{W} : \|\bar{w}\|_{\mathcal{W}} \leq r_0\} \quad (11.16)$$

and

$$r_0 = \frac{1 - \sqrt{1 - 2\tilde{C}_1}}{\tilde{C}_1} \tilde{C}_2. \quad (11.17)$$

Moreover, the sequence  $\bar{u}^n = (\lambda^n, \mathbf{u}^n)$ ,  $n \geq 1$ , obtained by the Newton algorithms (11.13) or (11.14), taking  $\bar{u}^0 = (0, \mathbf{0}) \in \mathcal{W}$ , converges to this solution.

The following error estimate holds for the Newton method (11.13):

$$\|\bar{u} - \bar{u}^n\|_{\mathcal{W}} \leq \frac{1}{2^n} (2\tilde{C}_1)^{2^n} \frac{\tilde{C}_2}{\tilde{C}_1}, \quad n \geq 0, \quad (11.18)$$

while for the modified Newton method (11.14) we have (if  $\tilde{C}_1 < 1/2$ ):

$$\|\bar{u} - \bar{u}^n\|_{\mathcal{W}} \leq \frac{\tilde{C}_2}{\tilde{C}_1} \left(1 - \sqrt{1 - 2\tilde{C}_1}\right)^{n+1}, \quad n \geq 0. \quad (11.19)$$

*Proof.* The proof, which is a corollary of Theorem A.3, is given in [13]. We report it here as well for sake of completeness. Consider  $\bar{u}^0 = (\lambda^0, \mathbf{u}^0) = (0, \mathbf{0}) \in \mathcal{W}$ . Then, for all  $\bar{w} = (\eta, \mathbf{w}) \in \mathcal{W}$ , we have:

$$\begin{aligned} \langle (P'(\bar{u}^0))(\bar{w}), \bar{w} \rangle &= a_f(\tilde{R}_f^1 \eta, \tilde{R}_f^1 \eta) + a_f(\mathbf{w}, \mathbf{w}) + \int_{\Gamma} \sum_{j=1}^{d-1} \frac{\nu \alpha_{BJ}}{\sqrt{K}} (\tilde{R}_f^1 \eta \cdot \boldsymbol{\tau}_j) (\tilde{R}_f^1 \eta \cdot \boldsymbol{\tau}_j) \\ &+ \int_{\Gamma} \sum_{j=1}^{d-1} \frac{\nu \alpha_{BJ}}{\sqrt{K}} (\mathbf{w} \cdot \boldsymbol{\tau}_j) (\mathbf{w} \cdot \boldsymbol{\tau}_j) + \int_{\Gamma} g(R_p \eta) \eta \\ &\geq \frac{C_{\kappa\nu}}{2} (|\tilde{R}_f^1 \eta|_1^2 + |\mathbf{w}|_1^2) = \frac{C_{\kappa\nu}}{2} \|\bar{w}\|_{\mathcal{W}}^2. \end{aligned}$$

Consequently,  $[P'(\bar{u}_0)]^{-1}$  exists and

$$\|[P'(\bar{u}^0)]^{-1}\|_{\mathcal{L}(\mathcal{W}', \mathcal{W})} \leq \frac{2}{C_\kappa \nu}.$$

Moreover,

$$\langle P(\bar{u}^0), \bar{w} \rangle = - \int_{\Omega_f} \mathbf{f}(\mathbf{w} + \tilde{R}_f^1 \eta) \leq \sqrt{2} C_{\Omega_f} \|\mathbf{f}\|_0 \|\bar{w}\|_{\mathcal{W}},$$

and therefore,

$$\|P(\bar{u}^0)\|_{\mathcal{W}'} \leq \sqrt{2} C_{\Omega_f} \|\mathbf{f}\|_0.$$

The second derivative of the operator  $P$  reads:

$$\begin{aligned} \langle (P''(\bar{u}))(\bar{v})(\bar{w}), \bar{\zeta} \rangle &= c_f(\mathbf{w} + \tilde{R}_f^1 \eta; \mathbf{v} + \tilde{R}_f^1 \mu, \mathbf{z} + \tilde{R}_f^1 \xi) \\ &\quad + c_f(\mathbf{v} + \tilde{R}_f^1 \mu; \mathbf{w} + \tilde{R}_f^1 \eta, \mathbf{z} + \tilde{R}_f^1 \xi), \end{aligned}$$

for  $\bar{u} = (\lambda, \mathbf{u})$ ,  $\bar{v} = (\mu, \mathbf{v})$ ,  $\bar{w} = (\eta, \mathbf{w})$ ,  $\bar{\zeta} = (\xi, \mathbf{z}) \in \mathcal{W}$ . Thus,

$$\begin{aligned} \langle (P''(\bar{u}))(\bar{v})(\bar{w}), \bar{\zeta} \rangle &\leq 2C_{\mathcal{N}} |\mathbf{w} + \tilde{R}_f^1 \eta|_1 |\mathbf{v} + \tilde{R}_f^1 \mu|_1 |\mathbf{z} + \tilde{R}_f^1 \xi|_1 \\ &\leq 4\sqrt{2} C_{\mathcal{N}} |\bar{v}|_{\mathcal{W}} |\bar{w}|_{\mathcal{W}} |\bar{\zeta}|_{\mathcal{W}}, \end{aligned}$$

so that

$$\|P''(\bar{u})\|_{\mathcal{L}(\mathcal{W}, \mathcal{L}(\mathcal{W}, \mathcal{W}'))} \leq 4\sqrt{2} C_{\mathcal{N}}.$$

Consequently, in our case, inequality (A.3) corresponds to (11.15).

Moreover, since the operator  $P$  is defined and has continuous second derivative on  $W$ , we can select a radius  $r$  satisfying (A.4)–(A.7) with  $r_0$  in (11.17) and

$$r_1 = \frac{1 + \sqrt{1 - 2\tilde{C}_1}}{\tilde{C}_1} \tilde{C}_2.$$

Finally, the error estimates (11.18) and (11.19) are directly obtained from (A.8) and (A.9), respectively.  $\square$

*Remark 11.3.* With the help of a little algebra we can see that  $\tilde{C}_1$  and  $\tilde{C}_2$  are related to the constants  $C_1$  and  $C_2$  in (6.28) as:  $C_1 = 2\sqrt{2}\tilde{C}_2/\tilde{C}_1$  and  $C_2 = 2\sqrt{2}\tilde{C}_2^2/\tilde{C}_1$ . Thus, condition (6.26) can be reformulated as  $\tilde{C}_1 \leq (3 + 2\sqrt{2})/8$ . If we compare it with (11.15), we can see that the condition required for the convergence of the Newton method is more restrictive than condition (6.26).

Finally, notice that  $r_m$  becomes

$$r_m = \frac{1 - \sqrt{1 - \sqrt{2}\tilde{C}_1}}{\tilde{C}_1} \sqrt{2}\tilde{C}_2.$$

Thus,  $r_m$  has a form similar to  $r_0$  in (11.17) and  $r_0 \geq r_m$ . Notice however that in the definition of  $\bar{B}_{r_m}$  (see (6.30)) we control only  $|\tilde{R}_f^1 \lambda|_1$ , while in  $\bar{B}_{r_0}$  in (11.16) we take the whole norm  $\|\bar{u}\|_{\mathcal{W}}$ . We can conclude that the well-posedness results of Lemma 6.5 and Proposition 11.2 are consistent.

**11.3. Some numerical experiments**

We consider the computational domain  $\Omega = (0, 1) \times (0, 2)$  with  $\Omega_f = (0, 1) \times (1, 2)$  and  $\Omega_p = (0, 1) \times (0, 1)$ , and uniform regular triangulations characterized by a parameter  $h$ . We use Taylor-Hood elements for the Navier-Stokes equations and quadratic Lagrangian elements for the Darcy equation.

In a first test, we set the boundary conditions in such a way that the analytical solution for the coupled problem is  $\mathbf{u}_f = (e^{x+y} + y, -e^{x+y} - x)$ ,  $p_f = \cos(\pi x) \cos(\pi y) + x$ ,  $\varphi = e^{x+y} - \cos(\pi x) + xy$ . In order to check the behavior of the iterative methods that we have studied with respect to the grid parameter  $h$ , to start with we set the physical parameters  $(\nu, K, g)$  all equal to 1.

The algorithms are stopped as soon as  $\|\mathbf{x}^n - \mathbf{x}^{n-1}\|_2 / \|\mathbf{x}^n\|_2 \leq 10^{-10}$ , where  $\|\cdot\|_2$  is the Euclidean norm and  $\mathbf{x}^n$  is the vector of the nodal values of  $(\mathbf{u}_f^n, p_f^n, \varphi^n)$ . Our initial guess is  $\mathbf{u}_f^0 = \mathbf{0}$ .

The number of iterations obtained using the fixed-point algorithm (11.1)–(11.3), and the Newton method (11.5)–(11.7) are displayed in Table 9. Both methods converge in a number of iterations which does not depend on  $h$ .

Table 9 – Number of iterations for the iterative methods with respect to  $h$ .

$h$	Fixed-point	Newton
0.1429	9	5
0.0714	9	5
0.0357	9	5

A second test is carried out in order to assess the influence of the physical parameters on the convergence rate of the algorithms. In this case, we consider the same computational domain, however the analytical solution now is  $\mathbf{u}_f = ((y-1)^2 + (y-1) + \sqrt{K}/\alpha_{BJ}, x(x-1))$ ,  $p_f = 2\nu(x+y-1)$ , and  $\varphi = K^{-1}(x(1-x)(y-1) + (y-1)^3/3) + 2\nu x$ . We choose several values for the physical parameters  $\nu$  and  $K$  as indicated in Table 10. The numerical results show that the smaller the parameters the higher the number of iterations.

Finally, we consider the computational domain illustrated in Figure 16 to represent the 2d section of a channel alongside a porous material. In this case, the boundary conditions are chosen in such a way that, if we would disregard the porous media, the Navier-Stokes equations would admit the following Kovaszny solution

$$\mathbf{u}_f = \left( 1 - e^{\lambda x} \cos(2\pi y), \frac{\lambda}{2\pi} e^{\lambda x} \sin(2\pi y) \right), \quad p_f = -\frac{e^{2\lambda x}}{2},$$

with  $\lambda = 0.5\text{Re} - \sqrt{0.25\text{Re}^2 + 4\pi^2}$ ,  $\text{Re} = 1/\nu$  and  $\nu = 0.025 \text{ m}^2/\text{s}$ . Moreover, we impose that the conormal derivative of the piezometric head is null on  $\Gamma_p^N$  and  $\varphi = -0.25 \text{ m}$  on  $\Gamma_p^D$ . The hydraulic conductivity coefficient is  $K = 10^{-1} \text{ m/s}$ .

Table 10 – Convergence behavior of the iterative methods with respect to the parameters  $\nu$  and  $K$ .

<i>Number of iterations for the fixed-point method</i>				
$\nu$	$K$	$h = 0.1429$	$h = 0.0714$	$h = 0.0357$
1	1	7	7	7
1	$10^{-4}$	5	5	5
$10^{-1}$	$10^{-1}$	10	10	10
$10^{-2}$	$10^{-1}$	15	15	15
$10^{-2}$	$10^{-3}$	13	13	13
<i>Number of iterations for the Newton method</i>				
$\nu$	$K$	$h = 0.1429$	$h = 0.0714$	$h = 0.0357$
1	1	4	4	4
1	$10^{-4}$	4	4	4
$10^{-1}$	$10^{-1}$	5	5	5
$10^{-2}$	$10^{-1}$	6	6	6
$10^{-2}$	$10^{-3}$	6	6	6

We have solved this problem using two different grids and adopting the Newton method. The convergence results are reported in Table 11, the computed velocity and piezometric head are displayed in Figure 17.

Table 11 – Newton iterations to solve the problem illustrated in Figure 16.

Grid elements	Newton iterations
792	7
3168	8

Concerning the computational costs, let us point out that the fixed-point algorithm requires at each iteration the assembly of the matrix corresponding to the linearization of the Navier-Stokes equations and the solution of a linear system involving the variables in both  $\Omega_f$  and  $\Omega_p$ . The Newton method is slightly more expensive since one has to assemble two matrices at each iteration and to update the right-hand side. The system to be solved features a similar structure to the one for fixed-point. These two methods are comparable since the additional cost required for assembling the Navier-Stokes system pays back with fewer iterations.

*Remark 11.4.* To solve (4.11)–(4.12), one could also consider the following *preconditioned Richardson method*: given  $\mathbf{u}_f^0 \in H_f$ ,  $\varphi^0 \in H_p$ , for  $n \geq 1$ , find  $\mathbf{u}_f^n \in H_f$ ,  $q_f^n \in Q$ ,



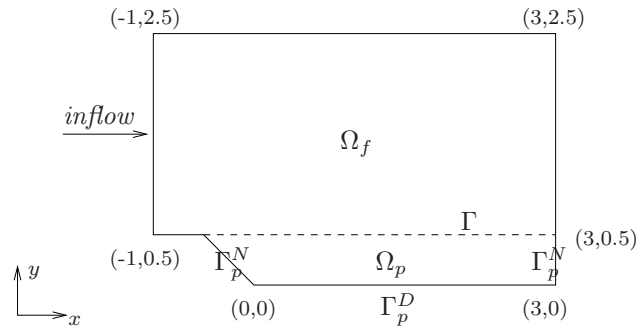


Figure 16 – Computational domain for the third test case.

$\varphi^n \in H_p$  such that, for all  $\mathbf{v} \in H_f$ ,  $q \in Q$ ,  $\psi \in H_p$ ,

$$\begin{aligned}
 & a_f(\mathbf{u}_f^n - \mathbf{u}_f^{n-1}, \mathbf{v}) + b_f(\mathbf{v}, p_f^n - p_f^{n-1}) + \int_{\Gamma} \sum_{j=1}^{d-1} \frac{\nu \alpha_{BJ}}{\sqrt{K}} ((\mathbf{u}_f^n - \mathbf{u}_f^{n-1}) \cdot \boldsymbol{\tau}_j)(\mathbf{v} \cdot \boldsymbol{\tau}_j) \\
 & = \theta \left[ \int_{\Omega_f} \mathbf{f} \cdot \mathbf{v} - a_f(\mathbf{u}_f^{n-1}, \mathbf{v}) - c_f(\mathbf{u}_f^{n-1}; \mathbf{u}_f^{n-1}, \mathbf{v}) - b_f(\mathbf{v}, p_f^{n-1}) \right. \\
 & \quad \left. - \int_{\Gamma} \sum_{j=1}^{d-1} \frac{\nu}{\varepsilon} (\mathbf{u}_f^{n-1} \cdot \boldsymbol{\tau}_j)(\mathbf{v} \cdot \boldsymbol{\tau}_j) - \int_{\Gamma} g \varphi^{n-1} (\mathbf{v} \cdot \mathbf{n}) \right], \\
 & b_f(\mathbf{u}_f^n - \mathbf{u}_f^{n-1}, q) = 0, \\
 & a_p(\varphi^n, \psi) = \int_{\Gamma} \psi (\mathbf{u}_f^n \cdot \mathbf{n}).
 \end{aligned}$$

$\theta > 0$  is a suitably chosen relaxation parameter. Unlike the fixed-point and the Newton methods, this algorithm requires to solve at each iteration two decoupled linear equations at each iteration: a Stokes system in the fluid subdomain  $\Omega_f$  and the Darcy equation in the porous media subdomain  $\Omega_p$ . Moreover, at each iteration the right-hand side of the Stokes system has to be updated and this corresponds to the residual of the equation (4.7).

Unfortunately, despite its attractiveness for its decoupling property, this algorithm performs quite poorly in practice. For the analysis and numerical results of the Richardson method we refer to [13].

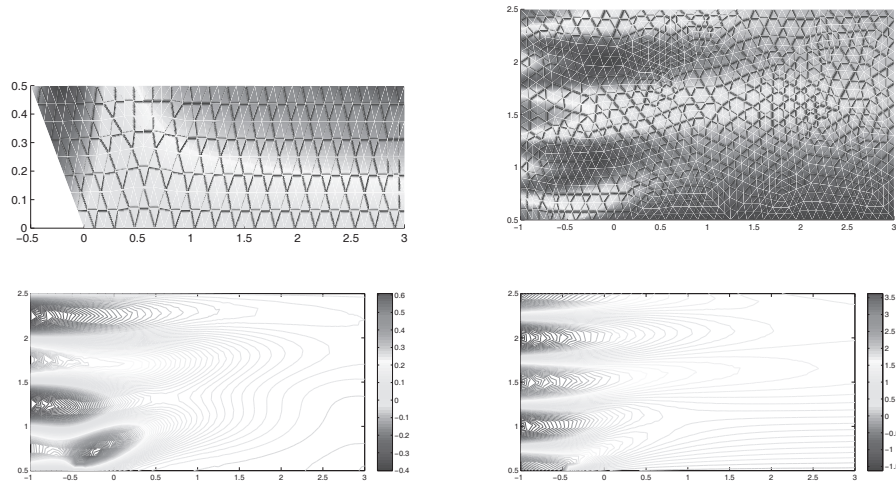


Figure 17 – Computed solution: piezometric head  $\varphi$  (top left), velocity field  $\mathbf{u}_f$  (top right), contour lines of the velocity in  $x$ - (bottom left) and  $y$ -direction (bottom right). Notice that the Kovasznay flow is modified in the presence of the porous media: indeed, the velocity in  $y$ -direction has negative values in correspondence to the porous media interface.

## 12. Problems of filtration through poroelastic media in hemodynamic applications

We consider a portion of a blood flow vessel as shown in Figure 1, right. The interior of the vessel, through which blood flows, is called lumen and it corresponds to our fluid domain  $\Omega_f$ . The lumen is surrounded by three layers of tissue called intima, media and adventitia, which form the arterial wall  $\Omega_p$ . Each layer has different physical properties. The plasma filtration and the transfer of molecules in such structure can be described by the so-called *multilayer model* (see [87]). However, here we make a simplification of the complex multilayered structure of the wall and we assume that the arterial wall is an homogeneous medium.

In large arteries (i.e., those whose diameter is roughly larger than 2 mm) blood can be assumed to behave as a Newtonian fluid [58], thus its motion can be described by the Navier-Stokes equations (2.1)–(2.2). Since the domain is changing in time due to blood flow pulsatility and to the elasticity of the arterial wall, usually the so-called Arbitrary Lagrangian Eulerian (ALE) framework is adopted for the mathematical setting (see, e.g., [103, 107]). For the sake of simplicity in our exposition we assume that displacements are negligible so that we can consider the domain fixed.

To describe the interaction between the blood flow and the arterial wall, we have

to consider a poroelastic model for the wall.

A porous medium is defined as a mixture of a solid material, called skeleton or matrix, and connecting pores filled with fluid. The fluid and the solid are assumed to be incompressible. Consequently, the dynamics of such a medium can be described by the Biot system [25, 26, 27]:  $\forall t > 0$ ,

$$\rho_p \partial_t \mathbf{u}_s + \rho_d \partial_t \mathbf{q} - \nabla \cdot \boldsymbol{\sigma}_s^E(\boldsymbol{\eta}) + \nabla p_p = \mathbf{f}_s \quad \text{in } \Omega_p, \quad (12.1)$$

$$\rho_d \partial_t \mathbf{u}_s + \rho_d \partial_t \frac{\mathbf{q}}{n} + K^{-1} \mathbf{q} + \nabla p_p = \mathbf{f}_d \quad \text{in } \Omega_p, \quad (12.2)$$

$$\nabla \cdot (\mathbf{u}_s + \mathbf{q}) = 0 \quad \text{in } \Omega_p. \quad (12.3)$$

The momentum equation for the balance of total forces is (12.1), while (12.2) is the momentum conservation equation for the fluid phase only, and (12.3) is the incompressibility constraint.  $\rho_d$  is the density of the fluid in the pores,  $\rho_p = \rho_s(1-n) + \rho_d n$  the density of the saturated porous medium,  $\rho_s$  the density of the solid material, and  $n$  the porosity. The latter is the ratio of the pore volume over the total volume (pore + skeleton) (see (2.3)).

We denote by  $\mathbf{u}_s = \partial_t \boldsymbol{\eta}$  the velocity of the skeleton, where  $\boldsymbol{\eta}$  is the displacement of the porous structure.  $\mathbf{q}$  is the filtration velocity, i.e., the relative velocity of the fluid phase with respect to the solid one:  $\mathbf{q} = n(\mathbf{u}_p - \mathbf{u}_s)$ . Here,  $\mathbf{u}_p$  is the velocity of the fluid in the porous medium,  $K$  is the hydraulic conductivity tensor (see (2.4)). The effective Cauchy stress tensor of the matrix is  $\boldsymbol{\sigma}_s^E$  and it is related to the displacement of the porous structure  $\boldsymbol{\eta}$  by a suitable constitutive law. For example, we can consider the linear Saint-Venant Kirchhoff three-dimensional elastic model:

$$\boldsymbol{\sigma}_s^E(\boldsymbol{\eta}) = 2\mu_\ell \boldsymbol{\epsilon}(\boldsymbol{\eta}) + \lambda_\ell (\nabla \cdot \boldsymbol{\eta}) \mathbf{I},$$

where  $\boldsymbol{\epsilon}(\boldsymbol{\eta}) = (\nabla \boldsymbol{\eta} + \nabla^T \boldsymbol{\eta})/2$ ,  $\mu_\ell$  and  $\lambda_\ell$  are the Lamé constants, representing the shear and dilation moduli of elasticity. The first constant accounts for distortion and the second for compression of the medium [46].

The pressure of the fluid in the pore is given by  $p_p$ . We define the total Cauchy stress for the poroelastic structure as

$$\boldsymbol{\sigma}_s = -p_p \mathbf{I} + \boldsymbol{\sigma}_s^E.$$

The right-hand side vectors  $\mathbf{f}_s$  and  $\mathbf{f}_d$  account for external body forces.

Typical values of the physical parameters in hemodynamic applications are reported in Table 12.

Notice that the Biot system (12.1)–(12.3) extends the Darcy equations taking into account not only the filtration through the porous medium but also the elastic properties of the porous medium itself.

In order for system (12.1)–(12.3) to be well-posed, proper initial and boundary conditions must be imposed. In the following, the boundary conditions on  $\partial\Omega_p \setminus \Gamma$  are

Table 12 – Values of the physical parameters in hemodynamic applications.

Fluid viscosity	$\mu = 0.035$ poise
Fluid density	$\rho_f = 1$ g/cm <sup>3</sup>
Fluid density in the pores	$\rho_f = 1$ g/cm <sup>3</sup>
Structure density	$\rho_s = 1.1$ g/cm <sup>3</sup>
Lamé constants	$\mu_\ell = 10^6$ dyne/cm <sup>2</sup>
	$\lambda_\ell = 1.73 \cdot 10^6$ dyne/cm <sup>2</sup>
Porosity	$n = 0.15$
Hydraulic conductivity	$K \sim 10^{-12}$ cm <sup>3</sup> s/g

chosen in a classical simple form, since they play no essential role in the interaction. On the exterior boundary of the porous medium we shall impose drained conditions  $p_p = 0$  on the pressure and clamped conditions  $\mathbf{u}_s = \mathbf{0}$  on the structure velocity at both the inlet and the outlet.

Any model of fluid in contact with a deformable and porous medium contains the filtration velocity, in addition to the displacement (or velocity) and stress variations of the porous matrix. These must be coupled to the Navier-Stokes flow. The differential model thus reads:  $\forall t > 0$ ,

$$\partial_t \mathbf{u}_f - \nabla \cdot \mathbb{T}(\mathbf{u}_f, p_f) + (\mathbf{u}_f \cdot \nabla) \mathbf{u}_f = \mathbf{f}_f \quad \text{in } \Omega_f, \tag{12.4}$$

$$\nabla \cdot \mathbf{u}_f = 0 \quad \text{in } \Omega_f, \tag{12.5}$$

$$\rho_p \partial_t \mathbf{u}_s + \rho_d \partial_t \mathbf{q} - \nabla \cdot \boldsymbol{\sigma}_s^E + \nabla p_p = \mathbf{f}_s \quad \text{in } \Omega_p, \tag{12.6}$$

$$\rho_d \partial_t \mathbf{u}_s + \rho_d \partial_t \frac{\mathbf{q}}{n} + K^{-1} \mathbf{q} + \nabla p_p = \mathbf{f}_d \quad \text{in } \Omega_p, \tag{12.7}$$

$$\nabla \cdot (\mathbf{u}_s + \mathbf{q}) = 0 \quad \text{in } \Omega_p. \tag{12.8}$$

We identify a physically consistent set of interface conditions which couple the Biot system (12.1)–(12.3) to the incompressible Navier-Stokes equations so that the variational statement of the resulting system is a well-posed initial-boundary-value problem.

The natural transmission conditions at the interface of a fluid and an impervious elastic solid consist of continuity of velocity and stresses, while the transmission relations for a fluid in contact with a rigid but porous solid matrix have been discussed in Section 3. More precisely, we consider the following set of conditions.

We begin with the mass-conservation requirement that the normal fluid flux must be continuous across the interface. Thus, the solution of (12.4)–(12.8) is required to satisfy the admissibility constraint:

$$\mathbf{u}_f \cdot \mathbf{n} = (\mathbf{u}_s + \mathbf{q}) \cdot \mathbf{n} \quad \text{on } \Gamma. \tag{12.9}$$

For the balance of the normal stresses in the fluid phase across  $\Gamma$ , we have

$$-\mathbf{n} \cdot \mathbb{T}(\mathbf{u}_f, p_f) \cdot \mathbf{n} = p_p. \quad (12.10)$$

The conservation of momentum requires that the total stress of the porous medium is balanced by the total stress of the fluid:

$$\boldsymbol{\sigma}_s \cdot \mathbf{n} = \mathbb{T}(\mathbf{u}_f, p_f) \cdot \mathbf{n}. \quad (12.11)$$

Finally, the fluid tangential stress (which is equal to the one of the solid phase) is assumed to be proportional to the slip rate according to the Beavers-Joseph-Saffman condition:

$$\boldsymbol{\tau}_j \cdot \mathbb{T}(\mathbf{u}_f, p_f) \cdot \mathbf{n} = -\frac{\alpha_{BJ}}{\sqrt{K}}(\mathbf{u}_f - \mathbf{u}_s) \cdot \boldsymbol{\tau}_j, \quad j = 1, \dots, d-1. \quad (12.12)$$

The global coupled system is then non-linear with a structure similar to the Navier-Stokes/Darcy system that we have analyzed in Section 6. Fixed-point of Newton methods can be used for the linearization of the Navier-Stokes/Biot coupled system. To solve the linear fluid-poroelastic-structure interaction problem, in [107, 18] several methods are proposed based both on the so-called monolytic approach and on domain decomposition methods. In the first case the linear system obtained after time and space discretizations is solved using direct or iterative methods with ad-hoc preconditioners (see [108, 17, 16]). On the other hand, partitioned procedures derived from a domain decomposition viewpoint feature similar structures to the Dirichlet-Neumann or Robin-Robin algorithms that we have illustrated in Section 8.4 and 10, respectively, for fluid-groundwater coupling. We refer to [107, 18] for an extensive analysis of these methods and for several numerical results.

Finally, let us point out that the finite element discretization of problem (12.4)–(12.12) can be carried out in analogous way to the Navier-Stokes/Darcy case using inf-sup stable finite element spaces or any convenient stabilization techniques. In particular, in [107] an effective stabilization strategy based on variational multiscale methods is investigated.

## Appendix

### A. Some existence and uniqueness results for non-linear problems

In this section we recall some existence and uniqueness results for non-linear saddle-point problems, referring the reader to, e.g., [35, 36, 37, 42, 74] for a rigorous study.

Let  $(X, \|\cdot\|_X)$  and  $(Y, \|\cdot\|_Y)$  be two real Hilbert spaces and consider a bilinear continuous form  $b(\cdot, \cdot) : X \times Y \rightarrow \mathbb{R}$ ,  $(v, q) \rightarrow b(v, q)$ , and a trilinear form  $a(\cdot; \cdot, \cdot) : X \times$

$X \times X \rightarrow \mathbb{R}$ ,  $(w, u, v) \rightarrow a(w; u, v)$ , where, for  $w \in X$  the mapping  $(u, v) \rightarrow a(w; u, v)$  is a bilinear continuous form on  $X \times X$ .

Then, we consider the following problem: given  $l \in X'$ , find a pair  $(u, p) \in X \times Y$  satisfying

$$\begin{aligned} a(u; u, v) + b(v, p) &= \langle l, v \rangle & \forall v \in X \\ b(u, q) &= 0 & \forall q \in Y. \end{aligned} \tag{A.1}$$

Introducing the linear operators  $A(w) \in \mathcal{L}(X; X')$  for  $w \in X$ , and  $B \in \mathcal{L}(X; Y')$ :

$$\begin{aligned} \langle A(w)u, v \rangle &= a(w; u, v) & \forall u, v \in X, \\ \langle Bv, q \rangle &= b(v, q) & \forall v \in X, \forall q \in Y, \end{aligned}$$

problem (A.1) becomes:

find  $(u, p) \in X \times Y$  such that

$$\begin{aligned} A(u)u + B^T p &= l & \text{in } X', \\ Bu &= 0 & \text{in } Y'. \end{aligned}$$

Taking  $V = \text{Ker}(B)$ , we associate (A.1) with the problem:

$$\text{find } u \in V : \quad a(u; u, v) = \langle l, v \rangle \quad \forall v \in V, \tag{A.2}$$

or, equivalently:

find  $u \in V$  such that  $\Pi A(u)u = \Pi l$  in  $V'$ , where the linear operator  $\Pi \in \mathcal{L}(X'; V')$  is defined by  $\langle \Pi l, v \rangle = \langle l, v \rangle$ ,  $\forall v \in V$ .

If  $(u, p)$  is a solution of problem (A.1), then  $u$  solves (A.2). The converse may be proved provided an inf-sup condition holds. Indeed, the following results can be proved.

**Theorem A.1** (Existence and uniqueness). *Suppose that:*

- (i) *The bilinear form  $a(w; \cdot, \cdot)$  is uniformly elliptic in the Hilbert space  $V$  with respect to  $w$ , i.e., there exists a constant  $\alpha > 0$  such that*

$$a(w; v, v) \geq \alpha \|v\|_X^2 \quad \forall v, w \in V.$$

- (ii) *The mapping  $w \rightarrow \Pi A(w)$  is locally Lipschitz-continuous in  $V$ , i.e., there exists a continuous and monotonically increasing function  $L : \mathbb{R}^+ \rightarrow \mathbb{R}^+$  such that for all  $m > 0$*

$$|a(w_1; u, v) - a(w_2; u, v)| \leq L(m) \|u\|_X \|v\|_X \|w_1 - w_2\|_X$$

$$\forall u, v \in V, \forall w_1, w_2 \in S_m \text{ with } S_m = \{w \in V : \|w\|_X \leq m\}.$$

- (iii) *It holds that*

$$\frac{\|\Pi l\|_{V'}}{\alpha^2} L \left( \frac{\|\Pi l\|_{V'}}{\alpha} \right) < 1.$$

Then (A.2) has a unique solution  $u \in V$ .

We consider now problem (A.1).

**Theorem A.2.** *Assume that the bilinear form  $b(\cdot, \cdot)$  satisfies the inf-sup condition: there exists a positive constant  $\beta > 0$ , such that*

$$\forall q \in Y, \quad \exists v \in X, v \neq 0 : \quad b(v, q) \geq \beta \|v\|_X \|q\|_Y.$$

Then for each solution  $u$  of (A.2) there exists a unique  $p \in Y$  such that the pair  $(u, p)$  is a solution of (A.1).

Finally, let us recall an important result on the convergence of Newton methods in Banach spaces.

Let  $X$  and  $Y$  be two Banach spaces. We consider the sphere of radius  $R > 0$  centered in  $x^0 \in X$ :  $\Omega = \{x \in X : \|x - x^0\|_X < R\}$ , and the closed sphere of radius  $0 < r < R$  centered in  $x^0$ :  $\Omega_0 = \{x \in X : \|x - x^0\|_X \leq r\}$ . We assume that  $\Omega$  contains a zero of an operator  $\mathcal{P} : \Omega \subset X \rightarrow Y$ , i.e., a point  $x^* \in \Omega$  such that  $\mathcal{P}(x^*) = 0$ .

If  $\mathcal{P}$  has a continuous Gâteaux derivative in  $\Omega$ , we can apply the Newton method to compute the zero  $x^*$ : given an initial approximation  $x^0 \in \Omega$  of  $x^*$ , for  $n \geq 0$ ,

$$x^{n+1} = x^n - [\mathcal{P}'(x^n)]^{-1}(\mathcal{P}(x^n)),$$

assuming that  $[\mathcal{P}'(x^n)]^{-1}$  exists.

Alternatively, we can use the modified Newton algorithm: given  $x^0 \in \Omega$ , for  $n \geq 0$ ,

$$x^{n+1} = x^n - [\mathcal{P}'(x^0)]^{-1}(\mathcal{P}(x^n)).$$

Concerning the convergence of these methods, we have the following theorem (see [86, Theorem 6 (1.XVIII), page 708]).

**Theorem A.3** (Kantorovich Theorem). *Let  $\mathcal{P}$  be defined on  $\Omega \subset X$  with continuous second derivative in  $\Omega_0$ . Moreover assume that:*

- (1) *There exists the continuous linear operator  $[\mathcal{P}'(x^0)]^{-1}$ .*
- (2) *There exists a positive constant  $K_1 > 0$  :  $\|[\mathcal{P}'(x^0)]^{-1}(\mathcal{P}(x^0))\|_X \leq K_1$ .*
- (3) *There exists a positive constant  $K_2 > 0$  :  $\|[\mathcal{P}'(x^0)]^{-1}\mathcal{P}''(x)\|_X \leq K_2$  for all  $x \in \Omega_0$ .*

If

$$K_3 = K_1 K_2 \leq \frac{1}{2}, \tag{A.3}$$

and the radius  $r$  of  $\Omega_0$  satisfies

$$r \geq r_0 = \frac{1 - \sqrt{1 - 2K_3}}{K_3} K_1, \quad (\text{A.4})$$

then, there exists a zero  $x^*$  of  $\mathcal{P}$  to which the Newton and the modified Newton methods converge. In this case,

$$\|x^* - x^0\|_X \leq r_0. \quad (\text{A.5})$$

Furthermore, if for  $K_3 < 1/2$

$$r < r_1 = \frac{1 + \sqrt{1 - 2K_3}}{K_3} K_1, \quad (\text{A.6})$$

or for  $K_3 = 1/2$

$$r \leq r_1, \quad (\text{A.7})$$

the solution  $x^*$  is unique in the sphere  $\Omega_0$ .

The convergence rate of the Newton method is characterized by

$$\|x^* - x^n\|_X \leq \frac{1}{2^n} (2K_3)^{2^n} \frac{K_1}{K_3}, \quad n \geq 0, \quad (\text{A.8})$$

while that of the modified method, for  $K_3 < 1/2$ , by

$$\|x^* - x^n\|_X \leq \frac{K_1}{K_3} (1 - \sqrt{1 - 2K_3})^{n+1}, \quad n \geq 0. \quad (\text{A.9})$$

**Acknowledgement.** The authors would like to acknowledge the anonymous referee for many useful comments and suggestions that have led to improving the original manuscript.

## References

- [1] J. Aarnes. Efficient domain decomposition methods for elliptic problems arising from flows in heterogeneous porous media. *Comput. Vis. Sci.*, 8(2):93–106, 2005.
- [2] J. Aarnes and Y. Efendiev. An adaptive multiscale method for simulation of fluid flow in heterogeneous porous media. *Multiscale Model. Simul.*, 5(3):918–939 (electronic), 2006.
- [3] J. Aarnes and B.-O. Heimsund. Multiscale discontinuous Galerkin methods for elliptic problems with multiple scales. In *Multiscale Methods in Science and Engineering*, volume 44 of *Lect. Notes Comput. Sci. Eng.*, pages 1–20. Springer, Berlin, 2005.
- [4] J. Aarnes and T.Y. Hou. Multiscale domain decomposition methods for elliptic problems with high aspect ratios. *Acta Math. Appl. Sin. Engl. Ser.*, 18(1):63–76, 2002.



- [5] J.E. Aarnes. On the use of a mixed multiscale finite element method for greater flexibility and increased speed or improved accuracy in reservoir simulation. *Multiscale Model. Simul.*, 2(3):421–439 (electronic), 2004.
- [6] R.A. Adams. *Sobolev Spaces*. Academic Press, New York, 1975.
- [7] V.I. Agoshkov. Poincaré-Steklov operators and domain decomposition in finite dimensional spaces. In *First International Symposium on Domain Decomposition Methods for Partial Differential Equations, Paris 1987*, pages 73–112. SIAM, Philadelphia, 1988.
- [8] V.I. Agoshkov and V.I. Lebedev. Variational algorithms of the domain decomposition method. *Sov. J. Numer. Anal. Math. Modelling*, 5(1):27–46, 1990. Originally published in Russian as Preprint No. 54, Dept. Numer. Math. URSS Acad. Sci. Moscow, 1983.
- [9] R.E. Alcouffe, A. Brandt, J.E. Dendy, and J.W. Painter. The multigrid method for the diffusion equation with strongly discontinuous coefficients. *SIAM J. Sci. Statist. Comput.*, 2(4):430–454, 1981.
- [10] T. Arbogast, J. Douglas, and U. Hornung. Derivation of the double porosity model of single phase flow via homogenization theory. *SIAM J. Math. Anal.*, 21(4):430–454, 1990.
- [11] D.N. Arnold, F. Brezzi, B. Cockburn, and L.D. Marini. Unified analysis of discontinuous Galerkin methods for elliptic problems. *SIAM J. Numer. Anal.*, 39(5):1749–1779, 2002.
- [12] I. Babuška and J.E. Osborn. Generalized finite element methods: their performance and their relation to mixed methods. *SIAM J. Numer. Anal.*, 20(3):510–536, 1983.
- [13] L. Badea, M. Discacciati, and A. Quarteroni. Numerical analysis of the Navier-Stokes/Darcy coupling. Technical report, Ecole Polytechnique Fédérale de Lausanne, IACS-CMCS, 2008.
- [14] S. Badia and R. Codina. Unified stabilized finite element formulations for the Stokes and the Darcy problems. Technical report, Universitat Politècnica de Catalunya, 2008.
- [15] S. Badia, F. Nobile, and C. Vergara. Robin-Robin preconditioned Krylov methods for fluid-structure interaction problems. Technical Report 19/2008, MOX - Politecnico di Milano, 2008.
- [16] S. Badia, A. Quaini, and A. Quarteroni. Modular vs. non-modular preconditioners for fluid-structure systems with large added-mass effect. *Comput. Methods Appl. Mech. Engrg.*, 197(49–50):4216–4232, 2008.
- [17] S. Badia, A. Quaini, and A. Quarteroni. Splitting methods based on algebraic factorization for fluid-structure interaction. *SIAM J. Sci. Comput.*, 30(4):1778–1805, 2008.
- [18] S. Badia, A. Quaini, and A. Quarteroni. Coupling Biot and Navier-Stokes problems for fluid-poroelastic structure interaction. Technical report, Universitat Politècnica de Catalunya, 2009. Available at <http://hdl.handle.net/2072/13533>.
- [19] P. Bastian. Higher order discontinuous Galerkin methods for flow and transport in porous media. In E. Baensch, editor, *Challenges in Scientific Computing CISC2002. Lecture Notes in Computational Science and Engineering (35)*, pages 1–22. Springer, Berlin and Heidelberg, 2003.

- [20] J. Bear. *Hydraulics of Groundwater*. McGraw-Hill, New York, 1979.
- [21] G.S. Beavers and D.D. Joseph. Boundary conditions at a naturally permeable wall. *J. Fluid Mech.*, 30:197–207, 1967.
- [22] C. Bernardi, Y. Maday, and F. Rapetti. *Discrétisations variationnelles de problèmes aux limites elliptiques*, volume 45 of *Mathématiques & Applications (Berlin) [Mathematics & Applications]*. Springer-Verlag, Berlin, 2004.
- [23] C. Bernardi, T.C. Rebollo, F. Hecht, and Z. Mghazli. Mortar finite element discretization of a model coupling Darcy and Stokes equations. *M2AN Math. Model. Numer. Anal.*, 42(3):375–410, 2008.
- [24] H. Berninger. *Domain Decomposition Methods for Elliptic Problems with Jumping Nonlinearities and Application to the Richards Equation*. PhD thesis, Freie Universität Berlin, 2007.
- [25] M.A. Biot. General theory of three-dimensional consolidation. *J. Appl. Phys.*, 12:155–164, 1941.
- [26] M.A. Biot. Theory of elasticity and consolidation for a porous anisotropic solid. *J. Appl. Phys.*, 25:182–185, 1955.
- [27] M.A. Biot. Theory of finite deformation of porous solids. *Indiana Univ. Math. J.*, 21:597–620, 1971/72.
- [28] A. Brandt. Multi-level adaptive solutions to boundary-value problems. *Math. Comp.*, 31(138):333–390, 1977.
- [29] F. Brezzi. On the existence, uniqueness and approximation of saddle-point problems arising from Lagrange multipliers. *Rev. Française Automat. Informat. Recherche Opérationnelle, sér. Rouge*, 8:129–151, 1974.
- [30] F. Brezzi, J. Douglas Jr., R. Durán, and M. Fortin. Mixed finite elements for second order elliptic problems in three variables. *Numer. Math.*, 51(2):237–250, 1987.
- [31] F. Brezzi, J. Douglas Jr., M. Fortin, and L.D. Marini. Efficient rectangular mixed finite elements in two and three space variables. *RAIRO Modél. Math. Anal. Numér.*, 21(4):581–604, 1987.
- [32] F. Brezzi, J. Douglas Jr., and L.D. Marini. Two families of mixed finite elements for second order elliptic problems. *Numer. Math.*, 47(2):217–235, 1985.
- [33] F. Brezzi and M. Fortin. *Mixed and Hybrid Finite Element Method*. Springer, New York, 1991.
- [34] F. Brezzi, L.P. Franca, T.J.R. Hughes, and A. Russo.  $b = \int g$ . *Comput. Methods Appl. Mech. Engrg.*, 145((3–4)):329–339, 1997.
- [35] F. Brezzi, J. Rappaz, and P.A. Raviart. Finite dimensional approximation of nonlinear problems. Part I: Branches of nonlinear solutions. *Numer. Math.*, 36:1–25, 1980.
- [36] F. Brezzi, J. Rappaz, and P.A. Raviart. Finite dimensional approximation of nonlinear problems. Part II: Limit points. *Numer. Math.*, 37:1–28, 1981.
- [37] F. Brezzi, J. Rappaz, and P.A. Raviart. Finite dimensional approximation of nonlinear problems. Part III: Simple bifurcation points. *Numer. Math.*, 38:1–30, 1981.

- [38] H.C. Brinkman. A calculation of the viscous force exerted by a flowing fluid on a dense swarm of particles. *Appl. Sci. Res. A*, 1:27–34, 1947.
- [39] E. Burman. Pressure projection stabilizations for galerkin approximations of Stokes' and Darcy's problems. *Numer. Methods Partial Differential Equations*, 24(1):127–143, 2008.
- [40] E. Burman and P. Hansbo. A unified stabilized method for Stokes' and Darcy's equations. *J. Comput. Appl. Math.*, 198(1):35–51, 2007.
- [41] E. Burman and P. Zunino. A domain decomposition method based on weighted interior penalties for advection-diffusion-reaction problems. *SIAM J. Numer. Anal.*, 44(4):1612–1638, 2006.
- [42] G. Caloz and J. Rappaz. Numerical Analysis for Nonlinear and Bifurcation Problems. In *Handbook of Numerical Analysis, Vol. V*, pages 487–637. North-Holland, Amsterdam, 1997.
- [43] Y. Cao, M. Gunzburger, F. Hua, and X. Wang. Coupled Stokes-Darcy model with Beavers-Joseph interface boundary conditions. *Comm. Math. Sci.*, 2008. To appear.
- [44] Z. Chen and T.Y. Hou. A mixed finite element method for elliptic problems with rapidly oscillating coefficients. *Math. Comput.*, 72:541–576, 2002.
- [45] P.G. Ciarlet. *The Finite Element Method for Elliptic Problems*. North-Holland Publishing Co., Amsterdam, 1978.
- [46] P.G. Ciarlet. *Mathematical elasticity. Vol. I*, volume 20 of *Studies in Mathematics and its Applications*. North-Holland Publishing Co., Amsterdam, 1988. Three-dimensional elasticity.
- [47] B. Cockburn, G. E. Karniadakis, and C.-W. Shu. The development of discontinuous Galerkin methods. In *Discontinuous Galerkin methods (Newport, RI, 1999)*, volume 11 of *Lect. Notes Comput. Sci. Eng.*, pages 3–50. Springer, Berlin, 2000.
- [48] R. Codina. Stabilized finite element approximation of transient incompressible flows using orthogonal subscales. *Comput. Methods Appl. Mech. Engrg.*, 191:4295–4321, 2002.
- [49] C. D'Angelo and P. Zunino. A finite element method based on weighted interior penalties for heterogenous incompressible flows. Technical Report 14/2008, MOX - Politecnico di Milano, 2008.
- [50] H. Darcy. *Les Fontaines Publiques de la Ville de Dijon*. Dalmont, Paris, 1856.
- [51] R. Dautray and J.-L. Lions. *Mathematical Analysis and Numerical Methods for Science and Technology*, volume 2. Springer, Berlin, 1988.
- [52] S. Deparis, M. Discacciati, and A. Quarteroni. A domain decomposition framework for fluid-structure interaction problems. In C. Groth and D.W. Zingg, editors, *Computational Fluid Dynamics 2004*, pages 41–58. Springer, New York, 2006.
- [53] M. Discacciati. *Domain Decomposition Methods for the Coupling of Surface and Groundwater Flows*. PhD thesis, Ecole Polytechnique Fédérale de Lausanne, Switzerland, 2004.
- [54] M. Discacciati. An operator-splitting approach to nonoverlapping domain decomposition methods. Technical Report 14, Section de Mathématiques, EPFL, 2004.

- [55] M. Discacciati, E. Miglio, and A. Quarteroni. Mathematical and numerical models for coupling surface and groundwater flows. *Appl. Numer. Math.*, 43:57–74, 2002.
- [56] M. Discacciati and A. Quarteroni. Analysis of a domain decomposition method for the coupling of Stokes and Darcy equations. In F. Brezzi, A. Buffa, S. Corsaro, and A. Murli, editors, *Numerical Mathematics and Advanced Applications, ENUMATH 2001*, pages 3–20. Springer. Milan, 2003.
- [57] M. Discacciati, A. Quarteroni, and A. Valli. Robin-Robin domain decomposition methods for the Stokes-Darcy coupling. *SIAM J. Numer. Anal.*, 45(3):1246–1268 (electronic), 2007.
- [58] D.A. Mc Donald. *Blood Flow in Arteries*. Edward Arnold Ltd., London, 1990.
- [59] M. Dorobantu and B. Engquist. Wavelet-based numerical homogenization. *SIAM J. Numer. Anal.*, 35:540–559, 1998.
- [60] M. Dryja, M.V. Sarkis, and O.B. Widlund. Multilevel Schwarz methods for elliptic problems with discontinuous coefficients in three dimensions. *Numer. Math.*, 72(3):313–348, 1996.
- [61] L.J. Durlofsky. Coarse scale models of two phase flow in heterogeneous reservoirs: volume averaged equations and their relationship to existing upscaling techniques. *Comput. Geosci.*, 2(2):73–92, 1998.
- [62] W. E and B. Engquist. The heterogeneous multiscale method. *Commun. Math. Sci.*, 1(1):87–132, 2003.
- [63] W. E and B. Engquist. Multiscale modeling and computation. *Notices Amer. Math. Soc.*, 50(9):1062–1070, 2003.
- [64] W. E and B. Engquist. The heterogeneous multi-scale method for homogenization problems. In *Multiscale Methods in Science and Engineering*, volume 43 of *Lect. Notes Comput. Sci. Eng.*, pages 89–110. Springer, Berlin, 2005.
- [65] Y.R. Efendiev, T.Y. Hou, and X.-H. Wu. Convergence of a nonconforming multiscale finite element method. *SIAM J. Numer. Anal.*, 37(3):888–910, 2000.
- [66] H.I. Ene and E. Sánchez-Palencia. Équations et phénomènes de surface pour l’écoulement dans un modèle de milieu poreux. *J. Mécanique*, 14(1):73–108, 1975.
- [67] P. Forchheimer. Wasserbewegung durch Boden. *Z. Ver. Deutsch. Ing.*, 45:1782–1788, 1901.
- [68] J. Galvis and M. Sarkis. BDD and FETI methods for mortar coupling of Stokes-Darcy. Technical Report Serie A 563, Instituto de Matematica Pura e Aplicada, Brazil, 2007. Submitted.
- [69] J. Galvis and M. Sarkis. Non-matching mortar discretization analysis for the coupling Stokes-Darcy equations. *Electron. Trans. Numer. Anal.*, 26:350–384, 2007.
- [70] J.C. Galvis and M. Sarkis. Inf-sup for coupling Stokes-Darcy. In A. Loula et al., editor, *XXV Iberian Latin American Congress in Computational Methods in Engineering, 2005, Recife. Proceedings of the XXV Iberian Latin American Congress in Computational Methods in Engineering, Recife, Brazil, 2004*. Universidade Federal de Pernambuco, 2004.

- [71] J.C. Galvis and M. Sarkis. Balancing domain decomposition methods for mortar coupling Stokes-Darcy systems. In D.E. Keyes and O.B. Widlund, editors, *Domain Decomposition Methods in Science and Engineering XVI*, pages 373–380. Springer, Berlin and Heidelberg, 2006.
- [72] G.N. Gatica, R. Oyarzúa, and F.-J. Sayas. Convergence of a family of Galerkin discretizations for the Stokes-Darcy coupled problem. Technical Report 08-11, Departamento de Ingeniería Matemática, Universidad de Concepción, 2008.
- [73] T. Giorgi. Derivation of the Forchheimer law via matched asymptotic expansions. *Transport in Porous Media*, 29:191–206, 1997.
- [74] V. Girault and P.A. Raviart. *Finite Element Methods for Navier-Stokes Equations. Theory and Algorithms*. Springer, Berlin, 1986.
- [75] V. Girault and B. Rivière. DG approximation of coupled Navier-Stokes and Darcy equations by Beaver-Joseph-Saffman interface condition. Technical Report TR-MATH 07-09, University of Pittsburgh, Department of Mathematics, 2007.
- [76] J.S. Hesthaven and T. Warburton. *Nodal Discontinuous Galerkin Methods*, volume 54 of *Texts in Applied Mathematics*. Springer, New York, 2008. Algorithms, analysis, and applications.
- [77] H. Hoteit, J. Erhel, R. Mosé, B. Philippe, and Ph. Ackerer. Numerical reliability for mixed methods applied to flow problems in porous media. *Comput. Geosciences*, 6:161–194, 2002.
- [78] T.Y. Hou and X. Wu. A multiscale finite element method for elliptic problems in composite materials and porous media. *J. Comput. Phys.*, 134(1):169–189, 1997.
- [79] T.Y. Hou, X. Wu, and Z. Cai. Convergence of a multiscale finite element method for elliptic problems with rapidly oscillating coefficients. *Math. Comp.*, 68(227):913–943, 1999.
- [80] T.J.R. Hughes. Multiscale phenomena: Green’s functions, the Dirichlet-to-Neumann formulation, subgrid scale models, bubbles and the origins of stabilized methods. *Comput. Methods Appl. Mech. Engrg.*, 127:387–401, 1995.
- [81] T.J.R. Hughes, G.R. Feijóo, L. Mazzei, and J.-B. Quincy. The variational multiscale method – a paradigm for computational mechanics. *Comput. Methods Appl. Mech. Engrg.*, 166(1–2):3–24, 1998.
- [82] O. Iliev, A. Mikelić, and P. Popov. On upscaling certain flows in deformable porous media. *Multiscale Model. Simul.*, 7(1):93–123, 2008.
- [83] W. Jäger and A. Mikelić. On the boundary conditions at the contact interface between a porous medium and a free fluid. *Ann. Scuola Norm. Sup. Pisa Cl. Sci.*, 23:403–465, 1996.
- [84] W. Jäger and A. Mikelić. On the interface boundary condition of Beavers, Joseph and Saffman. *SIAM J. Appl. Math.*, 60(4):1111–1127, 2000.
- [85] W. Jäger, A. Mikelić, and N. Neuss. Asymptotic analysis of the laminar viscous flow over a porous bed. *SIAM J. Sci. Comput.*, 22(6):2006–2028, 2001.

- [86] L.V. Kantorovich and G.P. Akilov. *Functional Analysis in Normed Spaces*. Translated from the Russian by D. E. Brown. Edited by A. P. Robertson. International Series of Monographs in Pure and Applied Mathematics, Vol. 46. The Macmillan Co., New York, 1964.
- [87] G. Karner and K. Perktold. Effect of endothelial injury and increased blood pressure on albumin accumulation in the arterial wall: a numerical study. *J. Biomech.*, 33:709–715, 2000.
- [88] W.L. Layton, F. Schieweck, and I. Yotov. Coupling fluid flow with porous media flow. *SIAM J. Num. Anal.*, 40:2195–2218, 2003.
- [89] T. Levy and E. Sánchez-Palencia. On the boundary conditions for fluid flow in porous media. *Int. J. Engng. Sci.*, 13:923–940, 1975.
- [90] J.L. Lions and E. Magenes. *Problèmes aux Limites Non Homogènes et Applications*, volume 1. Dunod, Paris, 1968.
- [91] P.L. Lions. On the Schwarz alternating method III: a variant for non-overlapping subdomains. In T.F. Chan et al., editor, *Third International Symposium on Domain Decomposition Methods for Partial Differential Equations*, pages 202–231. SIAM, Philadelphia, 1990.
- [92] A.F.D. Loula, F.A. Rochinha, and M.A. Murad. High-order gradient post-processings for second-order elliptic problems. *Comput. Meth. Appl. Mech. Engrg.*, 128:361–381, 1995.
- [93] Y. Maday and F. Magoulès. Optimized Schwarz methods without overlap for highly heterogeneous media. *Comput. Methods Appl. Mech. Engrg.*, 196(8):1541–1553, 2007.
- [94] L.D. Marini and A. Quarteroni. A relaxation procedure for domain decomposition methods using finite elements. *Numer. Math.*, 55:575–598, 1989.
- [95] E. Marušić-Paloka and A. Mikelić. The derivation of a nonlinear filtration law including the inertia effects via homogenization. *Nonlin. Anal.*, 42:97–137, 2000.
- [96] A. Masud and T.J.R. Hughes. A stabilized mixed finite element method for Darcy flow. *Comput. Meth. Appl. Mech. Engrg.*, 191:4341–4370, 2002.
- [97] E. Miglio. *Mathematical and Numerical Modeling for Enviromental Applications*. PhD thesis, Università degli Studi di Milano, Politecnico di Milano, 2000.
- [98] E. Miglio, A. Quarteroni, and F. Saleri. Coupling of free surface and groundwater flows. *Comput. Fluids*, 32(1):73–83, 2003.
- [99] J. Nečas. *Les Méthodes Directes en Théorie des Équations Elliptiques*. Masson, Paris, 1967.
- [100] J.-C. Nédélec. Mixed finite elements in  $\mathbb{R}^3$ . *Numer. Math.*, 35:119–136, 1980.
- [101] J.-C. Nédélec. A new family of mixed finite elements in  $\mathbb{R}^3$ . *Numer. Math.*, 50(1):57–81, 1986.
- [102] N. Neuss, W. Jäger, and G. Wittum. Homogenization and multigrid. *Computing*, 66(1):1–26, 2001.
- [103] F. Nobile. *Numerical Approximation of Fluid-Structure Interaction Problems with Applications to Haemodynamics*. PhD thesis, Ecole Polytechnique Fédérale de Lausanne, Switzerland, 2001.

- [104] J.T. Oden and K.S. Vemaganti. Estimation of local modeling error and goal-oriented adaptive modeling of heterogeneous materials. I. Error estimates and adaptive algorithms. *J. Comput. Phys.*, 164(1):22–47, 2000.
- [105] L.E. Payne and B. Straughan. Analysis of the boundary condition at the interface between a viscous fluid and a porous medium and related modelling questions. *J. Math. Pures Appl.*, 77:317–354, 1998.
- [106] D. Peaceman and H. Rachford. The numerical solution of parabolic and elliptic differential equations. *J. SIAM*, 3:28–41, 1955.
- [107] A. Quaini. *Algorithms for Fluid-Structure Interaction Problems Arising in Hemodynamics*. PhD thesis, Ecole Polytechnique Fédérale de Lausanne, Switzerland, 2008. Submitted.
- [108] A. Quaini and A. Quarteroni. A semi-implicit approach for fluid-structure interaction based on an algebraic fractional step method. *Math. Models Methods Appl. Sci.*, 17(6):957–983, 2007.
- [109] A. Quarteroni and A. Valli. *Numerical Approximation of Partial Differential Equations*. Springer, Berlin, 1994.
- [110] A. Quarteroni and A. Valli. *Domain Decomposition Methods for Partial Differential Equations*. Oxford University Press, New York, 1999.
- [111] P.-A. Raviart and J. M. Thomas. A mixed finite element method for 2nd order elliptic problems. In *Mathematical Aspects of Finite Element Methods (Proc. Conf., Consiglio Naz. delle Ricerche (C.N.R.), Rome, 1975)*, pages 292–315. Lecture Notes in Math., Vol. 606. Springer, Berlin, 1977.
- [112] B. Rivière. Analysis of a discontinuous finite element method for the coupled Stokes and Darcy problems. *J. Sci. Comput.*, 22(1):479–500, 2005.
- [113] B. Rivière and I. Yotov. Locally conservative coupling of Stokes and Darcy flows. *SIAM J. Numer. Anal.*, 42(5):1959–1977, 2005.
- [114] Y. Saad. *Iterative Methods for Sparse Linear Systems*. Society for Industrial and Applied Mathematics, Philadelphia, second edition, 2003.
- [115] P.G. Saffman. On the boundary condition at the interface of a porous medium. *Stud. Appl. Math.*, 1:93–101, 1971.
- [116] G. Sangalli. Capturing small scales in elliptic problems using a residual-free bubbles finite element method. *Multiscale Model. Simul.*, 1(3):485–503, 2003.
- [117] L. Tartar. Incompressible fluid flow in a porous medium: convergence of the homogenization process. In *E. Sánchez-Palencia: Non-Homogeneous Media and Vibration Theory. Lecture Notes in Physics 127*, pages 368–377. Springer, Berlin, 1980.
- [118] J.M. Thomas. *Sur l'Analyse Numérique des Méthodes d'Eléments Finis Hybrides et Mixtes*. PhD thesis, Université Pierre et Marie Curie, 1977.
- [119] A. Toselli and O. Widlund. *Domain Decomposition Methods - Algorithms and Theory*. Springer, New York, 2005.
- [120] U. Hornung, editor. *Homogenization and Porous Media*, volume 6 of *Interdisciplinary Applied Mathematics*. Springer, New York, 1997.

- [121] B.I. Wohlmuth. *Discretization Methods and Iterative Solvers Based on Domain Decomposition*, volume 17 of *Lecture Notes in Computational Science and Engineering*. Springer-Verlag, Berlin, 2001.
- [122] X.H. Wu, Y. Efendiev, and T.Y. Hou. Analysis of upscaling absolute permeability. *Discrete Contin. Dyn. Syst. Ser. B*, 2(2):185–204, 2002.
- [123] K. Yosida. *Functional Analysis*. Springer, Berlin, 1974.
- [124] P. Zunino. *Mathematical and Numerical Modeling of Mass Transfer in the Vascular System*. PhD thesis, Ecole Polytechnique Fédérale de Lausanne, Switzerland, 2002.
- [125] P. Zunino. Mortar and discontinuous Galerkin methods based on weighted interior penalties. In U. Langer et al., editor, *Domain Decomposition Methods in Science and Engineering XVII*, volume 60 of *Lect. Notes Comput. Sci. Eng.*, pages 321–327, Berlin, 2008. Springer.